**REPUBLIC OF TURKEY**
**YILDIZ TECHNICAL UNIVERSITY**
**GRADUATE SCHOOL OF NATURAL AND APPLIED SCIENCES**

# INVESTIGATION OF NOVEL, NICOTINAMIDE ADENINE DINUCLEOTIDE PHOSPHATE DEPENDENT FORMATE DEHYDROGENASE ENZYMES

**SAADET ALPDAĞTAŞ**

**Ph. D. THESIS**
**DEPARTMENT OF BIOENGINEERING**
**PROGRAM OF BIOENGINEERING**

**ADVISER**
**PROF. DR. SEVİL YÜCEL**

**CO-ADVISER**
**ASSOC. PROF. DR. BARIŞ BİNAY**

**İSTANBUL, 2018**

**REPUBLIC OF TURKEY**

**YILDIZ TECHNICAL UNIVERSITY**

**GRADUATE SCHOOL OF NATURAL AND APPLIED SCIENCES**

# INVESTIGATION OF NOVEL, NICOTINAMIDE ADENINE DINUCLEOTIDE PHOSPHATE DEPENDENT FORMATE DEHYDROGENASE ENZYMES

A thesis submitted by Saadet ALPDAĞTAŞ in partial fulfillment of the requirements for the degree of **DOCTOR OF PHILOSOPHY** is approved by the committee on 26.11.2018 in Department of Bioengineering, Bioengineering Program.

**Thesis Adviser**

Prof. Dr. Sevil YÜCEL

Yıldız Technical University

**Co- Adviser**

Assoc. Prof. Dr. Barış BİNAY

Gebze Technical University

**Approved By the Examining Committee**

Prof. Dr. Sevil YÜCEL

Yıldız Technical University _____

Prof. Dr. Osman Uğur SEZERMAN

Acıbadem University _____

Prof. Dr. Musa TÜRKER

Yıldız Technical University _____

Assist. Prof. Dr. Alper YILMAZ

Yıldız Technical University _____

Assist. Prof. Dr. Pınar HATIR ÇAKIR

İstanbul Arel University _____

This study was supported by Research Fund of the Yildiz Technical University (Project Number: FDK-2018-3331).

# ACKNOWLEDGEMENTS

This study titled "Investigation of Novel, Nicotinamide adenine dinucleotide phosphate Dependent Formate Dehydrogenase Enzymes" was prepared as a PhD thesis with the financial support of Research Fund of the Yildiz Technical University (Project Number: FDK-2018-3331) in the field of Bioengineering of Graduate School of Natural and Applied Sciences.

I would like to thank my superviser, Prof. Dr. Sevil Yücel and co-adviser Assoc. Prof. Dr. Barış Binay for their valuable guidance, scientific and moral supports in all stages of my thesis. I would like to extend my thanks to Prof. Dr. Osman Uğur SEZERMAN and Assist. Prof. Dr. Alper YILMAZ for their favorable contributions and comments during thesis progress and also my all friends from Yildiz Technical University and Gebze Technical University, particularly many thanks to my labmates Fatma Ertan, Gülden Aşçı Yetiş, Ünzile Güven Gülhan, Atike Nur Seyitoğlu and Aişe Ünlü for their kindly help and foresights in all experimental stages.

For enabling the fulfillment of this study, I would like to thank the Scientific Research Projects Unit of Yildiz Technical University, the members of Graduate School of Natural and Applied Sciences, the Dean of Chemistry and Metallurgy Faculty and particularly faculty members of Bioengineering Department.

I am always grateful to my family for their constant patient, love, support and encouragement throughout my whole life and particularly my PhD stage.

November, 2018

Saadet ALPDAĞTAŞ

## TABLE OF CONTENTS

Page

LIST OF SYMBOLS ..... viii

LIST OF ABBREVIATIONS ..... ix

LIST OF FIGURES ..... x

LIST OF TABLES ..... xii

ABSTRACT ..... xiii

ÖZET ..... xv

CHAPTER 1

INTRODUCTION ..... 1

1.1 Literature Review ..... 1
1.2 Objective of the Thesis ..... 5
1.3 Hypothesis ..... 6

CHAPTER 2

GENERAL INFORMATION ..... 7

2.1 Biocatalysis ..... 7
2.2 Chiral Compounds ..... 7
2.3 Oxidoreductases ..... 9
2.4 Cofactor Regeneration ..... 11
2.5 Formate Dehydrogenase (FDH) ..... 15
2.5.1 Other Applications of FDH ..... 17
2.5.1.1 Diagnosis of Methanol Poisoning ..... 17
2.5.1.2 Diagnosis of Nephrolithiasis ..... 17
2.5.1.3 Diagnosis of Trichomonas vaginalis ..... 18
2.5.1.4 Sequestration of Greenhouse Gases ..... 19

CHAPTER 3

MATERIAL METHOD ..... 20

3.1 Material ..... 20

3.2 Mining Protein Sequences for $NADP^+$ Dependent FDH …….....20
3.3 Cloning, Expression and Purification of N-terminus His Tagged FDH from *Burkholderia dolosa* PC543……...21
3.3.1 N-Terminus His Tag Primer Design and Polymerase Chain Reaction (PCR).....21
3.3.2 Cloning of Bdfdh Gene into pET14b..... 22
3.3.2.1 Isolation of Cloning Vector (pET14b)..... 22
3.3.2.2 Restriction Reactions of PCR product and pET14b-Ss_Ntr Plasmid DNA.....22
3.3.2.3 Ligation Reaction of Bdfdh Gene and pET14b Vector ..... 23
3.3.2.4 Selection and Characterization of Recombinant *E. coli* Colonies 23
3.3.3 Expression and Purification of BdFDH ..... 23
3.3.3.1 Production of Recombinant Enzyme *via* IPTG Induction ..... 23
3.3.3.2 Purification of Recombinant Enzyme *via* Autoinduction..... 24
3.3.3.3 Purification of N-Terminus His Tagged FDH Using Ni-Affinity Column..... 24
3.4 Cloning, Expression and Characterization of BdFDH into C-Terminus His Tagged Form ..... 25
3.4.1 C-Terminus His Tag Primer Design and the fdh Gene Amplification *via* PCR ..... 25
3.4.2 Cloning of Bdfdh into pET22b ..... 25
3.4.2.1 Isolation of Cloning Vector (pET22b) and Restriction Reactions of PCR Product and Plasmid DNA ..... 25
3.4.2.2 Ligation Reaction of Bdfdh Gene and pET22b Vector ..... 26
3.4.3 Expression and Purification of BdFDH ..... 26
3.4.3.1 Production of C-Terminus His Tagged Recombinant Enzyme *via* IPTG Induction and Autoinduction ..... 26
3.4.3.2 SDS/Native-PAGE Analysis and Determination of Protein Concentration..... 27
3.4.4 Determination of Protein Mass by MALDI-TOF Analysis ..... 27
3.4.5 Determination of Recombinant BdFDH Properties..... 27
3.4.5.1 Ionic Strength Effect on BdFDH Enzyme ..... 27
3.4.5.2 The Effect of pH and Temperature on BdFDH Enzyme ..... 28
3.4.5.3 Effects of Metallic Compounds and Organic Solvents on BdFDH ..... 29
3.4.5.4 Steady State Kinetics and Enzyme Assay..... 29
3.5 Cloning, Expression and Characterization of FDH from *Lactobacillus buchneri* NRRL B-30929 (LbFDH)..... 30
3.5.1 Lbfdh Gene Mutation and Amplification *via* Overlap PCR ..... 30
3.5.2 Cloning of Lbfdh into pET23b ..... 31
3.5.2.1 Restriction Reactions of PCR Product and Plasmid DNA (pET23b (+))..... 31
3.5.2.2 Ligation Reaction of Lbfdh Gene into pET23b Vector ..... 31
3.5.3 Expression and Purification of LbFDH ..... 32
3.5.4 SDS/Native-PAGE Analysis and Bradford Assay..... 32
3.5.5 Determination of Recombinant LbFDH Properties ..... 33
3.5.5.1 The Effect of pH and Temperature on LbFDH..... 33
3.5.5.2 Effects of Metallic Compounds and Organic Solvents on LbFDH.. .....33
3.5.5.3 Enzymatic Assay and Steady State Kinetic Reactions ..... 34

3.6 Statistical analysis ..... 35

CHAPTER 4

RESULTS AND DISCUSSION ..... 36

4.1 Cloning, Expression and Biochemical Characterization of FDH from *Burkholderia dolosa* PC543 ..... 36
4.1.1 Cloning of BdFDH as N-terminal His Tagged Form ..... 36
4.1.2 Confirmation of Ligation Reaction ..... 40
4.1.3 Expression and Purification of N-terminus His Tagged BdFDH ..... 42
4.1.4 Cloning of BdFDH as C-terminus His Tagged Form ..... 46
4.1.5 Ligation Reaction Confirmation ..... 49
4.1.6 Expression and Purification of C-terminus His Tagged BdFDH ..... 49
4.1.7 Ionic strength, pH and Temperature Effect on BdFDH ..... 52
4.1.8 Effect of Metallic Ions and Organic Solvents on BdFDH ..... 55
4.1.9 Enzymatic Assay and Steady State Kinetics ..... 57
4.2 Cloning, Expression and Characterization of FDH from *L. buchneri* NRRL B-30929 ..... 60
4.2.1 Cloning of LbFDH as C-terminal His Tagged Form ..... 61
4.2.2 Expression and Purification of C-terminus His Tagged LbFDH ..... 65
4.2.3 Effect of pH and Temperature on LbFDH ..... 67
4.2.4 Effects of Metal Ions and Organic Solvents on Enzyme ..... 70
4.2.5 Enzymatic Assay and Steady State Kinetics ..... 72

REFERENCES ..... 82

APPENDIX-A

MEDIUMS/SOLUTIONS ..... 91

APPENDIX-B

PRIMERS FOR CLONING AND MUTAGENESIS ..... 93

CURRICULUM VITAE ..... 94

## LIST OF SYMBOLS

| | |
|---|---|
| kcat | Turnover number |
| kDa | Kilo dalton |
| M | Molarity |
| mL | Milliliter |
| mM | Millimolar |
| Vmax | Maximum velocity |
| ºC | Centigrade degree |
| Ɛ | Absorptivity coefficient |
| µg | Microgram |
| µM | Micromolar |

## LIST OF ABBREVIATIONS

| | |
|---|---|
| APS | Ammonium persulfate |
| BSA | Bovine serum albumin |
| CboFDH | *Candida boidinii* FDH |
| CmFDH | *Candida methylica* FDH |
| DMSO | Dimethyl sulfoxide |
| dNTP | Deoxyribonucleotide triphosphates |
| EDTA | Ethylenediaminetetraacetic acid |
| FDH | Formate dehydrogenase |
| *fdh* | Formate dehydrogenase gene |
| IPTG | Isopropyl β-D-1-thiogalactopyranoside |
| MALDITOF | Matrix Assisted Laser Desorption/Ionization - Time of Flight Mass Spectrometry |
| Min | Minute |
| NADH | Nicotinamide adenine dinucleotide (Reduced form) |
| NAD(P)H | Nicotinamide adenine dinucleotide phosphate (Reduced form) |
| Ni-NTA | Nickel-Nitrilotriacetic acid |
| PAGE | Polyacrylamide gel electrophoresis |
| PCR | Polymerase chain reaction |
| pH | Potential of hydrogen |
| PMSF | Phenylmethylsulfonyl fluoride |
| *Pse*FDH | *Pseudomonas* sp. 101 FDH |
| SDS | Sodium dodecyl sulfate |
| TEMED | Tetramethylethylenediamine |
| UV-Vis | Ultraviolet and Visible |

## LIST OF FIGURES

Page


Figure 2.1 Principles of green chemistry and benefits of biocatalysis..... .8
Figure 2.2 Distribution of enzymatic activities registered in BRENDA ..... .10
Figure 2.3 Nicotinamide adenine dinucleotides..... .11
Figure 2.4 Whole-cell biocatalytic reduction via coexpressing CtXR and CbFDH....12
Figure 2.5 Reaction mechanism for L-tert-leucine (L-Tle) production..... .15
Figure 2.6 The reaction catalyzed by formate dehydrogenase..... .16
Figure 4.1 Sequence comparison of BdFDH with reported NAD(P)$^+$ FDHs.....37
Figure 4.2 pET14b vector sequence and map..... 38
Figure 4.3 PCR program and gel electrophoresis for amplification of Bdfdh.....38
Figure 4.4 PostPCR product of Bdfdh (N-terminus His tagged) on agarose gel.....39
Figure 4.5 Restriction reaction products of pET14b-Ss-ntr and PCR products..... .39
Figure 4.6 Construction of pET14b-Bdfdh recombinant plasmid. ..... .40
Figure 4.7 Colony PCR products on 0.8 % agarose gel..... .41
Figure 4.8 Restriction reaction products of recombinant plasmid on agarose gel..... .41
Figure 4.9 Overnight and induction cultures for protein expression. ..... .42
Figure 4.10 The expression profile of N-term His tagged BdFDH at 30 °C. ..... .43
Figure 4.11 The purification of BdFDH after IPTG induction..... .43
Figure 4.12 The expression profile of BdFDH at ~22 °C for 8 h ..... .44
Figure 4.13 Purification of BdFDH after IPTG induction at 16°C for 8h. ..... .44
Figure 4.14 Expression profile of BdFDH by autoinduction at 16 ° C for 20 hours. .. .45
Figure 4.15 SDS-PAGE analysis of N-terminus His tagged BdFDH..... .46
Figure 4.16 pET22b vector sequence and map..... .47
Figure 4.17 Post PCR product of Bdfdh (C-terminus His tagged) ..... .48
Figure 4.18 Restriction reaction products of pET22b-X and PCR products ..... ..48
Figure 4.19 Colony PCR products on 0.8 % agarose gel..... .49
Figure 4.20 The expression profile of C-term His tagged BdFDH at 30 °C. ..... .....50
Figure 4.21 SDS-PAGE result for purification of BdFDH..... .50
Figure 4.22 SDS-PAGE analysis of purified C-terminal His tagged BdFDH..... .51
Figure 4.23 Native-PAGE analysis of purified BdFDH protein. ..... .52
Figure 4.24 MALDI-TOF MS results of C-terminus His tagged BdFDH..... .53
Figure 4.25 The effect of ionic strength on the enzyme activity. ..... .53
Figure 4.26 Activity-pH profile of BdFDH ..... .54
Figure 4.27 Relative activity–temperature profile of BdFDH.....55
Figure 4.28 Thermostability of BdFDH..... .55
Figure 4.29 Effect of metallic ions on BdFDH.....56
Figure 4.30 Residual activity of BdFDH in some organic solvents..... 57
Figure 4.31 Michaelis–Menten curves for BdFDH in presence of $NAD^+$ or $NADP^+$...58
Figure 4.32 Sequence comparison of BdFDH with NAD(P)$^+$ dependent FDH.....60

Figure 4.33 pET23b(+) vector sequence and map ..... .61
Figure 4.34 Post PCR product of Lbfdh on 1% agarose gel ..... .62
Figure 4.35 Post PCR products obtained by combining PCRI and PCRII products ... .63
Figure 4.36 Combined PCRI and PCR II product on 1 % agarose gel. ..... .64
Figure 4.37 Restriction reaction products of pET23b-Lys and PCR products. ..... .64
Figure 4.38 Colony PCR products on 0.8 % agarose gel. ..... .64
Figure 4.39 Colonies from transformation of ligation reaction. ..... 65
Figure 4.40 The expression profile of C-terminus His tagged LbFDH at 30 °C ..... .65
Figure 4.41 SDS-PAGE and Native-PAGE analysis of LbFDH ..... .66
Figure 4.42 Theoretical calculation of molecular weight of recombinant LbFDH ..... .67
Figure 4.43 MALDI-TOF MS analysis for LbFDH ..... .67
Figure 4.44 pH-activity profile of LbFDH. ..... .68
Figure 4.45 Activity-temperature profile of LbFDH ..... .69
Figure 4.46 Thermostability of LbFDH. ..... .69
Figure 4.47 Differential Scanning Calorimetry (DSC) analysis of LbFDH ..... .70
Figure 4.48 Metal ions effect on LbFDH activity. ..... .70
Figure 4.49 Organic solvent stability of LbFDH ..... .72
Figure 4.50 Stability profile of LbFDH in different storage conditions ..... .72
Figure 4.51 Michaelis-Menten graphs for LbFDH. ..... .....73

## LIST OF TABLES

Page


Table 1.1 Kinetic constants of some native and mutant FDHs.....2
Table 1.2 Kinetic parameters for FDHs reported for having specificity to $NADP^+$....5
Table 2.1 Enzyme classes based on activities registered in BRENDA.....9
Table 2.2 Cofactor regeneration routes.....13
Table 4.1 Kinetic constants of natural $NADP^+$ dependent FDHs for cofactors.....59
Table 4.2 Kinetics parameters of the FDHs in terms of formate (BdFDH).....59
Table 4.3 Kinetics parameters of the *Bd*FDH for substrates.....60
Table 4.4 Residual activity profile for *Lb*FDH in various cosolvents.....71
Table 4.5 Kinetic constants for $NADP^+$ dependent FDHs.....74
Table 4.6 Kinetic constants of FDHs for formate.....75

## ABSTRACT

# INVESTIGATION OF NOVEL, NICOTINAMIDE ADENINE DINUCLEOTIDE PHOSPHATE DEPENDENT FORMATE DEHYDROGENASE ENZYMES

Saadet ALPDAĞTAŞ

Department of BioEngineering

Ph. D. Thesis

Adviser: Prof. Dr. Sevil YÜCEL

Co-Adviser: Assoc. Prof. Dr. Barış BİNAY

NADPH dependent oxidoreductases are remarkable biocatalysts for industrial production of chiral chemicals. For in situ regeneration of required expensive cofactors, Formate dehydrogenases (FDHs) are quite important. It is a significant necessity to determine the FDHs which have $NADP^+$ dependency and also multi-directional stability for cofactor recycling process.

In this study, it was aimed to get two, new $NADP^+$ dependent FDHs *via* recombinant DNA technologies and protein engineering methods from natural sources, a pathogenic bacterium *Burkholderia dolosa* PC543 (*Bd*FDH) and ethanol tolerant bacterium *Lactobacillus buchneri* NRRL B-30929 (*Lb*FDH), and also investigate the effect of N- and C- terminus His tag extensions on solubility and activity of *Bd*FDH. Two novel $NADP^+$ dependent FDHs from these microorganisms were cloned, purified and characterized with their unique features. The first enzyme is a new, DMSO tolerant formate dehydrogenase, which has dual cofactor specificity and tolerance to acidic conditions and obtained from *B. dolosa* PC543 (*Bd*FDH). The expression of N- and C-terminus His-tagged *Bd*FDHs were performed, separately and it was determined that the C-terminus His-tagged enzyme was active and soluble whereas the N-terminal version of enzyme was not. The other putative $NADP^+$ dependent formate dehydrogenase gene was obtained from *L. buchneri* NRRL B-30929. It was determined that LbFDH has high activity at an acidic pH range (pH 4.8-6.2) and at high temperatures. Its $T_m$ value has been obtained as 78 °C by differential scanning calorimetry (DSC) as an unusual value for equivalent enzymes. The specific activity of *Lb*FDH (24.6 U/mg) with $NADP^+$ is a beneficial feature among all $NADP^+$ dependent FDHs at 60 °C. If these enzymes are

compared in terms of its kinetic constants, it can be said that *Bd*FDH has a great interaction with formate ion and LbFDH has a beneficial affinity towards $NADP^+$, due to these capabilities, both of FDHs can be utilized as model enzymes for protein engineering studies.

In conclusion, these two novel enzymes with their performance in acidic pH values, DMSO tolerance and coenzyme preference, have great potential to recycle cofactors in biocatalysis of chiral intermediates in various industries.

**Key words:** Cofactor regeneration, $NADP^+$ dependent formate dehydrogenase, *Lactobacillus buchneri* NRRL B-30929, *Burkholderia dolosa* PC543, Biochemical and kinetic characterization.

# ÖZET

## YENİ, NİKOTİNAMİD ADENİN DİNÜKLEOTİD BAĞIMLI FORMAT DEHİDROJENAZ ENZİMLERİNİN ARAŞTIRILMASI

Saadet ALPDAĞTAŞ

Biyomühendislik Anabilim Dalı

Doktora Tezi

Tez Danışmanı: Prof. Dr. Sevil YÜCEL

Eş Danışman: Doç. Dr. Barış BİNAY

NADPH bağımlı oksidoredüktazlar, kiral bileşiklerin endüstriyel üretimi için değerli biyokatalizörlerdir. İhtiyaç duydukları yüksek maliyetli kofaktörlerin, yerinde rejenerasyonu için Format dehidrojenaz enzimleri (FDH) oldukça değerli bir seçenektir. $NADP^+$ bağımlılığı ve çok yönlü kararlılık gibi özelliklere sahip olabilecek FDH enzimlerinin tespit edilmesi, koenzim rejenerasyonu açısından bir gerekliliktir.

Bu çalışmada iki ayrı $NADP^+$ bağımlı FDH enziminin rekombinant DNA teknikleri ve protein mühendisliği metodları kullanılarak doğal kaynaklardan, biri patojenik bakteri olan *Burkholderia dolosa* PC543 (*Bd*FDH) ve diğeri etanole toleransı olan bir bakteri olan *Lactobacillus buchneri* NRRL B-30929 (*Lb*FDH), elde edilmesi ve ayrıca amino / karboksil uçlarına ekli histidin uzantısının *Bd*FDH enzimi üzerine olan etkisinin incelenmesi amaçlanmıştır. Bu mikroorganizmalardan iki yeni $NADP^+$ bağımlı FDH enzimi klonlanmış, saflaştırılmış ve karakterize edilmiştir. İlk FDH, *B. dolosa* PC543 bakterisinden elde edilmiş, çift koenzim spesifitesi olan ve asidik pH değerlerinde çalışabilen, DMSO toleransına sahip yeni bir enzimdir. Amino / karboksil ucunda histidin uzantısı olan *Bd*FDH' ler, ayrı ayrı ifade edilmiş ve karboksil ucunda histidin etiketi olan enzimin çözünür halde ve aktif iken amino ucunda histidin uzantısı olan FDH enziminin inklüzyon cisimciği şeklinde olduğu ve aktivitesinin olmadığı tespit edilmiştir. Diğer putatif $NADP^+$ bağımlı format dehidrojenaz geni *L. buchneri* NRRL B-30929 bakterisinin genomik DNA' sından klonlanmış ve elde edilen *Lb*FDH enzimin asidik koşullarda (pH 4.8-6.2) oldukça aktif olduğu ve yüksek sıcaklık değerlerinde optimum aktiviteye sahip olduğu belirlenmiştir. Enzimin, eşdeğerleri arasında sıradışı bir Tm değerine (78 °C) sahip olduğu diferansiyel taramalı kalorimetri ile belirlenmiştir. Dahası,

*Lb*FDH' ın 60 °C'de ve $NADP^+$ varlığında elde edilen spesifik aktivitesi (24.6 U/mg) tüm $NADP^+$ bağımlı FDH'ler arasında sıradışı bir özelliktir. Enzimler kinetik sabitleri yönüyle değerlendirildiğinde *Bd*FDH enziminin özellikle format iyonu ile LbFDH enziminin ise kofaktör ile etkileşimi oldukça dikkat çekicidir ve protein mühendisliği çalışmaları için model olarak kullanılabileceği düşünülmektedir.

Sonuç olarak, DMSO toleransı, asidik koşullara olan dayanıklılık ve koenzim tercihi nedeniyle bu iki yeni enzim, kiral ara bileşiklerin biyokatalizinde kofaktör geri dönüşümünde kullanım için büyük bir potansiyele sahiptir.

**Anahtar Kelimeler:** Kofaktör rejenerasyonu, $NADP^+$ bağımlı format dehidrojenaz, *Lactobacillus buchneri* NRRL B-30929, *Burkholderia dolosa* PC543, biyokimyasal ve kinetik karakterizasyon

# CHAPTER 1

# INTRODUCTION

## 1.1 Literature Review

Nicotinamide cofactor (NAD(P)H) dependent enzymes are quite significant for the synthesis of chiral intermediates. Such biocatalytic processes can be commercialized. Due to high cost of nicotinamide cofactors, it is not economically feasible to add the cofactor into the system in stoichiometric quantities. Instead of this, an appropriate in situ recycling technique should be used for cofactor regeneration. An $NAD^+$ dependent formate dehydrogenase (FDH) has been used as a recycler enzyme for the synthesis of L-*tert*-leucine in large scale [1]. Most of reported formate dehydrogenases prefer $NAD^+$ over $NADP^+$ and display weak affinity or no ability to catalyse the reduction of $NADP^+$ in reactions [2]. There is a number of extremely useful NADPH dependent enzymes for chiral synthesis. Therefore, to produce new FDHs with desired properties to recycle NADPH in such reactions, protein engineering of FDHs with the scope of change their cofactor preference to $NADP^+$ is a beneficial method. In this technique, the gene encoding the enzyme is mutagenized and a library of mutant enzymes is obtained. Then, this library is screened for desired enzyme. This method has been successfully performed in some studies to enhance several properties of enzymes including coenyzme specificity, however the mutant enzymes frequently have not been improved in desired aspect. Another solution is to mine native $NADP^+$ dependent FDHs from various natural sources, these FDHs might be better than engineered ones [2], [3], [4]. There are various papers on these two points.

Until 2009, all studies focused on protein engineering of existing FDHs. The first study was conducted by Tishkov et al. [5], through engineering of the FDH from Pseudomonas sp. 101(PseFDH) [5]. The catalytic efficiency value of this mutant for $NADP^+$ was only 3-fold less than the catalytic efficiency value of wild type enzyme for $NAD^+$ [6].

Gul-Karaguler et al. [7] investigated the replacement of aspartic acid residue, in interaction with the adenine ribose of the $NAD^+$ cofactor, by serine in *Candida methylica* FDH (*Cm*FDH) to change the coenzyme preference from $NAD^+$ to $NADP^+$. The alteration of cofactor specificity in *Cm*FDH by the D195S mutation indicated that an aspartic acid residue at cofactor binding position in the Rossmann fold is a major determinant of $NAD^+/NADP^+$ recognition. The affinity of the *Cm*FDH for $NADP^+$ was increased to 10,000-fold *via* Asp195Ser substitution, however, the obtained mutant *Cm*FDH still displayed 40 times higher $k_{cat}/K_M$ value with $NAD^+$ than in presence of $NADP^+$ [7].

Serov et al. reported a mutant of *Saccharomyces cerevisiae* FDH (*Sce*FDH) with its coenzyme preference switched to $NADP^+$ [8].The $NADP^+$ preference of mutant *Sce*FDH was improved and higher than that of reported for the *Cm*FDH D195S mutant mentioned above. However, the Michaelis constant for formate was increased via D196A/Y197R mutation in *Sce*FDH and the total catalytic activity of this mutant was quite lower than that of the mutant $NADP^+$ dependent FDH of Pseudomonas sp. 101 [8], [9] (Table 1.1).

Table 1.1 Kinetic constants of some native and mutant FDHs [8]

| Formate dehyrogenase | $K_m^{NAD^+}$ ($\mu$M) | $k_{cat}$ with $NAD^+$ ($s^{-1}$) | $K_m^{NADP^+}$ ($\mu$M) | $k_{cat}$ with $NADP^+$ ($s^{-1}$) | $K_m^{formate}$ (mM) | $\frac{k_{cat}^{NADP^+}}{K_m^{NADP^+}} / \frac{k_{cat}^{NAD^+}}{K_m^{NAD^+}}$ |
|---|---|---|---|---|---|---|
| Wild-type SceFDH [8] | 36 ± 5 (0.25 M formate) | 6.5 ± 0.4 | ND* | ND | 5.5 ± 0.3 | $< 3.3 \times 10^{-10}$ |
| SceFDH D196A/Y197R [8] | 7600 ± 800 (0.25 M formate) | 0.095 ± 0.01 (0.25 M formate) | 4500 ± 500 (0.25 M formate) | 0.13 ± 0.01 (0.25 M formate) | 1000 ± 200 (40 mM $NADP^+$) | 2.3 (0.25 M formate) |
| | 8400 ± 900 (0.5 M formate) | 0.12 ± 0.02 (0.5 M formate) | 7600 ± 900 (0.5 M formate) | 0.16 ± 0.02 (0.5 M formate) | | 1.5 (0.5 M formate) |
| Wild-type CmeFDH [7] | 55 ± 4 (0.2 M formate) | 1.4 ± 0.1 | ND | ND | NR† | $< 4 \times 10^{-6}$ |
| CmeFDH D195S [7] | 4700 ± 300 (0.2 M formate) | 1.6 ± 0.1 | ND (> 0.4 M‡) | ND | NR | $2.4 \times 10^{-2}$ (0.2 M formate) |
| Wild-type PseFDH [8] | 60 ± 5 (0.3 M formate) | 10.0 ± 0.6 | > 0.4 M | ND | 7.0 ± 0.8 | $4.2 \times 10^{-4}$ (0.3 M formate) |
| Mutant $NADP^+$-specific PseFDH [8] | 1000 ± 150 (0.3 M formate) | 5.0 ± 0.4 | 150 ± 25 (0.3 M formate) | 2.5 ± 0.15 | 9.0 ± 3.0 | 3.5 (0.3 M formate) |

* ND, not detectable.
† NR, not reported.
‡ Estimated from data [7]

Nanba et al. [10], [11] reported two FDHs with a few affinity towards $NADP^+$. The FDH from *Thiobacillus sp*. KNK66MA [10] and *Ancylobacter aquaticus* KNK607M [11] has $NADP^+$ affinity only 4.2% and 2.4% of those with $NAD^+$, respectively. *Candida boidinii* formate dehydrogenase (*Cbo*FDH) has a high affinity towards $NAD^+$ and essentially it is unable to catalyze the reduction of $NADP^+$. Andreadeli et al. [12] redesigned the coenzyme preference of *Cbo*FDH *via* site-saturation mutagenesis and resulted mutant, Asp195Gln /Tyr196His, displayed more than $2.10^7$-fold enhancement in catalytic efficiency. Although, the mutant enzyme shows high $K_M$ for $NADP^+$ and formate [12].

In spite of all of these engineering efforts, the $(k_{cat}/K_M)^{NADP+}$ values for these mutant enzymes are quite low. Therefore, it still has a great importance to screen and identify particularly native $NADP^+$ dependent FDHs. In order to fill the gap, Davis et al. [2] focused on this point and obtained two native $NADP^+$ dependent FDHs from *Burkholderia* sp 383 (*Bsp*383FDH) and *Burkholderia cenocepacia* PC184 (*Bsp*184FDH). Both of these novel FDHs have strong preferences for $NADP^+$. The $(k_{cat}/K_M)^{NADP+}/(k_{cat}/K_M)^{NAD+}$ value is 73 for *Bsp*184FDH and 39 for *Bsp*383FDH. The catalytic efficiency values for *Bsp*184FDH and *Bsp*383FDH are 2.79 and 3.96 and the *Bsp*383FDH has better affinity for $NADP^+$ than *Bsp*184FDH [2].

Labrou et al. [13] estimated that the beneficial way to switch the coenzyme preference of *Cbo*FDH to $NADP^+$ was to change the residues Gln197 and Asp195 via mutagenesis resulted on molecular modeling and affinity labeling studies [13]. They suggested that such mutagenesis might discard the repulsion between Asp195 residue and the phosphate group of $NADP^+$ and it provides an area required for the phosphate group of $NADP^+$. On the other hand, the adenine ring is likely to interact with Tyr196 and His232 in crystal structures of *Cbo*FDH mutants [14]. Thus, it can be said that, the Asp195, Tyr196 and Gln197 residues might have significant role in tuning the cofactor specificity of enzyme. Based on this inference, Wu et al. [15] investigated the roles of residues 195, 196 and 197 in the cofactor specificity for *Cbo*FDH and performed site saturation mutagenesis on Tyr196 an Asp195 residues of *Cbo*FDH resulted in D195S/Y196P and D195Q/Y196R double mutants which have a remarkable $NADP^+$ preference. The $(k_{cat}/K_M)^{NADP+}$ values were $1.14x10^4$ and $2.9\times10^3$ $M^{-1}$ $s^{-1}$, respectively. The $NADP^+$ preference value, $(k_{cat}/K_M)^{NADP+}/(k_{cat}/K_M)^{NAD+}$, of D195S/Y196P and D195Q/Y196R mutants were 0.2 and 2.1, respectively. Moreover, to alter the residue Gln197 of D195Q/Y196R to Asn enhanced the catalytic efficiency of enzyme $(k_{cat}/K_M)^{NADP+}$ to $29.1\times10^3$ $M^{-1}$ $s^{-1}$ and the $(k_{cat}/K_M)^{NADP+}/(k_{cat}/K_M)^{NAD+}$ value to 17.1, This value is quite higher than mutant *Pse*FDH [15].

In 2010, Hatrongjit and Packdibamrung focused on the *Burkholderia cepacia* complex (BCC) as a new FDH source to get native $NADP^+$ dependent FDHs. The research revealed a new, native $NADP^+$ dependent formate dehydrogenase from *Burkholderia stabilis* 15516 (*Bst*FDH) with a wide range pH and temperature stability. This enzyme has a clear specificity for both $NADP^+$ and $NAD^+$. The native *Bst*FDH act on $NADP^+$ as a natural cofactor with approximately 2.6-fold specific activity over that of $NAD^+$. The affinity

($K_M$ values) for $NADP^+$, $NAD^+$ and sodium formate, are 0.16, 1.43 and 55.5 mM, respectively [4].

In another study, to obtain an $NADP^+$ dependent enzyme, Hoelsch et al. [16] engineered the FDH from *Mycobacterium vaccae* N10 (*Myc*FDH). The $NAD^+$ binding pattern region was used for mutagenesis. Among the obtained mutants, A198G/D221Q had the highest $k_{cat}/K_M$ value in the presence of $NADP^+$. In addition, the substitution of two cysteines (C145S/C255V) both provided a good tolerance to α-haloketone ethyl 4-chloroacetoacetate (ECAA) and also increased the $k_{cat}/K_M$ value for 6-fold. This C145S/A198G/D221Q/C255V mutant had a specific activity of 4.00 U/mg and a $K_M^{NADP+}$ of 0.147 mM at room temperature and neutral pH. The another mutant C145S/D221Q/ C255V had the best specific activity of 10.25 U/mg and the $K_M^{NADP+}$ value is 0.92. These results indicated that the A198G substitution had a beneficial effect on the kinetic values of the *Myc*FDH [16].

Ihara et al. [17] also obtained some mutants to switch the cofactor preference from $NAD^+$ to $NADP^+$ (Table 1.2). Among these mutants; Gln/Asn (QN) mutants for Pseudomonas FDH and *Arabidopsis* FDH, Gln/His (QH) mutant for *potato* FDH and Gln/Arg/Asn (QRN) mutant for *Candida boidinii* FDH displayed high $NADP^+$ dependency. PseFDH (QN) showed low $K_M$ values with $NADP^+$ and formate [17].

Despite all efforts in protein engineering for $NAD^+$ dependent FDHs to switch their cofactor specificity, still, glucose dehydrogenases or phosphite dehydrogenases are generally preferred for regeneration of $NADP^+$. Therefore, to obtain a feasible $NADP^+$ dependent FDH, Fogal et al. [3] screened and performed the characterization of an FDH from *Granulicella mallensis* MP5ACTX8. The kinetic characterization showed that the novel FDH is able to use both cofactors, with better specificity towards the $NADP^+$. The $k_{cat}^{NADP+}$ is comparable with *Bst*FDH (3.96 vs.4.75 $s^{-1}$). The $K_M^{NADP+}$ is 5.3-fold higher than that of *Bst*FDH. The low affinities for substrates indicate that the *Gra*FDH needs to be optimized for utilization in biotransformations [3] (Table 1.2).

Table 1.2 Kinetic parameters for FDHs reported for having specificity to $NADP^+$ [3]

| FDH | $K_m$ $NAD^+$ mM | $k_{cat}$ $NAD^+$ $s^{-1}$ | $K_m$ $NADP^+$ mM | $k_{cat}$ $NADP^+$ $s^{-1}$ | $K_m$ formate mM |
|---|---|---|---|---|---|
| *Sce*FDH [8] | 8.40 | 0.12 | 7.60 | 0.16 | 1000.00 |
| D196A/Y197R | | | | | |
| *Cbo*FDH [12] | 1.80 | 0.49 | 1.70 | 0.44 | 80.00 |
| D195Q/Y196H | | | | | |
| *Cbo*FDH [15] | 0.36 | 0.62 | 0.029 | 0.79 | n.d. |
| D195Q/Y196R/Q197N [17] | n.d | | 0.18 | | 150.00 |
| *Bst*FDH [4] | 1.43 | 1.66 | 0.16 | 4.75 | 55.50 |
| *Myc*FDH [16] | 1.09 | 8.22 | 0.92 | 7.89 | 113.00 |
| C145S/D221Q/C255V | | | | | |
| 3 M formate | | | | | |
| *Myc*FDH [16] | 4.10 | 5.18 | 0.15 | 3.08 | 98.00 |
| C145S/A198G/D221Q/C255V | | | | | |
| 4 M formate | | | | | |
| *Ath*FDH [17] | n.d. | | 0.91 | | 96.00 |
| D227Q/L229N | | | | | |
| *Pot*FDH [17] | n.d. | | 0.62 | | 120.00 |
| D195Q/L197H | | | | | |
| *Pse*FDH [17] | 1.00 | | 0.35 | | 63.00 |
| D222Q/H224N | | | | | |
| *Gra*FDH [3] | 6.50 | 5.77 | 0.85 | 3.96 | 80.00 ($NAD^+$) 200.00 ($NADP^+$) |

As known, *Candida methylica* FDH (*Cm*FDH) is a remarkable catalyst for NADH regeneration in chemical industry. Özgün et al. [18] performed the site saturation mutagenesis to change the coenzyme preference of this robust enzyme in terms of $NADP^+$ and increase its thermal resistance. The positions at 195, 196, and 197 are used for mutagenesis in the coenzyme binding region. The obtained mutants, D195S/Q197T and D195S/Y196L, increase the catalytic efficiency for $NAD^+$ to $5.6 \times 10^4$-fold and $5 \times 10^4$-fold value, respectively [18].

## 1.2 Objective of the Thesis

A broad range of chemical reactions can be catalyzed by oxidoreductases with a great specificity, selectivity and efficiency. Most of these enzymes strictly require expensive nicotinamide cofactors [19]. In several industries, the cost of the cofactor prevents its utilization in stoichiometric quantities for NAD(P)H dependent dehydrogenase based biotransformations. Due to the numerous advantages of FDH, it can be used as an *in situ* cofactor regenerator in the production of optically active intermediates *via* $NAD(P)^+$ dependent dehydrogenases. In such biotransformations, to regenerate the cofactor, the formate conversion has been used as an auxiliary reaction. Most of the FDH enzymes

reported up to now have strictly dependency towards $NAD^+$. This preference is the main disadvantage, since various crucial dehydrogenases used in industrial biocatalysis are strongly $NADP^+$ dependent. There are different studies including various approaches to change the cofactor specificity, nevertheless none of them reach acceptable efficiency [6], [7], [8], [12], [15], [16], [18]. Even though a preference for $NADP^+$ is generally achieved in different degrees, a decrease or loss of efficiency frequently is inevitable as an undesired situation [19]. Therefore, these studies still have not been enough to circumvent this problem and their implementation has not yet achieved as an applicable way in organic synthesis. In order to obtain novel, robust and natural $NADP^+$ dependent FDHs to regenerate NADPH, we aimed to perform protein sequence mining studies by using computational tools through considering conserved coenzyme binding region and key residues. By this approach, determination of putative *fdh* genes and their expression as a soluble protein, purification and biochemically characterization were targeted. Briefly, our aim is to provide a contribution towards the economical regeneration of NAD(P)H coenzyme. To elucidate the N- and C-terminus His tag effect on the protein activity and solubility is another aspect of this study. It allows us to understand the impact of an intervention on structure and its reflection on function.

### 1.3 Hypothesis

Oxidoreductases are quite significant enzymes in the biosynthesis of chiral substances. Most of these enzymes particularly require the $NADP^+$ cofactor, which is expensive and prevents the utilization of enzymes at large scale. The formate dehydrogenase enzymes have great potential for recovery of the cofactor used in the reaction system. In particular, the presence of enzymes that have affinity towards $NADP^+$ is a crucial way to recycle reduced cofactor and provide the system continuity. It is thought that this study reveal the production and the characterization of two different FDH enzymes through screening of $NADP^+$ dependent formate dehydrogenase enzymes from natural sources *via* recombinant DNA techniques as promising candidates for industrial utilization.

# CHAPTER 2

# GENERAL INFORMATION

## 2.1 Biocatalysis

Biocatalysis has been applied in almost all types of biotransformations in the last few decades. The fine chemical and pharmaceutical research industries benefited biocatalysts greatly day by day. The development of a biocatalytic process in an economical manner highly depends on the accessibility of biocatalysts with high selectivity, stability, robust performance and activity. Advances in recombinant DNA technologies, bioinformatics, protein and strain engineering will promote the discovery and design of the new favorable enzymes with applications and also the soluble production of promising enzymes [20], [21], [22].

## 2.2 Chiral Compounds

In pharmaceutical, agricultural and other chemical industries chirality plays a key role. Chiral molecules cannot be superimposed on their mirror image, like right and left hands. Enantiomers are two non-superimposable mirror-image forms of chiral molecules. They are also called as optical isomers due to the optical activity features of chiral molecules. The levorotary (l-isomer) or dextrorotary (d-isomer) are two enantiomers of such compounds depending on whether they rotate polarized light in a left (-) or right (+) handed manner, respectively. The racemic mixture includes an equimolar mixture of the two enantiomers of a chiral compound. It has not any optical activity. The optical isomers have the same physical and chemical features, but they have differences in their optical activity. The body act as an efficient chiral molecule selector. When a racemic drug taken

into body, our metabolism uses different pathways to utilize each enantiomers and reveal different pharmacological activity. Therefore, one of these isomers may be active and produce the healing effect, while the other may be toxic or inactive [23]. Production of optically active compounds can be performed by separation racemic mixtures of enantiomers or by asymmetric synthesis. The synthesis of single enantiomers has become more and more crucial for the pharmaceutical synthesis. Single enantiomers can be obtained either by biocatalytic or chemical routes for preparation of drugs and their intermediates [24]. Conventional chemical methods are laborious, inefficient and time-consuming. In comparison with chemical catalysts, enzymes are considerably useful catalysts contributing much more competitive processes [25]. Since they include only L-amino acids and also their active sites constitute asymmetric environments which are likely to react distinctly with different enantiomers [26].

The substitution of chemical procedures with safer, cleaner and more eco-friendly biocatalytic procedures is required for global demand on green technologies [25]. Biocatalysis with numerous benefits over chemical synthesis is one of the best way to achieve Green Chemistry to obtain pharmaceutical intermediates [22] (Figure 2.1).

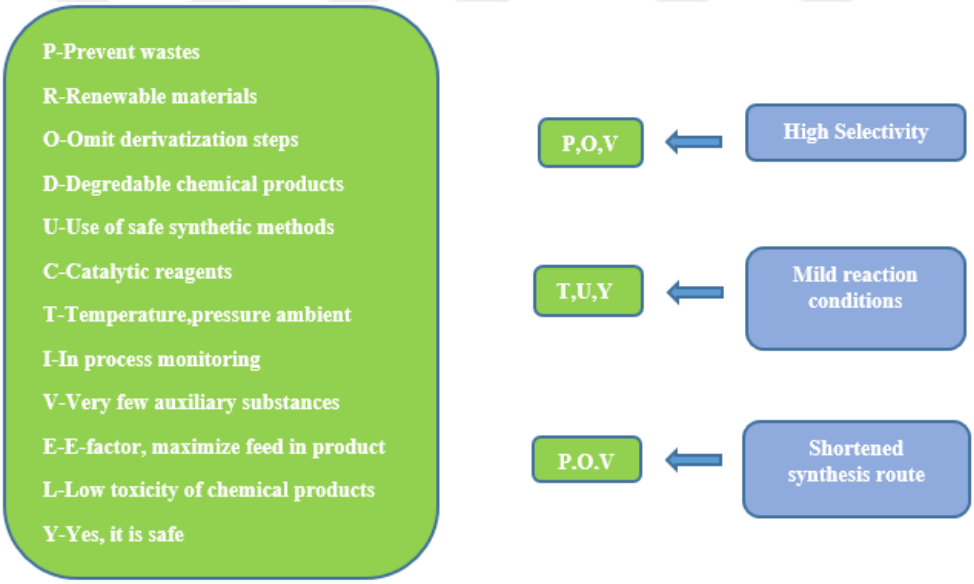



Figure 2.1 Principles of green chemistry and benefits of biocatalysis [22]

Since enzymatic processes generally provide a reduced amount of waste, process period and number of reaction steps, applications of enzymes to produce several types of materials have become an approved method in several industries particular in pharmaceutical industries [27]. In particular, utilization of enzymes is a significant route

of obtaining enantiomeric compounds *via* their high chemoselectivity, stereoselectivity and regioselectivity [28]. Their usage is less exposed to social examination and environmental regulations [29]. Enzymes are the most proficient biocatalysts, providing more competitive processes than the chemical catalysts and have a broad field of applications on the industrial scale [25], [30]. There are six major groups of enzymes based on their catalyzed reactions [31] (Table 2.1). Oxidoreductases, particularly dehydrogenases, can use nonchiral compounds to produce optically active intermediates with a high optical purity (99.9-99.99%) [9].

Table 2.1 Enzyme classes based on activities registered in BRENDA [31], [34]

| Enzyme Class | Examples | Reaction Catalyzed |
|---|---|---|
| **Oxidoreductases** | oxidase, oxygenase, dehydrogenase, peroxidase | oxidation or reduction |
| **Transferases** | Transaminase, glycosyltransferase, transaldolase | transfer of a group from one molecule to another |
| **Hydrolases** | esterase, nitrilase, nitrile hydratase, lipase, protease, glycosidase, phosphatase | hydrolysis reaction in $H_2O$ |
| **Lyases** | dehydratase, deoxyribose-phosphate aldolase decarboxylase | Nonhydrolytic bond cleavage |
| **Isomerases** | racemase, mutase | İntramolecular rearrangement |
| **Ligases** | DNA Ligase | Bond formation requiring triphosphate |

## 2.3 Oxidoreductases

As a large group of enzymes, oxidoreductases (EC.1.X.X.X) are remarkable biocatalysts for industrial utilization and can catalyze the electron transfer reactions. They constitute about one third of all enzymatic reactions defined in the BRaunschweig ENzyme Database, BRENDA (Figure 2.2). These enzymes can use a broad range of organic substrates including amines, ketones and alcohols and also inorganic substrates such as cations and anions. The water can also be used by them as a solvent which facilitates the transformations. Thus, oxidoreductases have various implementations particularly in

pharmaceutical industries, in production of several chemicals such as polymers, amino acids, fuels, nutraceuticals and cosmetics [32], [33], [34].

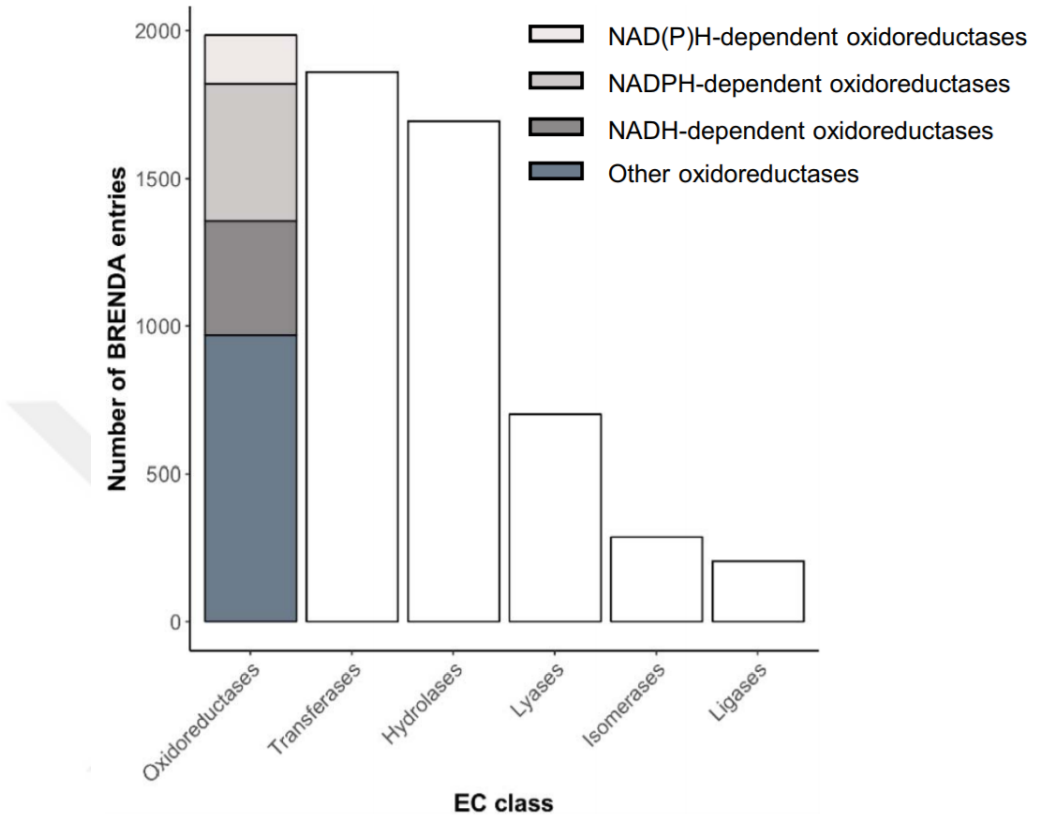



Figure 2.2 Distribution of enzymatic activities registered in BRENDA [34]

They generally require bound cofactors as prosthetic groups for their activity. These group is the permanent part of the enzyme. They can also use coenzymes. These molecules can be an external electron acceptors or donors and they are required in stoichiometric amounts for the biotransformation [35]. Oxidoreductases catalyze about 30% of all the BRENDA enzymatic reactions. Among them, approximately 50% use NADPH/$NADP^+$ and/or NADH/$NAD^+$ [34]. Nicotinamide adenine dinucleotide ($NAD^+$) and its phosphorylated equivalent, nicotinamide adenine dinucleotide phosphate ($NADP^+$), both in their reduced and oxidized forms, are typical coenzymes (Figure 2.3). These structures have two fragments; (i) the adenosine part, containing the the hydroxyl group ($NAD^+$) or phosphate group ($NADP^+$) in the 2'-position of the ribose. Which distinguishes two coenzymes, (ii) the nicotinamide part, accepting or donating a hydride group, which gives the coenzyme its electrochemical property [36].

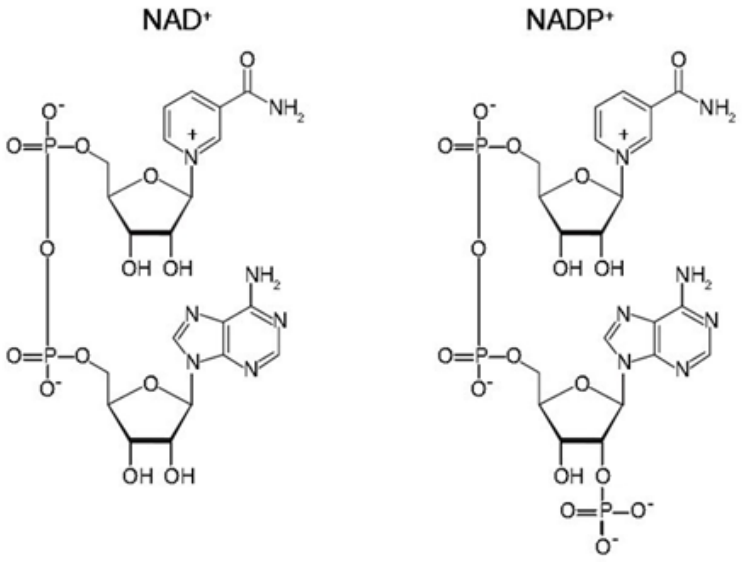



Figure 2.3 Nicotinamide adenine dinucleotides [37]

NAD(P)H dependent oxidoreductases are attractive enzymes in industrial manner since they can catalyze the critical reactions to obtain many hard-to-synthesize chemicals, under desirable conditions. For instance, there are various chemical routes for oxidization of primary alcohols, though mentioned methods generally laborious and can result in toxic products. The enzymatic catalysis can circumvent this difficulty. Moreover, NAD(P)H dependent oxidoreductases have some features which give them remarkable benefits for organic chemosynthesis, such as stereoselectivity, regioselectivity and also their suitability for redesign to have the desired kinetic parameters and substrate specificity [38].Hence, these enzymes have been utilized widely in metabolic engineering studies to produce valuable compounds [34]. Nevertheless, the high cost of cofactor is still an obstruction in biocatalysis applications [39]. The applications containing these enzymes is not feasible economically, due to high cost of NADH and particularly NADPH. To eliminate this problem, the recycling of $NAD(P)^+$/NAD(P)H is a viable alternative [9].

## 2.4 Cofactor Regeneration

The nicotinamide cofactors, electron carriers in oxidoreductions, are fundamental components of the cell. There is a recycling process in the aspect of cofactors, they are produced and regenerated [40]. However, the biosynthetic processes in industrial applications require reduced cofactors like NADH and NADPH [24]. The nicotinamide

cofactors, particularly in their reduced form, are quite expensive for being used in stoichiometric quantities. Methods for cofactor recycling have been grouped by Chenault and Whitesides [41] into various titles: electrochemical, biological, enzymatical, chemical and photochemical (Table 2.2).

To supply a constant source of enzymes and cofactors, whole-cell biocatalysts can be used. As known, whole-cells have their cofactor reserves, however during reaction cofactor deficiency can be a problem [40]. There are numerous studies for whole cell regeneration system. One of which demonstrated, coexpression the xylose reductase gene from *Candida tenuis* (*Ctxr*) and the formate dehydrogenase gene from *Candida boidinii* (*Cbofdh*) in the recombinant *E. coli* strain to produce ethyl-4 cyanobenzoyl formate [42] (Figure 2.4). Another example is coexpressing of *Cbofdh* and cyclohexanone monooxygenase gene (*chmo*) originated from *Acinetobacter calcoaceticus* NCIMB 9871 in *E. coli* BL21 (DE3). To synthesize chiral phenyl methyl sulfoxide (PMSO), this coexpression system was utilized as a wholecell biocatalyst [43]. In addition, an *in vivo* system was designed for the transformation of D-fructose into D-mannitol *via* the production of the mannitol dehydrogenase (MDH) in *Bacillus megaterium*. The cofactor for MDH activity were recycled *via* coexpression of the gene *fdh* encoding *Mycobacterium vaccae* N10 FDH [44].

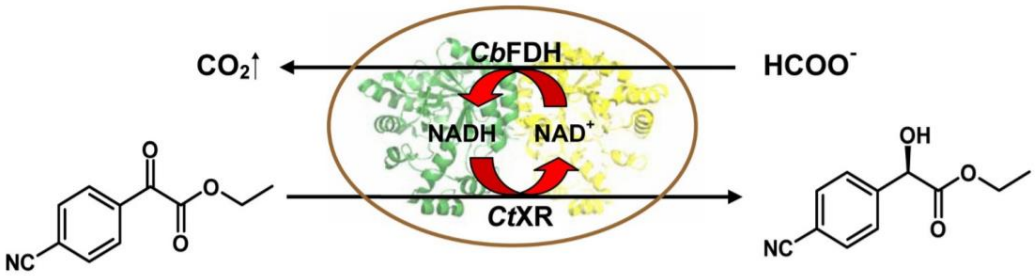



Figure 2.4 Whole-cell biocatalytic reduction *via* coexpressing *Ct*XR and *Cbo*FDH [42]

Table 2.2 Cofactor regeneration routes [41]

| Strategy | Advantages | Disadvantages |
|---|---|---|
| **Biological-Microbiological** | Cheap, inexpensive recycling reagents<br>Great selectivity | Relatively primitive state of development<br>Complicated product isolation<br>Limited stability<br>Low enantiomeric purity<br>Controlling the enzyme activity |
| **Enzymatic:**<br>**Substrate-coupled**<br>**Enzyme-coupled** | High selectivity, especially for NAD(P) to NAD(P)H<br>Compatibility with enzyme-catalysed synthesis<br>High rates for some systems<br>Easy monitoring of reaction progress | The cost of enzyme<br>Immobilization in some cases<br>Complexity of product isolation<br>Low rates |
| **Electrochemical** | Low cost of electricity<br>No stoichiometric regenerating reagent<br>Readily conrolled redox potential<br>Easy product isolation<br>Easy monitoring of reaction progress | Incompatibility with many biochemical systems<br>Poor selectivity (especially for reductive regeneration)<br>Complex apparatus and procedures |
| **Chemical** | Generally inexpensive and commercially available reagents<br>No requirement for added enzymes<br>High redox potentials | Limited compatibility with biochemical systems<br>Complexity of product isolation in some cases<br>Low product yields |
| **Photochemical** | No stoichiometric regenerating reagent in some systems<br>No requirement for added enzymes | Limited compatibility with biochemical systems<br>Limited stability<br>Requirement for photosensitizers and redox dyes |

The systems that utilize the isolated enzymes to perform biosynthetic catalysis should include another reaction mechanism for the cofactor regeneration [40]. Coupling another

oxidoreductase to the system that recycles the cofactor at the cost of a inexpensive substrate is a general strategy [16].

The enzymatic mechanisms that regenerate cofactors *via* utilization of $NAD(P)^+$ dependent enzymes have been investigated *via* a number of studies such as *in vitro* systems utilizing glucose-6-phosphate dehydrogenases [45], alcohol dehydrogenases [46], [47], formate dehydrogenases [6], [47] and phosphite dehydrogenases [48], [49] or pyridine nucleotide transhydrogenases [50], [51]. Each recycling processes have its own advantages and disadvantages. The strategy of preference usually depends on the stability of the enzymes in organic solvents and the effect of substrate and product on the enzyme activity [52]. Formate dehydrogenase (FDH) and Glucose dehydrogenase (GDH) are widely used coenzyme-regeneration systems for NADH regeneration. The cofactor recycling systems including GDH have some benefits, such as great specific activity and affinity for both cofactors. However, in this reaction glucose is used and gluconic acid is produced as a waste product, which is environmentally unfriendly and interferes with purification. In comparison with GDH, FDH requires a cheap substrate, formate, and oxidizes it to a volatile compounds ($CO_2$). Therefore, no waste and byproduct is produced [53], [54]. Currently, the most profitable method is the utilization of FDH for NADH regeneration in either cases in which purified enzymes are used or whole cells when conditions are favorable [52]. FDHs can be used efficiently, because of the irreversible reaction, broad pH optimum (pH 6–9) [6] and environment-friendly process [55]. In addition, the reaction substrate is cheap and the by-product ($CO_2$) is volatile, inert and does not inhibit the productivity and activity of enzyme. Due to its easily removal from the reaction system, there is not any interference for the purification of the product [16]. The most typical instance of the industrial application of formate dehydrogenase as a cofactor recycler in the large scale production of tert-L-leucine by the company Evonik [56]. In this process, leucine dehydrogenase is used as main enzyme, NADH as an electron carrier and the formate dehydrogenase as a regenerator enzyme and then, L-*tert*-leucine is produced from trimethyl pyruvate (Figure 2.5 ) [57].

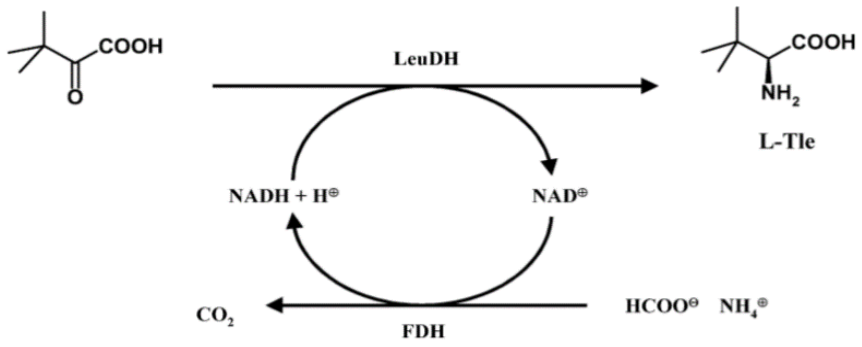



Figure 2.5 Reaction mechanism for L-*tert*-leucine (L-Tle) production [57]

In the pharmaceutical field, it can be utilized successfully for the enzymatic production of various chiral molecules, such as L-lactic acid [58], aromatic alpha-keto esters [42], 6-hydroxybispiron (the main metabolite of Buspiron, a drug used in the treatment of anxiety and depression) and (S) -N-boc-adamantane glycin (a remarkable compound required for the synthesis of Saxagliptin, type 2 diabetes mellitus drug) [59], [60].

## 2.5 Formate Dehydrogenase (FDH)

Formate dehydrogenase (FDH, EC 1.17.1.9) is a group of enzyme that plays an important role for its sources and also it is an attractive enzyme for recycling of reduced cofactor in the chiral synthesis reactions [6]. This enzyme belongs to the superfamily of D-isomer specific 2-hydroxyacid dehydrogenases [61]. FDH oxidizes formate into $CO_2$ and reduces cofactor simultaneously. Moreover, it can act on the conversion of $CO_2$ into formate in convenient conditions (Figure 2.6). Therefore, it can be said that FDHs are significant enzymes not only in recycling of coenzyme but also in $CO_2$ sequestration. Formate dehydrogenases are found in almost all domains of life such as archaea, bacteria, fungi, yeasts and plants [62], FDHs display a large diversity in substrate specificity, cellular localization, quaternary structures, presence of prosthetic groups and different metal ions (molybdenum, tungsten) [63], [64].

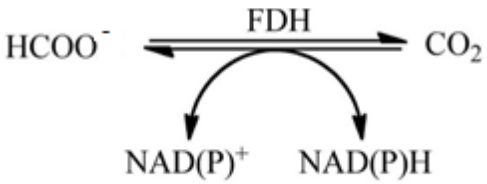



Figure 2.6 The reaction catalyzed by formate dehydrogenase [65]

Based on the differences in their structure there are three FDH enzyme groups. The first group is called $NAD(P)^+$ independent/metal including formate dehydrogenases which is found in anaerobic microorganisms and archae. These FDHs have heterooligomers with a complex quaternary structure. They are usually characterized with their iron sulphur clusters, molybdenum and tungsten ions in their active site as their prosthetic groups. Being sensitive to oxygen and having high molecular weight are the other feature of the FDHs [66]. The second group includes $NAD(P)^+$ dependent and metal containing formate dehydrogenases and the third one is $NAD(P)^+$ dependent/metal independent FDHs [62]. The latter FDHs contain no prosthetic groups or metal ions in their active region and have a high specificity towards both substrates. These FDHs can be found in bacteria, yeast and plants, and have a homodimer structure consisting of two identical subunits, each composed of 360–400 residues with a molecular weight in the range of 35-50 kDa [61], [67]. Each subunit of enzyme contains of two domains: the peripheral catalytic domain and the internal coenzyme binding domain. Each domain has the same Rossmann-fold topology and high structural homology. Two domains of enzyme separated by deep cleft, and the active site is localized in this cleft and accepts cofactor to do transition state of enzyme. The active region is also in contact to the solvent *via* a wide and long substrate channel [14], [68]. FDH can exist in so-called 'open' and 'closed' forms like many other $NAD^+$ dependent dehydrogenases. The transition from open to the closed form is fundamental for catalysis [69].

The transfer of a hydride ion directly from formate to the C4 atom of the nicotinamide ring of $NAD^+$ is the molecular mechanism of FDH [61]. Thus, for investigating the mechanism of hydride transfer in the active region of $NAD^+$ dependent dehydrogenases, FDHs can be analyzed as a model enzyme [66].

The cellular localization of FDHs depends on their functions. The FDHs that reduces the $CO_2$ are located in cytoplasm. They are hosted in symbionts, acetogens and other fermentative organisms [70]. The FDHs in methanogens located in cytoplasm and use formate as an energy source, which is transformed into $CO_2$ to be used in the methanogenic route [71]. The FDHs from bacteria, yeast and fungi are also cytoplasmic. In plant cells, the enzyme is expressed in cytoplasm then it is localized in mitochondria. Plant FDH genes have a special sequence at the beginning of the *fdh* gene. A signal peptide is encoded by this sequence and it is responsible for the transfer of enzyme from cytoplasm to mitochondria. In plants and pathogenic microorganisms, FDHs perform as

stress proteins [72]. During various stress inducers such as thermal discontinuity, drought, heavy metal, hypoxia and pathogen infection, the expression level of FDH in plants increases [2], [73], [74].

### 2.5.1 Other Applications of FDH

Beside its beneficial utilization in cofactor regeneration, FDHs also have a number of significant practical applications.

#### 2.5.1.1 Diagnosis of Methanol Poisoning

Methanol has a weak odor, no color and is a volatile liquid, which is found in de-icers, paints, varnishes, wood stains, paint thinners and cleaning products [75]. Methanol has a relatively low intrinsic toxicity, however, it is transformed to highly toxic compounds *in vivo*. These products can cause coma, blindness and metabolic disturbances that can result in death [76]. For treatment of methanol poisoning, early diagnosis is crucial. The detection of methanol generally needs a gas chromatographic method and it is not found in most hospitals. The calculation of the osmolal and anion gap can be used for indirect detection of methanol. Due to low concentrations and the sensitivity, this indirect method is not reliable. Another way of determining methanol poisoning is direct measurement of formate in serum [77]. Alcohol dehydrogenase oxidizes the methanol to formaldehyde in the liver. Then, formaldehyde dehydrogenase convert the formaldehyde to formic acid [78]. Therefore, formate can be detected in any biological sample such as plasma, serum, urine, or whole blood. In the presence of FDH, formic acid is oxidized and $NAD^+$ is reduced. The quantity of reduced cofactor is measured at 340 nm and a measurement can be performed for the formic acid quantity in sample [79] Formate analysis by means of formate dehydrogenase is highly sensitive and specific [80]. Detection of formate ion by FDH in the diagnosis of methanol poisoning is an enzymatic method applied in most routine biochemistry laboratories.

#### 2.5.1.2 Diagnosis of Nephrolithiasis

The most common type of kidney stone diseases is nephrolithiasis (oxalate urolithiasis). Oxalate partially comes from food and largely as a metabolic byproduct from various intermediates produced in the liver. Oxalate concentrations in urine and plasma can be changed by oxalate absorption and excretion or its metabolic routes affected by various

food intake. The removal of oxalate is frequently done by kidneys and partially *via* intestinal excretion. After reaching certain conditions, oxalate can precipitate in kidneys and the formation of stones is initiated [81]. Detection of the urinary oxalate can be done in different ways such as chemical, physical and enzymatic methods. Because of the specificity of enzymes and the beneficial usage of them, the enzymatic assays are preferred to non-specific ones. The oxalate decarboxylase and oxalate oxidase can be utilized for the detection of oxalate in urine. When oxalate decarboxylase was used, oxalate is firstly converted to the formate, then it is oxidized by FDH in the presence of $NAD^+$. Oxalate analysis is performed by measuring the absorbance of the NADH which is stoichiometrically increased by the oxidation of the formate at 340 nm. This method is preferred because the activity of oxalate decarboxylase and FDH enzymes is not inhibited by the substances in the urine, and a large number of samples can be automatically run [82].

#### 2.5.1.3 Diagnosis of *Trichomonas vaginalis*

*Trichomonas vaginalis* is a sexually transferred protozoan parasite which causes vaginitis in women. It is not a part of the flora of the genitourinary tract, therefore, it is considered as an invasive pathogen. A common symptom related with trichomonas caused vaginitis is a profuse frothy discharge. Due to the low cost of and ease of microscopic method which can be done on fresh vaginal specimens, it has been widely used to detect the motile trichomonads. However, the accuracy of microscopy is weak, since accuracy depends upon presence of motile trichomonads. Non-motile trichomonads are not discernible. In addition, immunological approaches for diagnosis have been reported, but the extent and nature of the antigenic heterogeneity of *Trichomonas vaginalis* isolates has caused slow progress. Another method is enzymatic method based upon formate production. Trichomonads grown on culture media produce formic acid in large quantities and is thought to give rise to strong inflammatory responses observed in the vaginal mucosa. It can be determined by a simple chromogenic detection of formate in vaginal sample. The technique includes the mixture of a vaginal fluid sample, formate dehydrogenase, the $NAD^+$ as an electron carrier. The chromogenic indicator produces a color change in the presence of NADH. The increased levels of formate in vaginal fluid is related with *Trichomonas vaginitis* in patients. This method is fast, simple and doesn't require intact cells and also the activity of the FDH is not affected by other materials in the sample [83].

#### 2.5.1.4 Sequestration of Greenhouse Gases

To recycle of carbon dioxide into valuable compounds such as fuels and remarkable chemicals, the photochemical, electrochemical, chemical and enzymatic methods can be applied. The enzymatic method is significant for $CO_2$ reduction due to their peculiar characteristics such as high selectivity, specificity and mild reaction conditions. The reduction of $CO_2$ into formate enzymatically could be performed by FDH and the product could be used for many purposes such as in preservation of silages, animal feed additives [84] and in paper/pulp production [85] and also fuel for low temperature fuel cells [86]. The tungsten including FDH from *Syntrophobacter fumaroxidans* has been used to convert $CO_2$ into formate as the most active catalyst [87]. In addition, FDH from *Pseudomonas oxalaticus* can be utilized to reduce $CO_2$ by aid of methyl viologen. However, these $NAD^+$ independent FDH enzymes are highly sensitive to $O_2$. In the presence of $O_2$, they are inactive and quite unstable. Therefore, Kim et al. [88] studied with the $NAD^+$ dependent FDH from *Candida boidinii* (*Cbo*FDH), due to its almost 100% selectivity and high stability for industrial utilization. The conversion rate can be enhanced within the electrochemical NADH regeneration reaction conditions [88]. Hence, stable FDHs should be found for an electroenzymatic technique.

Beside these remarkable applications, particularly due to its significance in the pharmaceutical industry as an NADH recycling catalyst, the identification, modification and implementation studies on FDH have always been a hot topic. Among FDH sources, especially bacterial FDHs have benefits over FDHs from other organisms in practical biotransformations due to their activity and stability [6].

# CHAPTER 3

# MATERIAL METHOD

## 3.1 Material

The pET14b and pET22b(+) used for cloning procedure were supplied by Novagen (Darmstadt, Germany) and pET23b was provided by Nova Lifetech (Mongkok Ki, Hong Kong). Restriction enzymes and 2X Tag Master Mix™ were obtained from New England BioLabs (NEB, GmbH, Germany) and T4 DNA ligase was from Fermentas. The Prime STAR™ HS DNA Polymerase kit was purchased from Takara (Japan). *E. coli* strains TOP 10 and BL21(DE3) utilized as a host for cloning and expression, respectively (Invitrogen). IPTG (isopropyl-β-d thiogalacto pyranoside) was supplied from Qiagen (ATQ Biotechnology, TR). Coomassie brilliant blue R-250, PMSF (phenylmethylsulfonyl fluoride), SDS (sodium dodecyl sulphate) were supplied by Sigma Aldrich. Nicotinamide cofactors ($NAD^+$ and $NADP^+$) were obtained from Roche Applied Science. Peptone, agar, glucose, lactose, acrylamide, bis-acrylamide, hydrochloric acid, glycerin, tetramethylethylenediamine (TEMED), fructose, sodium citrate, sodium phosphate monobasic from Merck, sodium phosphate dibasic, citric acid from Riedel de Haen. Bradford reagent, agarose and sodium dodecyl sulfate, proteinase K, sodium chloride, potassium dihydrogen phosphate were purchased from Sigma. Other reagents were obtained from several companies in analytical grade.

## 3.2 Mining Protein Sequences for $NADP^+$ Dependent FDHs

The Protein Blast (blastp) / Pattern-Hit Initiated BLAST (PHIBLAST) tool [89] in GenBank (hosted in NCBI- National Centre for Biotechnology Information) was used for pattern based screening of protein sequences. Due to our aim, the $NADP^+$ dependent

protein sequences should be used as a query sequence. Therefore, the protein sequence of an $NADP^+$ dependent FDH from *Burkholderia stabilis* (BstFDH; ACF35003.1) was utilized as a query sequence to obtain new $NADP^+$ dependent FDHs from PHIBLAST. An alignment of protein sequences resulted from PHIBLAST search was carried out by using Constraint Based Multiple Alignment Tool (COBALT) [90]. As output of this search, two microorganisms were obtained to work on. One of them was *Burkholderia dolosa* PC543 and the other one was as *Lactobacillus buchneri* NRRL B-30929 isolated from an ethanol treatment plant.

## 3.3 Cloning, Expression and Purification of N-terminus His Tagged FDH from *Burkholderia dolosa* PC543

### 3.3.1 N-Terminus His Tag Primer Design and Polymerase Chain Reaction (PCR)

The genome of *Burkholderia dolosa* PC543 was sequenced by Workentine et al. [91] and shared in GenBank (NCBI accession no. NZ_AWRY00000000). The genomic DNA of this strain was kindly provided by Dr. Steve Bernier from McMaster University, Canada. The FDH coding region from the *Burkholderia dolosa* PC543 genomic DNA was used as a template for PCR reaction using the following primers; FP1 (5'-CGGTGTCCATATGGCGAAAGTGCTTTGCG-3') and RP1 (5'CGCTGGATCCCTACGTCAGGCTGTACG-3'). These primers contain *Nde*I and *BamH*I restriction sites at their 5'end to facilitate cloning process. The PCR reaction included 2X Taq Master Mix™ (1X), reverse and forward primers (1.6 pmol/µL), genomic DNA (3.2 ng/µl) and distilled water (15 µL) in a final volume of 50 µL. The PCR steps include and initial denaturation for 5 min at 95 ˚C and then 29 cycles of amplification (95 ˚C, 1 min; 52 ˚C, 1 min; 72 ˚C, 1.5 min) followed by a final extension at 72 ˚C for 10 min. The post PCR product was mixed with 10 µl of 6X loading buffer. The product was loaded onto 0.8% agarose gel with the marker DNA and electrophoresis was conducted for 10 min at 30 V and then for 50-55 min at 120 V. The PCR product was recovered from the agarose gel by using the QIAquick Gel Extraction Kit (QIAGEN). The purified DNA was stored at -20 ºC for restriction procedure.

### 3.3.2 Cloning of Bdfdh Gene into pET14b

#### 3.3.2.1 Isolation of Cloning Vector (pET14b)

The pET14b cloning vector was obtained by digestion of recombinant plasmid DNA, pET14b-Ss-Ntr. This plasmid was transferred into *E. coli* Top10 competent cells. In the transformation process, 5 µl of plasmid was mixed with 50 µl of competent cells which thawed on ice. Then, the mixture was incubated at 42 °C for 50 seconds and followed by 5 min incubation on ice. Under sterile conditions, 250 µL of SOC (Super Optimal broth with Catabolite repression) reagent was put into the mixture and incubated at 37 °C in a shaker at 230 rpm for 60 min. 15-30 µl of the transformation mixture was spreaded on LB-agar plate including 100 µg/mL ampicillin and incubated for 16 hours at 37 °C. LB-agar / Amp plates was used for isolation of pET14b-Ss-Ntr plasmid from *E. coli* Top10 cells. A selected colony was inoculated into 5 mL of LB / Amp liquid medium and allowed to grow for 16-17 hours at 37 ° C. The plasmid isolation kit (QIAGEN, QIAprep Spin Miniprep Kit, Germany) was used for the plasmid isolation. The 5 µl of plasmid DNA was run on the gel for quantification. Then, the plasmid DNA was stored at -20ºC for restriction reaction.

#### 3.3.2.2 Restriction Reactions of PCR product and pET14b-Ss_Ntr Plasmid DNA

The reaction volume was 120 µl for PCR product restriction with *Nde*I and *BamH*I and the reaction included following components; PCR product (100 µl, ~26 ng / µl), reaction buffer (12 µl, 10 × NEB Buffer 4), BSA (4 µl, 30X), *Nde*I (2 µl, 20,000 U / mL, NEB) and *BamH*I (2 µl, 20,000 U / mL, NEB). The reaction was incubated at 37 ° C for 2 h. The plasmid was also restricted with the same enzymes. The restriction reaction volume was 60 µl. Reaction components were; plasmid DNA (35 µl, ~ 32 ng / µl), reaction buffer (12 µl, 10X NEB Buffer 4), BSA (4 µl, 30X), *Nde*I (2 µl, 20,000 U / mL, NEB), *BamH*I (2 µl, 20,000 U / mL, NEB) and 13 µl distilled water. The reaction was incubated for 2 hours at 37 ° C. Restriction reaction products were run on the gel. DNA was recovered from gel as previously described method. The DNA quantification was performed *via* NanoDrop spectrophotometer. Then, the DNA was stored at -20 ºC for ligation.

#### 3.3.2.3 Ligation Reaction of Bdfdh Gene and pET14b Vector

The reaction volume was 20 µl. It included restricted PCR product (2.85 µl, 13.1 ng / µl), restricted cloning vector (5,05 µl, ~9,9 ng / µl), T4 DNA ligase (1 µl, 200 CEU / µl, Fermentas), T4 DNA ligase reaction buffer (2 µl, 10 ×) and distilled water (9,1 µl). The mixture was incubated at 16 ° C for overnight. Then, 5 µl of the ligation mixture was transferred into ultra-competent cells as described above (Section 3.3.2.1). The mixture was spreaded onto agar plates containing 100 µg/mL amp and incubated for 18-21 hours at 37 ° C.

#### 3.3.2.4 Selection and Characterization of Recombinant *E. coli* Colonies

To test whether recombinant plasmids were obtained or not, the colony PCR reaction was carried out. 25 µl colony PCR reactions were set up for 3 different ligation colonies and the colonies were tested for recombinant plasmid. These reactions were the same with optimized PCR reaction as mentioned in section 3.3.1 except for DNA source. The ligation colonies were used as DNA source. In addition, to make a double check the insert, the purified recombinant plasmids were digested with restriction endonucleases. In restriction reactions, 10 µl of the recombinant plasmid and the control plasmid (pET14b-Ss-Ntr) were used. Total reaction volumes were 20 µl. Reaction components of *Nde*I-*BamH*I restriction reaction were; reaction buffer (2 µl, Buffer 4 (10X), NEB), *Nde*I (1 µl, 20,000 U / mL, NEB), *BamH*I (1 µl, 20,000 U / mL, NEB) and 5 µl of distilled water. In the single restriction reaction with *Nde*I, the reaction components were; reaction buffer (2 µl, Buffer 4 (10 X), NEB), *Nde*I (1 µl, 20,000 U / mL, NEB) and 6.5 µl of distilled water. The same restriction reactions were performed with control plasmid. The comparison of the sizes of restriction reaction products were checked in agarose gel to assess ligation reaction.

### 3.3.3 Expression and Purification of BdFDH

#### 3.3.3.1 Production of Recombinant Enzyme *via* IPTG Induction

The recombinant construct was used to obtain N-terminal His tagged enzyme. Therefore, it is transferred into the *E. coli* BL21 (DE3) for overexpression of protein and spreaded on agar plate including ampicillin. In addition, as a control group, the plasmid pET14b was transferred to the same competent cells. Then, a colony from plates was inoculated

into LB liquid medium including ampicillin (100 μg/mL) at 37 ˚C with agitation for overnight. Then, this pre-culture was used for the inoculation of LB medium containing 100 mg/mL ampicillin and expression was induced *via* IPTG (with 0.5 mM IPTG at 37 ˚C and $OD_{600}$: 0.6-0.8). This induction was performed at various temperatures (30 ˚C, ~22 ˚C and 16 ˚C) with agitating at 180 rpm for 6-8 h to get active and soluble enzyme. Aliquots were withdrawn at certain times in various temperatures and loaded onto the SDS-PAGE.

#### 3.3.3.2 Purification of Recombinant Enzyme *via* Autoinduction

The autoinduction procedure modified from Studier [92] was used. This medium with recombinant strain was incubated at 16 ˚C with agitation for 16 h. Then, the cells were harvested and stored at 4 ° C for lysis. In addition, autoinduction was repeated at 37 ˚C for 8 h and followed by 8 h at 16 ˚C for monitoring the protein expression. The expression was also repeated for 20 hours of autoinduction to make the time optimization.

#### 3.3.3.3 Purification of N-Terminus His Tagged FDH Using Ni-Affinity Column

After expression, the autoinduced cells were centrifuged at 5800 rpm and 4 °C for 10 minutes. The resulted pellet was suspended on ice in the lysis buffer including 4 mL of chilled buffer A (20 mM Tris/Cl, 0.5 M NaCl, 5 mM imidazole, pH 7.8), 8 μl of 0.1 M PMSF and 80 μl of lysozyme enzyme per gram pellet for 30 min. Cell lysate were disrupted by sonication (15 sec burst, 45 sec interval). The lysate was centrifuged at 11800 rpm and 4 ° C for 30 min. Before loading supernatant onto column, the resin column was regenerated. To remove nickel ion and regenerate the column following solvents were used respectively, in 10 column volumes; Buffer B (50 mM EDTA, 0.5 M NaCl, 20 mM sodium phosphate buffer pH 7.4), 1.5 M NaCl solution, 1 M NaOH solution, 30% isopropanol (washing with 10 column volume distilled water between each step). In the last step, 0.5 M $NiSO_4$ solution were passed through and then distilled water was used for column washing. Finally, the equilibration buffer (20 mM Tris/HCl, 0.5 M NaCl, pH 7.8) was passed through the column and the supernatant was poured onto a 0.5 mL Nickel HiTrap™ column. The column was washed with buffer A for several times to get rid of unbound fraction. The undesired proteins were then discarded by using with 5 column volumes of 30 mM and 100 mM imidazole in buffer A (20 mM Tris/HCI, 0.5 M NaCI, pH 7.8) before elution of the recombinant *Bd*FDH by Buffer A with 400 mM

imidazole. Subsequently, active fractions were collected and the buffer of the purified proteins was replaced with 100 mM sodium phosphate, pH 7.0 *via* a column for desalting (Amersham Biosciences). In addition, protein expression and purification steps were determined by SDS-PAGE electrophoresis.

## 3.4 Cloning, Expression and Characterization of BdFDH into C-Terminus His Tagged Form

### 3.4.1 C-Terminus His Tag Primer Design and the fdh Gene Amplification *via* PCR

The *fdh* gene was obtained from genomic DNA by the following primers for C-terminus his tagged cloning. FP2 (5'-CGGTGTC**CATATG**GCGAAAGTGCTTTGCG-3') and RP2 (5'-ATAAAT **GCGGCCGC**CGACGTCAGGCTGTACGACGC-3'). The recognition sites for *Nde*I and *Not*I were inserted into the primers and underlined. The final concentration of components in PCR reaction were; 2X Taq Master Mix™ (1X), primers (1.6 pmol/µL), genomic DNA (1.25 ng/µl) in a reaction volume of 50 µL. The PCR program consisted of folllowing steps; initial denaturation step for 5 min at 95 ˚C, 29 cycles of amplification (95 ˚C, 1 min; 55 ˚C, 1 min; 72 ˚C, 1.5 min) and a final extension at 72 ˚C for 10 min. The PCR reaction products were electrophoresed as aforementioned in section 3.3.1. The PCR product was recovered from the gel and stored at -20 ºC for restriction procedure.

### 3.4.2 Cloning of Bdfdh into pET22b

#### 3.4.2.1 Isolation of Cloning Vector (pET22b) and Restriction Reactions of PCR Product and Plasmid DNA

The pET22b cloning vector was obtained by digestion of recombinant plasmid DNA, pET22b-X. This plasmid was transferred to *E. coli* Top10 cells as aforementioned in section 3.3.2.1. Then, the plasmid was isolated by using the plasmid isolation kit and electrophoresed for quantification. The plasmid DNA was stored at -20 ºC for restriction reaction. The pET22b (+) plasmid and PCR product were restricted with *Nde*I/*Not*I enzymes. The reaction volume was 105 µl for PCR product restriction with *Nde*I and *Not*I and the reaction included following components; PCR product (74 µl, ~25 ng / µl), Tango buffer (21 µl, 10X, Fermentas), BSA (3,675 µl, 30X), *Nde*I (2 µl, 20,000 U / mL, NEB) and *Not*I (2 µl, 10 U / µl, Fermentas) and 2,325 µl distilled water. The reaction mixture

was incubated at 37 °C for 2 h. The recombinant construct (74 µl, ~31 ng/µl) was also restricted with the same enzymes in the same reaction conditions. Restriction reaction products were exposed to electrophoresis and resulted DNA was stored at -20ºC for ligation.

#### 3.4.2.2 Ligation Reaction of Bdfdh Gene and pET22b Vector

The ligation reaction included restricted PCR product (1.59 µl, 20.22 ng/µl), restricted cloning vector (0.64 µl, ~77.58 ng/µl), T4 DNA ligase (2 µl, 200 CEU / µl, Fermentas), T4 DNA ligase buffer (2 µl, 10 X) and distilled water (13.77 µl). The mixture was incubated at 16 ° C for overnight. Then, the transformation and incubation were performed as described above (Section 3.3.2.3.). To test whether recombinant plasmids were obtained or not, the colony PCR reaction was carried out with 2 of ligation colonies as mentioned above (section 3.3.2.4). Then, the recombinant plasmid was purified from transformants and the desired gene was sequenced on each strands by MEDSANTEK company (Ankara, Turkey) to ensure the identity of sequence. The T7 terminator and T7 promotor primers were used for DNA sequencing procedure. The results were analysed by performing the BioEdit software packages (Ibis Therapeutics, CA).

### 3.4.3 Expression and Purification of BdFDH

#### 3.4.3.1 Production of C-Terminus His Tagged Recombinant Enzyme *via* IPTG Induction and Autoinduction

The recombinant construct was used to get C-terminal His Tagged enzyme. This construct was transferred into *E. coli* BL21 (DE3) for FDH overexpression and and the product was spreaded on agar containing ampicillin. In addition, as a control group, the plasmid pET22b was transferred to the same competent cells. Then, a colony from plates was inoculated in LB medium including ampicillin at 37 ˚C with agitation for 16 hours. Then, 1 mL of the starter culture was utilized for the induction of 50 mL of LB medium containing 100 mg/mL ampicillin in a 100 mL baffled flask and approximately after 3-4 hours, the expression of protein was induced *via* IPTG induction at the aforementined concentration. The induction was performed at 30 ˚C, with agitation at 180 rpm for 6 h. The induced cells were harvested and the protein expression profile was monitored by

SDS-PAGE. The autoinduction was also performed with recombinant strain at 30 ˚C and 180 rpm for 16 h. Finally, the cells were harvested and stored at 4 °C for lysis.

#### 3.4.3.2 SDS/Native-PAGE Analysis and Determination of Protein Concentration

All protein purification step were performed as indicated in section 3.3.3.3. The purity of the recombinant FDH was visualised on 12% SDS–PAGE carried out on Mini-PROTEAN II electrophoresis cell system (Bio-Rad). Native-PAGE was performed to estimate the overall molecular mass of the enzyme and to estimate its quaternary structure. The obtained protein concentrations were detected with the Bradford protein quantification assay [93] by using bovine serum albumin (BSA) as a reference protein. Protein standards were prepared at different dilutions (0.1 mg/mL to 1 mg/mL) and 10 µl of standards and samples were placed into wells separately, then, 200 µl of the Bradford solution were added to wells, mixed carefully and incubated at least 5 minutes at room temperature, finally, the plate was used for the measurement of absorbance at 595 nm.

### 3.4.4 Determination of Protein Mass by MALDI-TOF Analysis

The MALDI-TOF MS using MicroFlex instruments (Bruker Daltonics, Billerica, MA) was used for mass spectrometry of the *Bd*FDH. The calibration was performed with the Bruker's protein standards II kit containing different protein fractions such as cytochrome c (12,360 Da), myoglobin (16,952 Da), trypsinogen (23,982 Da), protein A (44,613 Da) and bovine serum albumin (BSA, 66,527 Da).

### 3.4.5 Determination of Recombinant BdFDH Properties

#### 3.4.5.1 Ionic Strength Effect on BdFDH Enzyme

The concentration of the reagents in the reaction performed to examine the ionic strength effect on the *Bd*FDH were; 8 µg/mL *Bd*FDH, 100 µM $NADP^+$ and 42.5 mM sodium formate with different sodium phosphate buffer concentrations. The buffer concentrations used are between 20-1000 mM (pH 6.2). The reaction was performed at 30 ° C in a quartz cuvette using UV spectrophotometer. The increment of reduced cofactor (NADPH) in the reaction was followed at 340 nm.

### 3.4.5.2 The Effect of pH and Temperature on BdFDH Enzyme

The acetic acid-sodium acetate buffer ($pK_2$, 50 mM, pH 3.8–5.8), citric acid–sodium citrate buffer ($pK_2$, 50 mM, pH 5.4-6.4), sodium phosphate buffer ($pK_2$, 50 mM, pH 6.2–8.0) Tris/HCl buffer (50 mM, pH 7.5–9.0) and ethanolamine buffer (50 mM, pH 8.5–10.5) were used for investigating of the pH profile of enzyme. The enzymatic assay was performed in the presence of $NADP^+$ at 30 °C. In addition, the pH range of enzyme was determined with the sodium phosphate buffer and citric acid-sodium citrate buffer in terms of each coenzymes at 37 °C. Specific activity results were detected in these buffers by using 20 µg/mL *Bd*FDH, 170 mM sodium formate and 100 µM $NAD(P)^+$ at final concentrations. In a standard reaction, the buffer including formate (680 µl) was added to on enzyme (40 µl) and the incubation was done for 5 min. By the addition of $NAD(P)^+$ (80 µl), the reaction was started and followed spectrophotometrically at 340 nm by using UV–vis spectrophotometer for 90 sec. The initial rates of reaction were calculated by using molar extinction coefficient of 6.22 $mM^{-1}$ $cm^{-1}$ for reduced NAD(P)H [94] and the values were given as a percentage expressions of the highest activity obtained at 37 °C.

The optimum temperature of enzyme was detected by assaying the enzymatic reactions between 15-60 °C. Activities were detected in 100 mM sodium phosphate buffer (pH 6.2). In a typical reaction, the buffer including formate (680 µl) and enzyme sample (40 µl, 2 µg/mL) were incubated at certain temperatures for 3 min. The $NAD(P)^+$ (1 mM) was used for initiation of the reaction. The reduced cofactor was visualised at 340 nm for about 2 min. The initial rates of reduced coenzyme increment were calculated as measured above. The temperature in UV-Vis spectrophotometer was fixed by using a circulating water bath equipment.

The thermostability of enzyme was also determined. 75 mM sodium phosphate buffer (pH 6.2) was used for pre-incubation of protein aliquotes (0.4 mg/mL, without glycerol) at 37, 45, 60 °C for 0-60 min. After incubation at certain time intervals (1, 5, 10, 20, 40, 60 min), the aliquotes of protein samples were taken and cooled on ice. The residual activity was calculated at 37 °C by using the standard assay with $NADP^+$ in a microplate reader and expressed as a percentage of the activity of control reaction performed without heat assay.

#### 3.4.5.3 Effects of Metallic Compounds and Organic Solvents on BdFDH

To find out the effects of cations on *Bd*FDH activity, the enzyme was incubated with several metal compounds ($ZnCl_2$, $MgSO_4$, $MnCl_2$, $CaCl_2$, $NiSO_4$, $FeCl_2$, $FeCl_3$, $CuSO_4$) at final concentrations, 1 mM and 10 mM. The final concentrations of reaction components were; 170 mM sodium formate in 64 mM sodium phosphate buffer (pH 6.2), 10 µg/mL *Bd*FDH and 1 mM $NADP^+$. The activity value of control reaction (assay without metal ion) was set to 100% as a reference and the resulted activities were analyzed in comparison with the reference reaction under the same conditions.

The enzyme was assayed in various percentages of different, water miscible solvents (methanol, acetonitrile, ethanol, DMSO, isopropanol) to detect the organic solvent effect on activity of enzyme. The assay was carried out in 96-well plate, (64 mM sodium phosphate buffer pH 6.2, 1 mM $NADP^+$, 170 mM sodium formate at final concentrations) with organic solvents (0-5-10-20-30-40-50%). The enzyme was added 10 µg/mL at final concentration and reaction was performed as abovementioned at 37 °C. The remaining activity was compared in reactions with and without cosolvent and given as percentage. In addition, the enzyme stability was measured by incubating the aliquotes of enzymes (0.4 mg/mL; without glycerol) in the presence of 30% DMSO in sodium phosphate buffer at room temperature for 1 hour to 5 hours. The residual activity was determined as aforementioned.

#### 3.4.5.4 Steady State Kinetics and Enzyme Assay

FDHs catalyse bisubstrate reactions. Therefore, to detect the steady-state kinetic values of *Bd*FDH for cofactors, the final concentration of formate was fixed at 4 M while final concentration of $NADP^+$ and $NAD^+$ were varied from 0.25 to 12.5 mM and 1.5 mM to 30 mM, respectively. To detect the kinetic parameters in terms of formate, the final concentrations of $NADP^+$ and $NAD^+$ were maintained at 20 mM and 75 mM, respectively, while the concentration of formate was varied from 4.25 mM to 403.75 mM. The measurements were done at 340 nm and 37 °C. All kinetic reactions were repeated at least triplicate by using microplate reader (SpectraMax Plus384™, Molecular Devices). The steady-state kinetic constants, such as Michaelis–Menten constant (Half saturation constant; $K_M$), turnover number ($k_{cat}$) and catalytic efficiency ($k_{cat}/K_M$) values for substrates were obtained by fitting the data to the Michaelis–Menten equation *via* Origin

v.8 software (OriginLab, Northampton, MA). In addition, the specific activity assay was carried out by using a plate reader based on the detection of reduced cofactor at 340 nm.

## 3.5 Cloning, Expression and Characterization of FDH from *Lactobacillus buchneri* NRRL B-30929 (LbFDH)

### 3.5.1 Lbfdh Gene Mutation and Amplification *via* Overlap PCR

Liu et al. sequenced the whole genome of *Lactobacillus buchneri* NRRL B-30929 [95] and shared the information in GenBank (NCBI accession no. NC_015428). The chromosomal DNA of this strain was kindly provided by Dr. Siqing Liu from USDA ARS, USA. It was used to get *fdh* gene. To perform the cloning step, *Nde*I and *Xho*I recognition sites were inserted into cloning primers and underlined, respectively as seen below. The *Lbfdh* gene has *Nde*I recognition site. Therefore, firstly the gene was mutated to get rid of *Nde*I site (CATATG to CACATG) by overlap mutagenesis procedure [96]. By using following mutagenesis and cloning primers, two different PCR (PCRI and PCRII) were carried out ($FP_{NdeI-}$: 5'CCCCACACATGTCCGGAACAAC-3' and $RP_{NdeI-}$: 5' CCGGACATGTGTGGGGTCATAGC-3'; FP: 5'-CGGTGTC**CATATG**ACCAAAG TGTTAGCAGTTC-3' and RP: 5'-ATAAAT**CTCGAGC**GACTTCTCAGCTTCCCC ACTTC-3', respectively). For this purpose, extrinsic forward primer with intrinsic reverse primer were used in PCR I reaction and intrinsic forward primer with extrinsic reverse primer were used in PCR II reaction, respectively. The components of 25 µl reaction mixture were; purified genomic DNA (1 µl, 0.22 ng/µl), primers (0.5µl, 0.2 pmol/µl), 5X PrimeSTAR (PS) buffer (1X, 5 µl), dNTP mix (2 µl, 2.5mM each), Prime Star HS DNA polymerase (0.25 µl) and distilled water. The PCR process designed as an initial denaturation step of 2 min at 95 ˚C and then 30 cycles of amplification ( 98 ˚C, 10 sec; 57 ˚C, 5 sec; 72 ˚C, 1.5 min) and a final extension step at 72 ˚C for 10 min. The PCR product was electrophoresed in the presence of marker DNA (Lambda DNA / EcoRI + HindIII) at 90 V for 45 min. The PCR products were recovered from agarose gel with the Thermo Scientific GeneJET Gel Extraction Kit according to the supplier's instructions. The concentration of the products was determined spectrophotometrically by using the NanoDrop.

Then, the combined reaction products were amplified by an additional PCR program including only cloning primers. The PCR reaction including; 5X Prime star Buffer

(TAKARA, 1X), dNTP mix (2.5 mM each), gel purified PCRI and PCRII product (4 ng/µl), the primers (0.2 pmol/µl) and HS DNA Polymerase (2.5U/µl). The PCR reaction was performed in Veriti®96 well Thermal Cycler™ and it consisted of 7 cycles of amplification without primers (98 ˚C, 10 sec; 57 ˚C, 5 sec; 72 ˚C, 1.5 min) and 23 cycles of amplification with primers (98 ◦C, 10 sec; 57 ˚C, 5 sec; 72 ◦C, 1.5 min) and a final extension at 72 ˚C for 10 min. A mutated gene fragment, approximately 1.2 kb, was amplified and DNA was stored at -20 ºC for restriction procedure.

### 3.5.2 Cloning of Lbfdh into pET23b

#### 3.5.2.1 Restriction Reactions of PCR Product and Plasmid DNA (pET23b(+))

The pET23b(+) cloning vector was obtained by digestion of recombinant plasmid DNA, pET23b-Lys. This plasmid was transferred to *E. coli* Top10 cells as aforementioned in section 3.3.2.1. Then, the plasmid was isolated by using the plasmid isolation kit and electrophoresed for quantification. The resulted PCR product and pET23b (+) were restricted with *Nde*I/*Xho*I enzymes. The reaction volume was 60 µl for PCR product restriction with *Nde*I and *Xho*I and the reaction included following components; PCR product (52 µl, ~5 ng / µl), reaction buffer (6 µl, 10X NEB Buffer 3), BSA (0.6 µl, 100X), *Nde*I (1 µl, 20,000 U / mL, NEB) and *Xho*I (1 µl, 20.000 U / mL, NEB). The plasmid was also restricted with the same enzymes. The reaction volume was 100 µl and the reaction included following components; *p*ET23b-*Lys* plasmid DNA (23 µl, ~30 ng/µl), reaction buffer (5 µl, 10X NEB Buffer 3), BSA (0.5 µl, 100X), *Nde*I (1 µl, 20.000 U/mL, NEB), *Xho*I (1 µl, 20.000 U/mL, NEB) and 19.5 µl distilled water. The restriction reactions were incubated at 37 °C for 2 hours then, the electrophoresis was performed with restriction products and gel purified DNA was stored at -20ºC for ligation.

#### 3.5.2.2 Ligation Reaction of Lbfdh Gene into pET23b Vector

The T4 DNA ligase was used for the ligation reaction according to the instructions (Fermentas). The reaction included restricted PCR product (5,5 µl, ~ 9 ng/µl), pET23b vector (1 µl,~ 50 ng/µl), T4 DNA ligase reaction buffer (2 µl, 10X), T4 DNA ligase (1 µl, 200 CEU / µl, Fermentas) and distilled water (10.5 µl). The control reaction included only cloning vector, reaction buffer and deionised water. The reaction was incubated at 16 °C for overnight. Then, the *E. coli* Top10 ultra-competent cells used for transfomation

process of ligation mixture. The transformation mixture was spreaded onto agar plates (in presence of ampicillin) and incubation for 18-21 hours at 37 °C was carried out. Then, the 25 µl PCR reactions were performed for 10 different ligation colonies to test the colonies for recombinant plasmids. The recombinant plasmid contains the dehydrogenase coding region with C-terminal His-tag was transferred into *E. coli* TOP10 and then, gel purified. To confirm the accuracy of product, DNA sequencing was performed. The BioEdit software packages was used for assembling and analyzing of sequencing results (Ibis Therapeutics, CA).

### 3.5.3 Expression and Purification of LbFDH

The control plasmid (pET23b, empty vector) and positive construct (pET23b-*Lbfdh*) were transferred into *E. coli* BL21(DE3) (Invitrogen) for gene expression and the transformation product was plated on LB-amp-agar. A colony from plates was used for inoculation of starter cultures. Then, with these pre-cultures, IPTG induction was performed (at 30 ˚C with 180 rpm for 8 h). After incubation, the cells were harvested *via* centrifugation at 8000xg and 4 ˚C. Aliquotes were withdrawn at determined periods and run onto SDS-PAGE to analyze the protein expression profile.

The autoinduction process was also performed [92]. A colony from petri plate was inoculated in pre- culture and utilized for autoinduction. After the centrifugation, the lysis buffer was used for resuspension of cell pellet and the cells were disrupted *via* sonication process. After centrifugation of resulted lysate, the supernatant was loaded onto affinity chromatography column. The recombinant protein was obtained with Buffer A including 100–400 mM imidazole and then, a desalting column was used to change the elution buffer at 4 ˚C.

### 3.5.4 SDS/Native-PAGE Analysis and Bradford Assay

The protein preparation was analyzed on 12% SDS–PAGE and visualised with Coomassie brilliant blue R-250. The Bradford protein quantification assay was used for detection of protein concentration. The MALDI-TOF analysis was carried to determine the mass of *Lb*FDH.

### 3.5.5 Determination of Recombinant LbFDH Properties

#### 3.5.5.1 The Effect of pH and Temperature on LbFDH

The 50 mM stock buffers at several pH ranges were assayed for determination of pH-activity profile of *Lb*FDH at 30 ˚C for both cofactor. As buffers, the acetic acid-sodium acetate ($pK_2$, 50 mM, pH 3.8–5.8), citric acid-sodium citrate ($pK_2$, 50 mM, pH 5.4–6.4), sodium phosphate ($pK_2$, 50 mM, pH 6.2–8.0), Tris/Cl (50 mM, pH 7.5–9.0), Ethanolamine (50 mM, pH 8.8–10.5) were used in assays. The 120 mM sodium formate, 1.1 µg/mL *Lb*FDH and 1 mM $NAD(P)^+$ were used for determination of activity values in each of these buffers. In a typical assay, the each buffer including sodium formate (120 mM) was added on enzyme (10 µl) then, the reaction was incubated for 3 min. After addition of $NAD(P)^+$ (20 µl), the reaction was followed at 340 nm and 30 ˚C. The initial rates were calculated as mentioned above.

The temperature profile assay was performed at several temperatures (15-68 ˚C) separately for each cofactor. In a standard assay, the 700 µl reaction mixture including sodium formate (0.15 M and 0.2 M for the assay with $NADP^+$ and $NAD^+$, respectively) was incubated at determined temperature. The enzyme (35µl) was added to reaction and it was incubated. After the initiation of reaction by $NAD(P)^+$, the activity was followed spectrophotometrically at 340 nm for 3 min. The calculation of initial rates for assays were done as previously described. To determine the thermostability of enzyme, the protein samples (0.5 mg/mL) were incubated at 50, 55, 60 and 65˚C for 0-24 h and samples were withdrawn at certain time. The remaining activity was performed with 150 mM of sodium formate in 100 mM acetate buffer (pH 4.8) in presence of $NADP^+$ as mentioned above and defined as a percentage of the reference reaction which is carried out without heat treatment. The thermostability of enzyme was also determined by differential scanning calorimetry method (DSC) in a Mettler Toledo DSC 1. The 0.1 M of sodium phosphate buffer (pH 7.0) was used as a reference buffer, the enzyme concentration was 1.2 mg/mL and the heating rate was at 1 K/min between 0-120 °C.

#### 3.5.5.2 Effects of Metallic Compounds and Organic Solvents on LbFDH

The effect of various cations on enzyme activity were examined by the presence of 1 mM and 10 mM $ZnCl_2$, $MgSO_4$, $MnCl_2$, $CaCl_2$, $NiSO_4$, $FeCl_2$, $FeCl_3$, $CuSO_4$, $Na_2MoO_4$ and $Na_2WO_4$ in the reaction medium, separately. The standard enzymatic assay was used for

the activity measurements. The remaining activity was determined in mixtures with and without metal and defined as relative activity.

The enzyme activity in organic solvent was carried out in 96-well plate, the reaction mixture including different percentages (from 0 to 50%) of various organic solvents (isopropanol, acetonitrile, ethanol, methanol, dimethyl sulfoxide). The enzyme was added 2 μg/mL at final concentration. The assay was initiated after 3 min *via* phosphorylated cofactor. The remaining activity was compared in reactions with and without solvent and defined as a percentage value. To determine the enzyme stability in different organic solvents, the *Lb*FDH was incubated in 20% of acetonitrile and DMSO at 25 ˚C for 1 h to 15 days and then the residual activity was checked.

The temperatures (-80 ˚C, -20 ˚C, +4 ˚C and 25 ˚C) were used for the investigation of the storage stability of the enzyme. The aliquots of enzyme were incubated at certain storage temperatures with and without glycerol for two weeks. The remaining activity was detected every week during storage. The assays were repeated at least in triplicates.

#### 3.5.5.3 Enzymatic Assay and Steady State Kinetic Reactions

In a standard assay with $NADP^+$, 0.15 M of sodium formate in 0.1 M acetate buffer (pH 4.8 ) was mixed with *Lb*FDH, then incubated for 3 min at 30 ˚C and the reaction was initiated *via* $NADP^+$ at various concentrations of 0.25–5 mM and and $NAD^+$ at 0.5-17.5 mM ranges, respectively. The same reaction was performed for $NAD^+$ with a different buffer; 0.2 M of sodium formate in 0.1 M citrate buffer pH 6.4. The assays were visualized spectrophotometrically at 340 nm during 5 min. To calculate the steady state kinetic parameters of enzyme, various concentrations of formate was used in the assay. In a standard reaction, several concentrations of sodium formate in the range of 0.036-1.8 M and 0.09-3.6 M were prepared in 0.1 M acetate buffer (pH 4.8) and 0.1 M citrate buffer (pH 6.4) for $NADP^+$ and $NAD^+$, respectively. The reaction was initiated by the addition of cofactor and monitored at 340 nm after for 3 min incubation (based on NAD(P)H formation ; $\varepsilon 340 = 6.22\ mM^{-1}\ cm^{-1}$).

The kinetic measurements were carried out at least triplicate *via* microplate reader (SpectraMax Plus384$^{TM}$, Molecular Devices). The Origin v.8 software (OriginLab, Northampton, MA) was used for Michaelis-Menten curve fittings. Specific activities (U/mg) were calculated using the protein mass of 44,27 kDa and the absorption coefficient of $\varepsilon 340 = 6.22\ mM^{-1}\ cm^{-1}$.

## 3.6 Statistical analysis

Statistical analysis of the experimental groups and control group were compared by using a one-way analysis of variance (ANOVA) and Paired Sample T test. A value of $p < 0.05$ was considered as a limit value for statistically significant. Statistical tests were carried out *via* SPSS version 25.5 PL for Windows.

# CHAPTER 4

# RESULTS AND DISCUSSION

## 4.1 Cloning, Expression and Biochemical Characterization of FDH from *Burkholderia dolosa* PC543

As an output of pattern based sequence screening and alignments, some microorganisms which have putative $NADP^+$ dependent *fdh* gene sequences were determined. According to the protein engineering studies in literature, particularly sequences which have a specific pattern for $NADP^+$ were selected. Among several putative formate dehydrogenase sources, the *Burkholderia dolosa* PC543, a pathogenic bacterium recovered from the lungs of cystic fibrosis patients, was determined and the sequence of putative $NADP^+$ dependent FDH (ETP61471.1) was obtained (Figure 4.1).

### 4.1.1 Cloning of BdFDH as N-terminal His Tagged Form

The vector pET14b was used for cloning putative gene and expression of N-terminus his tagged protein (Figure 4.2). Thus, it was aimed to easily perform protein purification using Ni-NTA affinity column.

For N-terminus His tag cloning procedure, oligonucleotide primers were designed according to the sequence of selected vector and the *fdh* gene. The putative *fdh* gene (1161 bp) was amplified with primers *via* PCR (Appendix-B Table 1, Figure 4.3, Figure 4.4). PCR products were recovered from agarose gel according to the gel extraction kit protocol. Then, the pET14b-SS-*ntr* plasmid DNA and PCR products were digested with *Nde*I and *BamH*I to get DNA with sticky ends for ligation process (Figure 4.5).




Figure 4.1 Sequence comparison of *Bd*FDH with reported NAD(P)$^+$ dependent FDHs.

The given abbreviations for FDHs are; Bsp184FDH for *Burkholderia cenocepacia* PC184 FDH, BstFDH for *Burkholderia stabilis* FDH, Bsp383FDH for *Burkholderia lata* FDH, GraFDH for *Granulicella mallensis* MP5ACTX8 FDH PseFDH for Pseudomonas sp. FDH, CboFDH for *Candida boidinii* FDH in alignment. The FDH from *Burkholderia dolosa* PC543 FDH is given as BdFDH. The residues that have significant role in the catalytic cavity are shown by a star symbol according to Tishkov and Popov [9]. The BioEdit software packages was used for alignment (Ibis Therapeutics, CA).

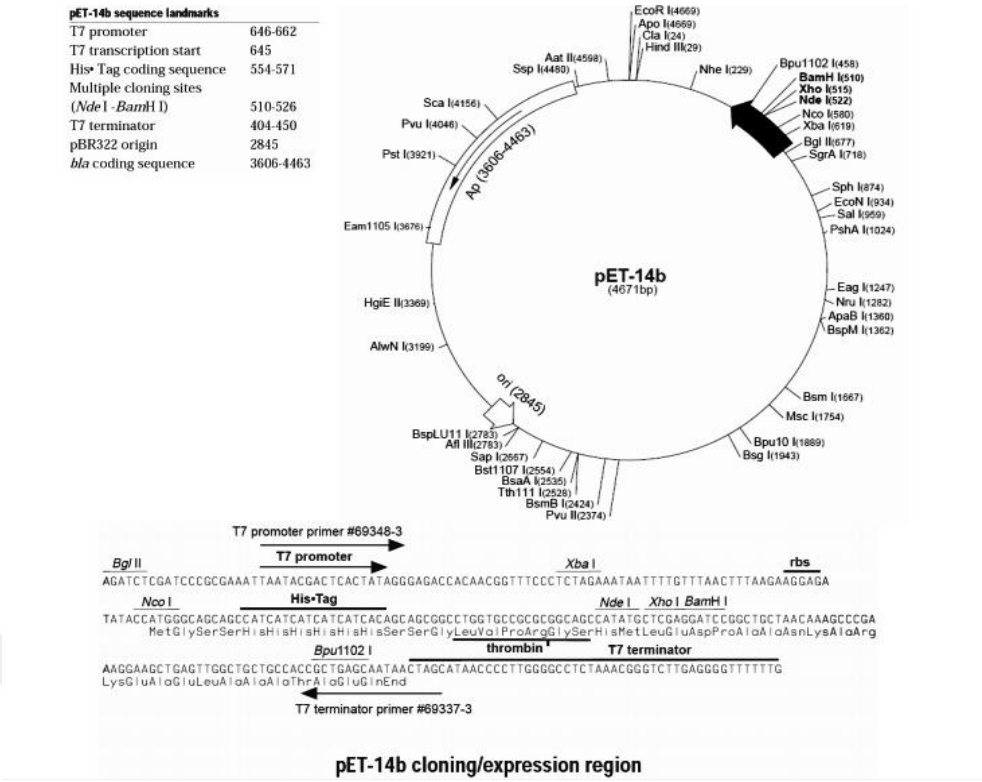
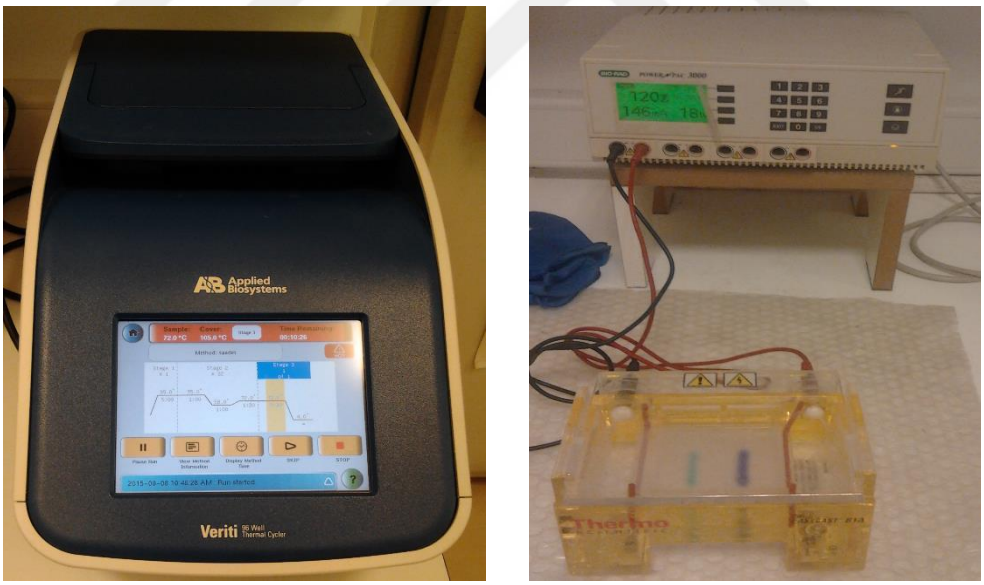



Figure 4.2 pET14b vector sequence and map [97]




**a** **b**

Figure 4.3 PCR program (a) and gel electrophoresis (b) for amplification of *Bdfdh.*

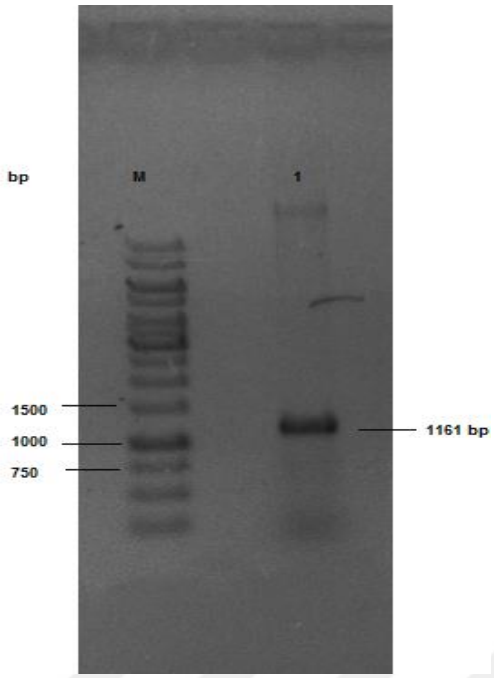



Figure 4.4 PostPCR product of *Bdfdh* (N-terminus His tagged) on agarose gel. Lanes: (M) 1 kb DNA marker; (1) *Bdfdh* PCR product.

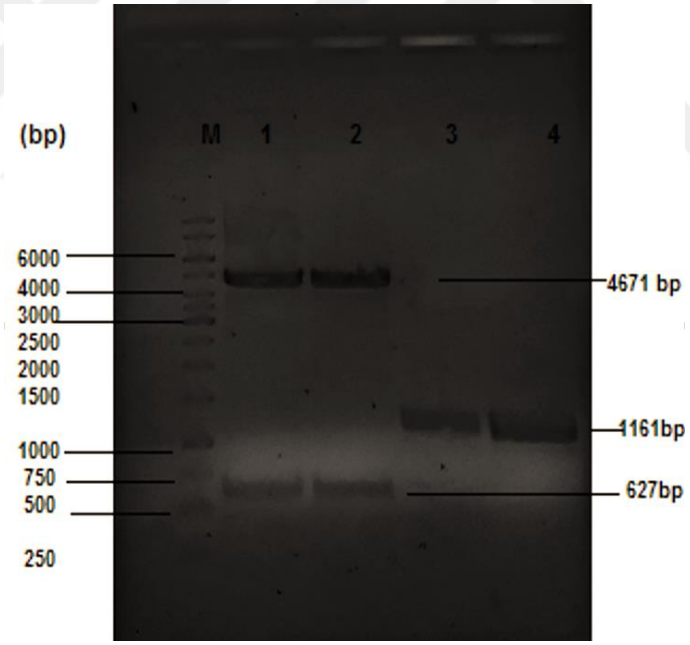



Figure 4.5 Restriction reaction products of pET14b-Ss-*ntr* and PCR products. (M) marker; (1,2) Digested plasmid; (3,4) Digested PCR product.

The insert and vector ratio was adjusted to 3:1 and DNA fragments were subjected to ligation process by using T4 DNA ligase enzyme (Figure 4.6).

### 4.1.2 Confirmation of Ligation Reaction

After chemical transformation of ligation products into *E. coli* Top10, the colony PCR with transformants and restriction reactions with isolated plasmids were carried out. To check the insertion of *Bdfdh* into plasmid, firstly, colony PCR was performed with 3 colonies from ligation transformants. 10 µl of the post PCR products were subjected to electrophoresis onto 0.8% agarose gel and the DNA bands confirmed the accuracy of ligation reaction (Figure 4.7). In addition, the recombinant plasmid was digested with *Nde*I/*BamH*I and only with *Nde*I to double check the ligation. The resulted DNA bands confirmed the integrity and insertion of desired gene into plasmid (Figure 4.8).

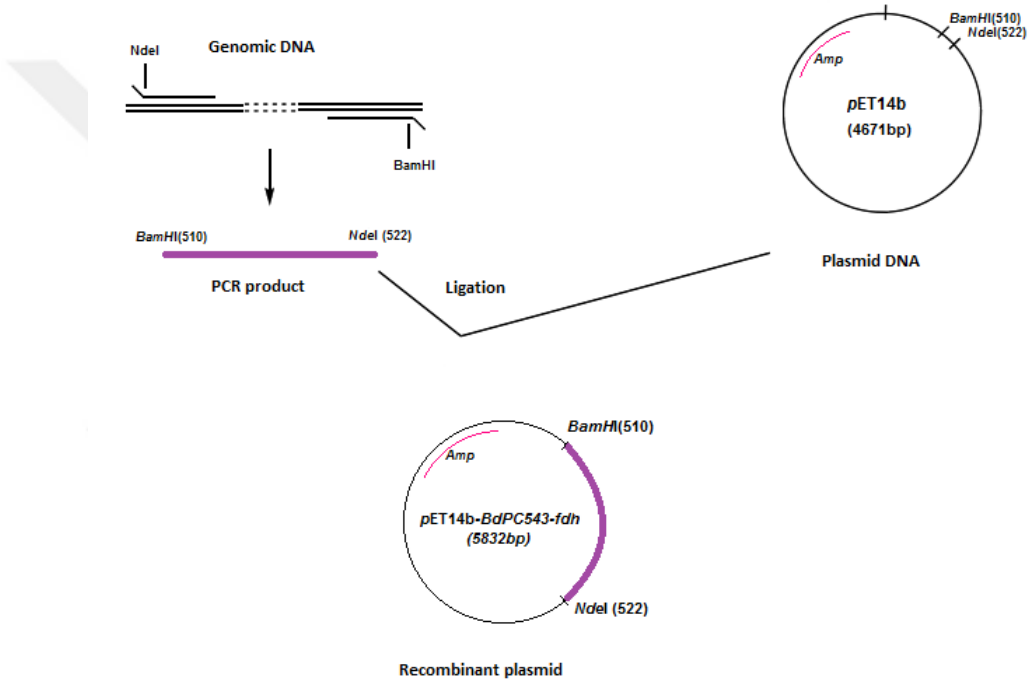



Figure 4.6 Construction of pET14b-*Bdfdh* recombinant plasmid.

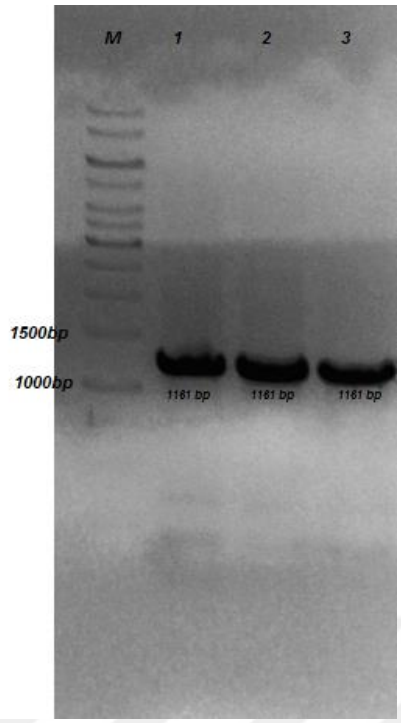



Figure 4.7 Colony PCR products on 0.8 % agarose gel. (M) DNA marker (1 kb); (1,2,3) PCR products of the 1st, 2nd and 3rd colonies from ligation transformants, respectively.

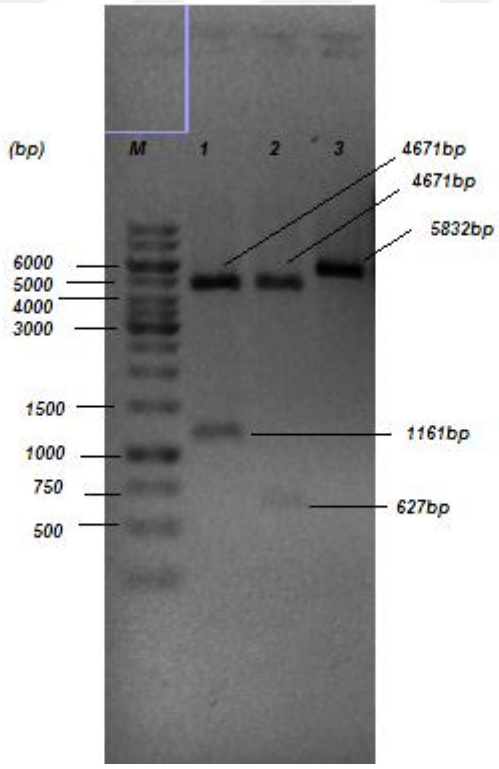



Figure 4.8 Restriction reaction products of recombinant plasmid on agarose gel. (M) 1kb DNA marker; (1) NdeI/BamHI digestion product of recombinant plasmid; (2) NdeI/BamHI digestion product of pET14b-Ss-*ntr* (*ntr* gene contain 627 bp); (3) NdeI digestion product of recombinant plasmid.

### 4.1.3 Expression and Purification of N-terminus His Tagged BdFDH

Then, the construct (pET14b-*fdh*) was transferred into *E. coli* BL21 (DE3) for production of N-terminus His tagged protein. The cells were grown at 37 °C until reach to required OD value at 600 nm, then the IPTG (final concentration 0.5 mM) was used to enhance the expression at 30 °C for 6 h. The protein expression increased gradually during six hours as seen on SDS-PAGE (Figure 4.9 and Figure 4.10). The SDS-PAGE result of the protein purification step indicated that the N-terminus his tagged *Bd*FDH accumulated in cells as an inclusion body (Figure 4.11).

To reduce the formation of inclusion body, the induction temperature was decreased. During the process, IPTG concentration was kept at a constant value (0.5 mM) and induction was firstly determined ~22 °C and then at 16 °C for 8 h, separately. The protein expression profile was confirmed that the protein was expressed at ~22 °C but not released into supernatant after sonication (Figure 4.12). At 16 °C, there was an expression and also the protein was released to supernatant, but the quantity of protein is still quite low (Figure 4.13 column 8).



a b

Figure 4.9 Pre-cultures (a) and induction cultures (b) for protein expression.

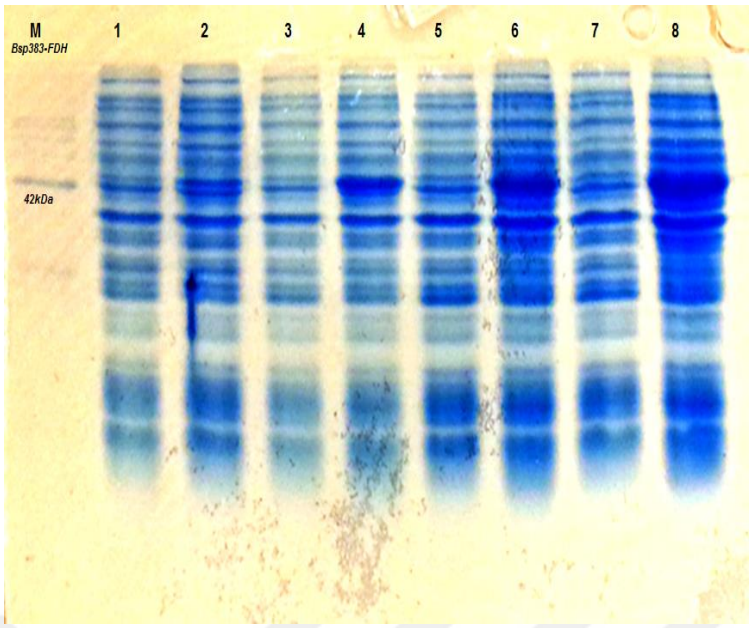



Figure 4.10 The expression profile of N-terminus His tagged *Bd*FDH at 30 °C. (M) Marker (Bsp383FDH); (1,2) cells with pET14b plasmid and recombinant plasmid, respectively before IPTG induction; (3,4) cells with pET14b plasmid and recombinant plasmid, respectively after IPTG induction for 2 hours; (5,6) after IPTG induction for 4 hours; (7,8) after IPTG induction for 6 hours.

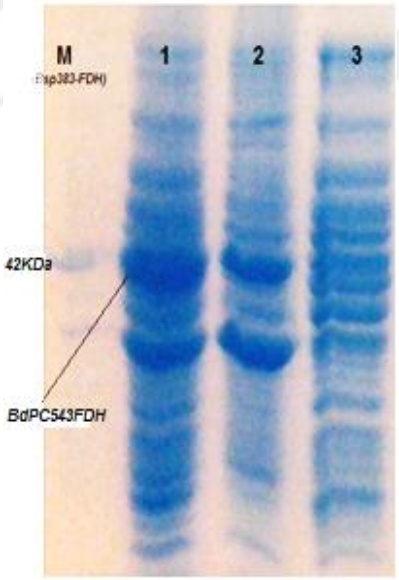



Figure 4.11 The purification of *Bd*FDH after IPTG induction for 6 h. (M) Marker (Bsp383-FDH); (1) post-induction cell pellet after 6 hours; (2) post-sonication pellet; (3) supernatant after sonication

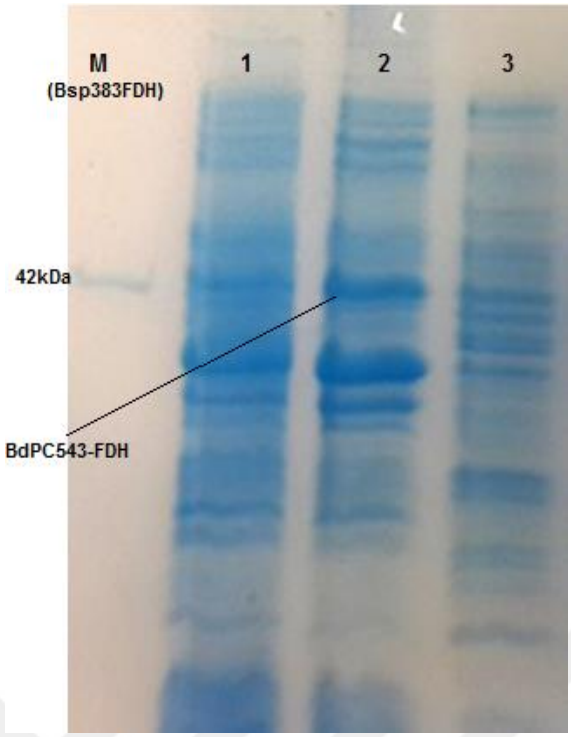



Figure 4.12 The expression profile of *Bd*FDH at ~22 °C for 8 hours in *E. coli* BL21 (DE3) cells. (M) Marker; (1) cell pellet after 8 h induction; (2) pellet after sonication; (3) supernatant after sonication

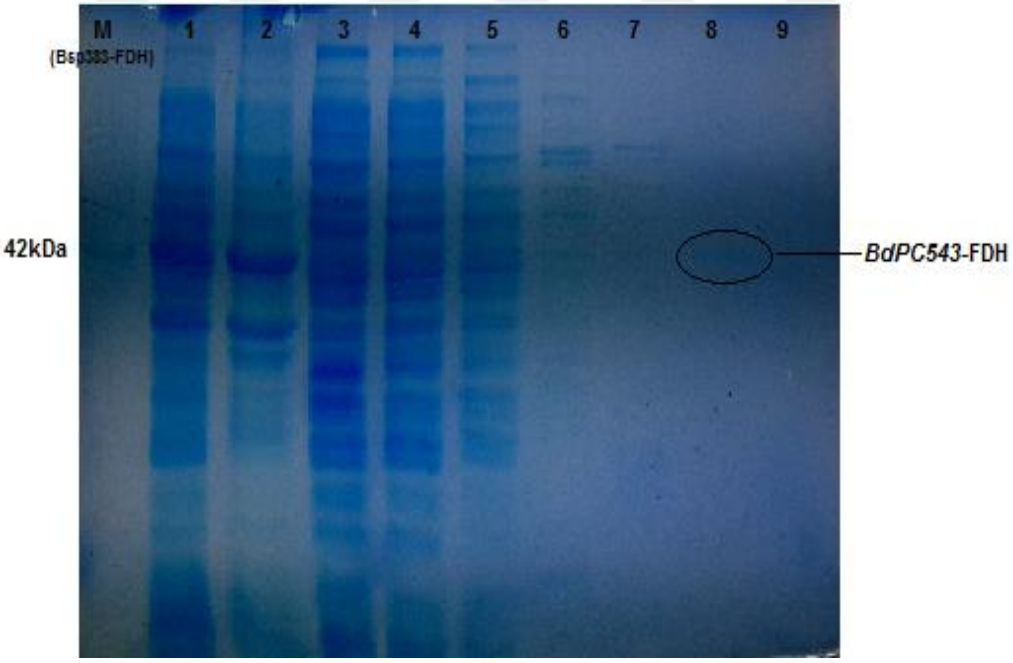
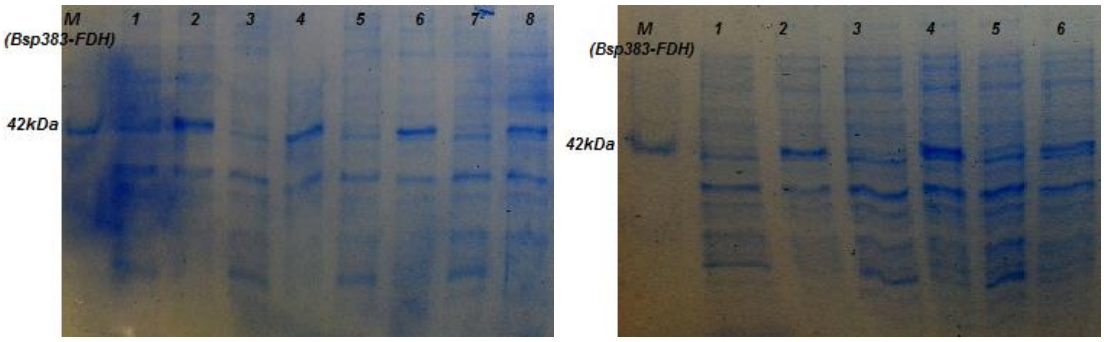



Figure 4.13 Purification of *Bd*FDH after IPTG induction at 16°C for 8h. (M) Marker ; (1) cell pellet; (2) cell pellet after sonication; (3) supernatant after sonication; (5) 5 mM imidazole; (6) 30 mM imidazole; (7) 100 mM imidazole; (8) 200 mM imidazole; (9) 400 mM imidazole




**a** **b**

Figure 4.14 Expression profile of *Bd*FDH by autoinduction at 16 ° C for 20 hours. (M) Marker; the columns indicated the expression profile of control group and the recombinant plasmid, respectively. (**a**) columns (1,2) after 8 hours; (3,4) after 10 hours; (5,6) after 12 hours; (7,8) after 14 hours of autoinduction. (**b**) columns (1,2) after 16 hours; (3,4) after 18 hours; (5,6) after 20 hours of autoinduction.

There was an enzyme activity in the presence of $NADP^+$ with the supernatant from IPTG induced cells at 16 °C for 8 h. Therefore, we tried to estimate the time range for better expression and activity by performing time dependent assay with autoinduction. Thus, 20 hours of autoinduction was performed at 16 °C to optimize the expression time. Particularly the expression at $8^{th}$, $10^{th}$ and $12^{th}$ hours were higher than the other time intervals (Figure 4.14). The enzymatic activity assay with the supernatant at $12^{th}$ h had the better result than $8^{th}$ and $10^{th}$ h. As understood from the SDS-PAGE result, in the following hours, the protein expression reduced and protein degraded.

Despite all these efforts, desired quantity of protein could not be obtained. Finally, we performed IPTG induction at 16 ˚C for 10 hours to induce the protein expression. Although, the resulted protein band was intense, it was not at desired level (Figure 4.15).

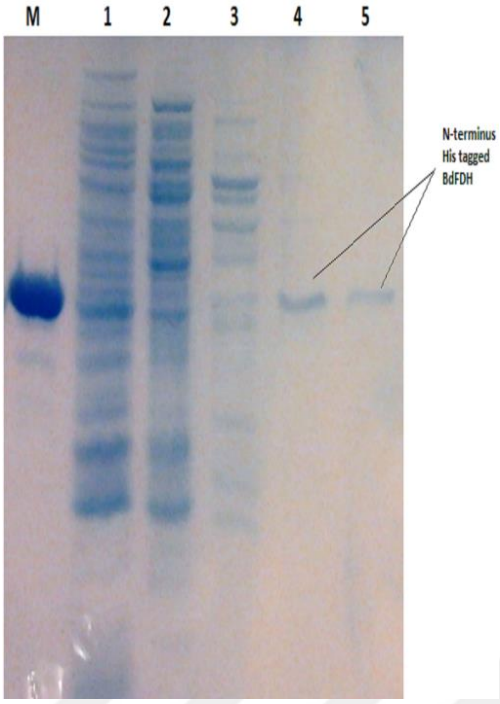



Figure 4.15 SDS-PAGE analysis of N-terminus His tagged *Bd*FDH (Purified fractions from IPTG induction at 16 ˚C for 10h). M, marker protein (molecular weight: 42kDa); 1 and 2, washing fraction; 3-5, elution buffers including 100, 200, 400 mM imidazole, respectively.

Only approximately 0.5 mg fused protein was obtained from purification at 16 ˚C *via* IPTG induction for 10 hours. The enzyme assay indicated that the specific activity values for *Bd*FDH were 0.25 and 0.36 U/mg with $NAD^+$ and $NADP^+$, respectively. Both IPTG induction and autoinduction assays indicated that the N-terminal His tagged protein was overexpressed in inclusion bodies at various temperatures (16 ˚C, ~22 ˚C, 30 ˚C) and its quantity and also activity was quite low. Therefore, we decided to get and investigate C-terminal His tagged *enzyme* for further studies.

### 4.1.4 Cloning of BdFDH as C-terminus His Tagged Form

The pET22b(+) vector was used for cloning and expression of enzyme as a C-terminus his tagged protein (Figure 4.16). Thus, it was aimed that to perform easily protein purification using Ni-NTA affinity column.

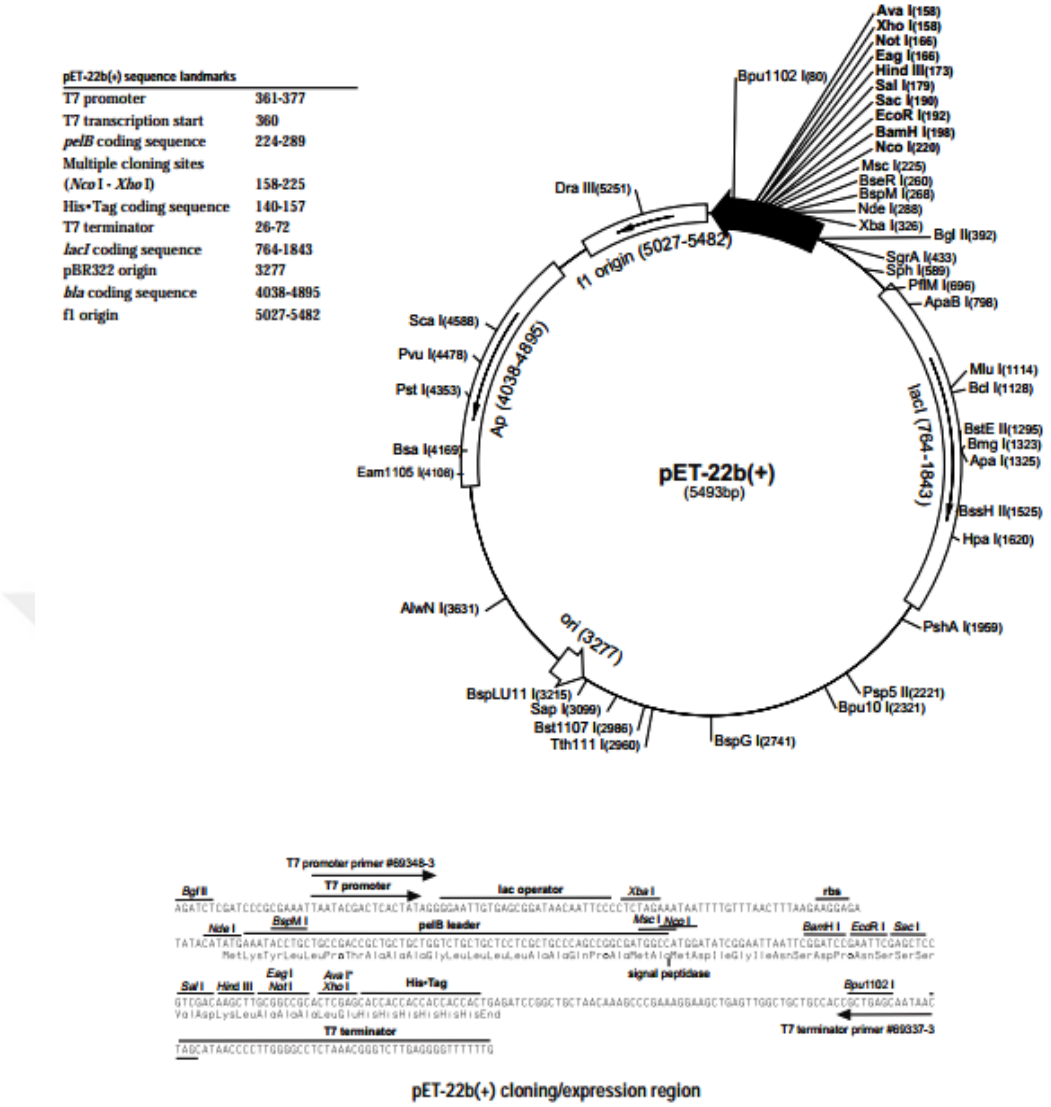






Figure 4.16 pET22b(+) vector sequence and map [98]

The whole *Bdfdh* gene was amplified with designed oligonucleotide primers *via* PCR as seen on Figure 4.17 (Appendix-B Table 2).

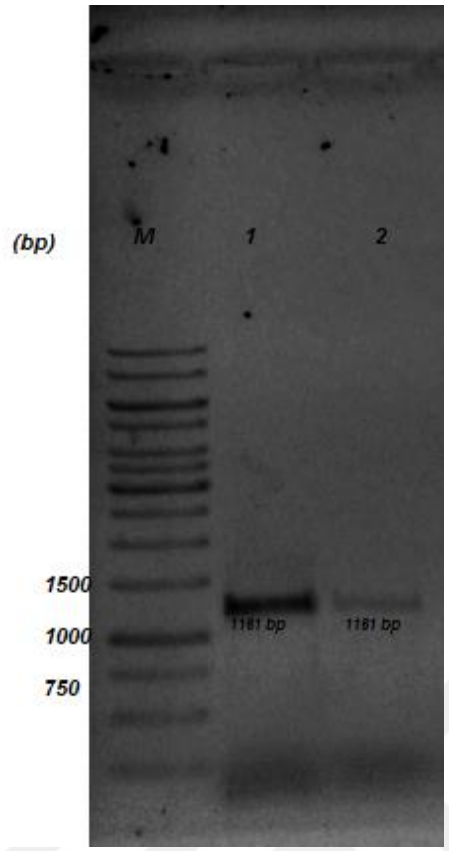



Figure 4.17 Post PCR product of *Bdfdh* (C-terminus His tagged) on 0.8% agarose gel. Lanes: (M), 1 kb DNA marker; (1,2) *Bdfdh* PCR product.

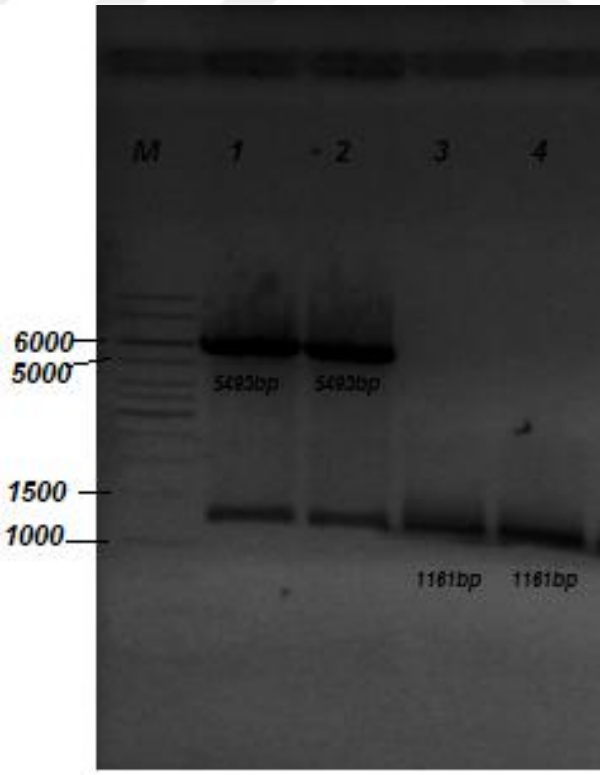



Figure 4.18 Restriction reaction products of pET22b-X and PCR products. (M) marker; (1,2) Digested plasmid; (3,4) Digested PCR product.

After recovery of PCR products from agarose gel, both plasmid for cloning (pET22b+X) and the PCR products were restricted with *Nde*I and *Not*I to get DNA fragments for ligation step (Figure 4.18). Then, the restriction reaction products (insert: 1161 bp and vector: 5493 bp) were purified from agarose gel. The insert vector ratio was adjusted to 3:1 and DNA fragments were subjected to ligation procedure by using T4 DNA ligase enzyme.

### 4.1.5 Ligation Reaction Confirmation

The ligation reaction products were transformed chemically into competent cells. Then, the colony PCR was carried out with 2 colonies from ligation transformants. The post PCR products were run onto gel and the resulted DNA bands confirmed the integrity of desired gene into the construct (Figure 4.19). The sequencing results confirmed that this gene has 1161 base pairs and it is successfully fused with the six histidine tag.

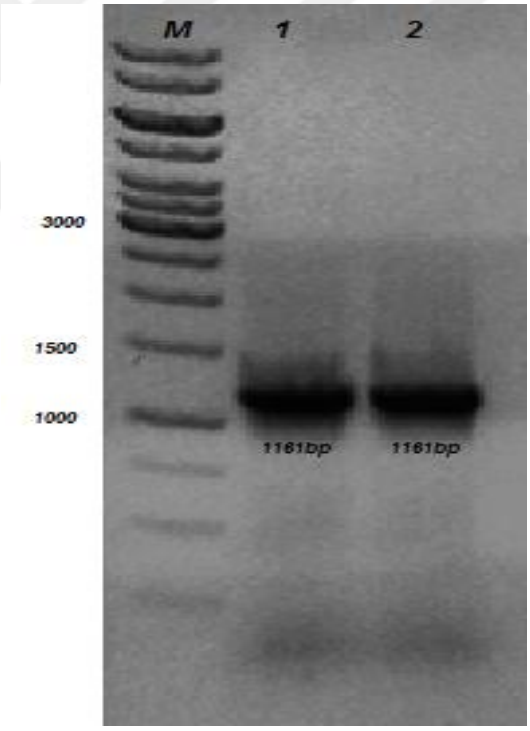



Figure 4.19 Colony PCR products on agarose gel. (M) DNA marker (1 kb); (1,2) PCR products of the 1st and 2nd colonies from ligation transformants, respectively.

### 4.1.6 Expression and Purification of C-terminus His Tagged BdFDH

The recombinant construct (pET22b-*fdh*) was transferred into the expression strain for production of C-terminus His tagged protein. The protein expression was enhanced with

IPTG (0.5 mM at final concentration) at 30 °C for 6 h. The protein expression increased gradually during six hours as seen on SDS-PAGE (Figure 4.20).

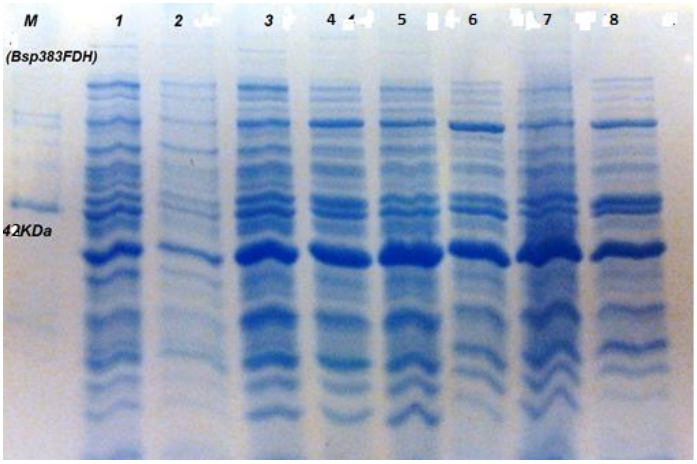



Figure 4.20 The expression profile of C-terminus His tagged *Bd*FDH at 30 °C. (M) Marker (Bsp383FDH); (1,2) cell pellets with pET22b plasmid and recombinant plasmid, respectively-before IPTG induction; (3,4) cell pellets with pET22b plasmid and recombinant plasmid, respectively -after IPTG induction for 2 hours; (5,6) after IPTG induction for 4 hours; (7,8) after IPTG induction for 6 hours.

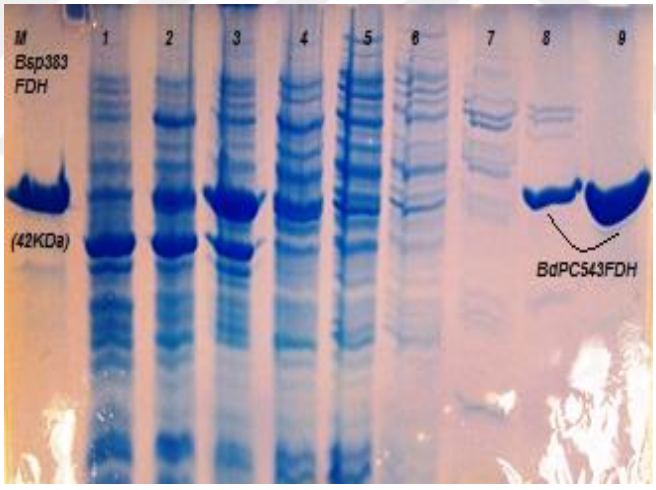



Figure 4.21 SDS-PAGE result for purification of *Bd*FDH (after autoinduction at 30 °C for 16 hours). (M) Marker (Bsp383FDH); (1) cell pellet with recombinant plasmid; (2) cell pellet after sonication, (3) supernatant after sonication, (4) column through (5) 5 mM imidazole, (6) 30 mM imidazole, (7) 100 mM imidazole,8) 200 mM imidazole, (9) 400 mM imidazole.

After the autoinduction process at 30 °C for 16 h, the His-trap affinity chromatography method was used for elution of protein. The enzyme was produced heterologously in *E. coli* as a soluble protein as seen on SDS-PAGE and the enzyme was pure ($8^{th}$ and $9^{th}$ columns in Figure 4.21). The protein, 43 kDa, was determined as seen as a pure protein band on a Coomassie-stained SDS-PAGE (Figure 4.22). According to native-PAGE

results, the molecular weight of native *Bd*FDH was thought to be about 90 kDa (Figure 4.23).

According to theoretical mass calculation, the enzyme was 43,126 Da. The molecular weight of the enzyme monomer was also detected by MALDI-TOF and found to be 43,909 Da (Figure 4.24). The enzymatic activity reaction performed by using cell extract shown that the enzyme had an affinity towards both $NAD^+$ and $NADP^+$.

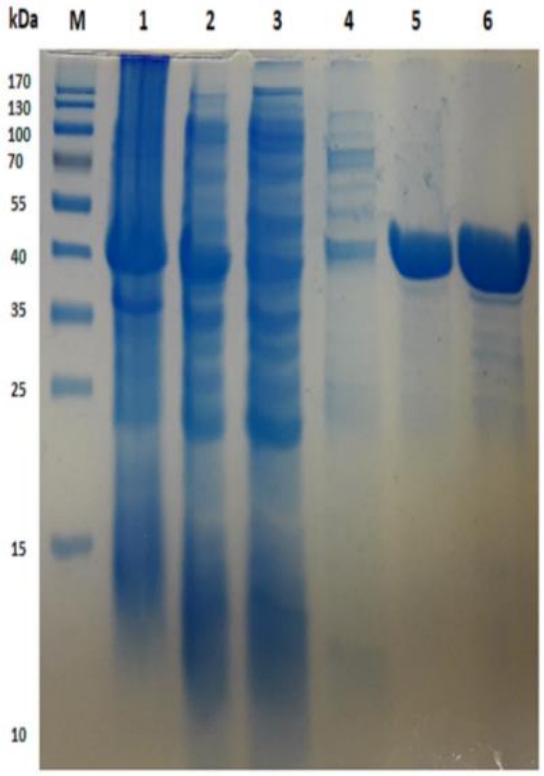



Figure 4.22 SDS-PAGE analysis of purified C-terminal his tagged *Bd*FDH. Lanes: M, Marker; 1, cell pellet; 2, cell free extract; 3 and 4, washing buffers; 5 and 6, 100 and 400 mM imidazole fractions, respectively. (autoinduction at 30 ˚C for 16 h)

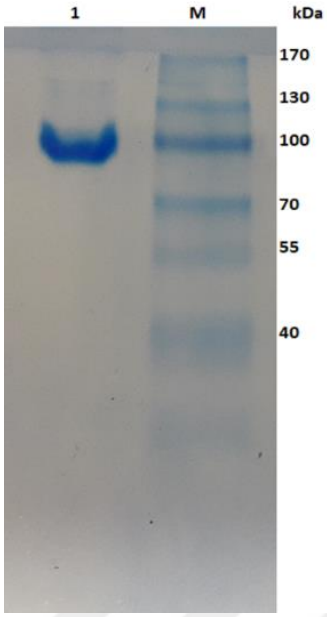



Figure 4.23 Native-PAGE results of purified *Bd*FDH protein. Lanes: M, molecular weight marker (Thermo Scientific); lane 1, purified BdFDH.

### 4.1.7 Ionic strength, pH and Temperature Effect on BdFDH

In all enzymatic reactions, the substrate (sodium formate) was prepared in related buffer. The total ionic strength of reaction medium was calculated by adding the ionic strength values of both buffer and the substrate. We realized that the BdFDH is affected by the ionic strength of reaction components. Due to this fact, we investigated the enzyme activity in terms of ionic strength parameter. The obtained data indicated that it has the optimum activity between $\mu$= 0.3-0.66 M and the activity is lost gradually outside this ionic strength range (Figure 4.25).

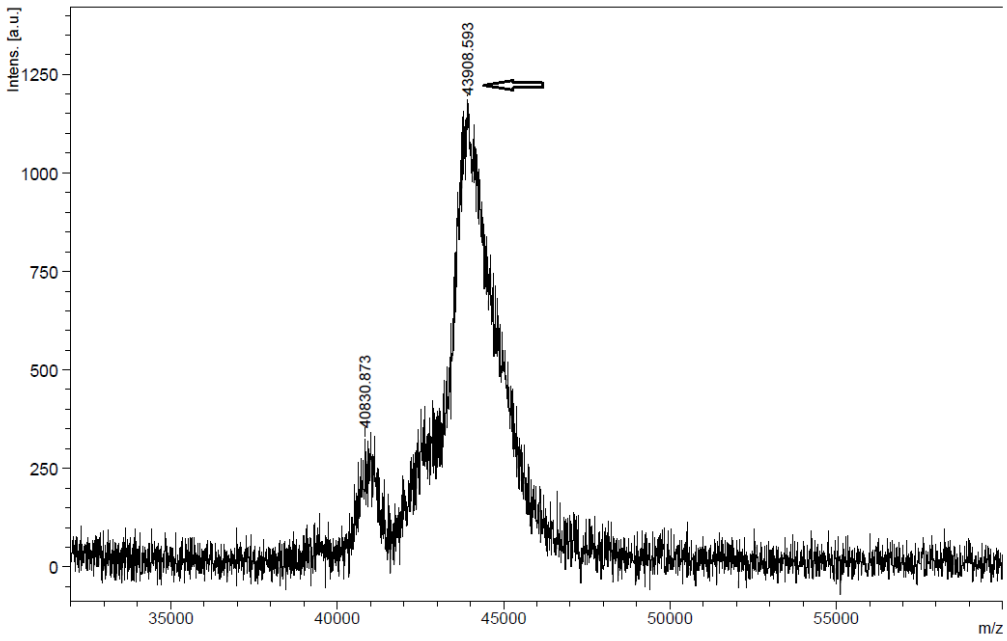



Figure 4.24 MALDI-TOF MS result for C-terminus His tagged *Bd*FDH (highlighted by arrow)

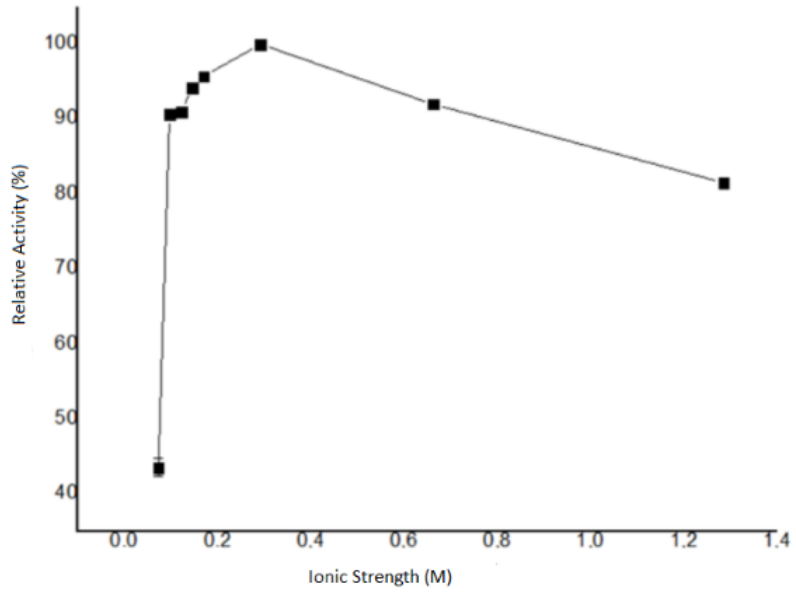



Figure 4.25 The ionic strength effect on enzyme activity

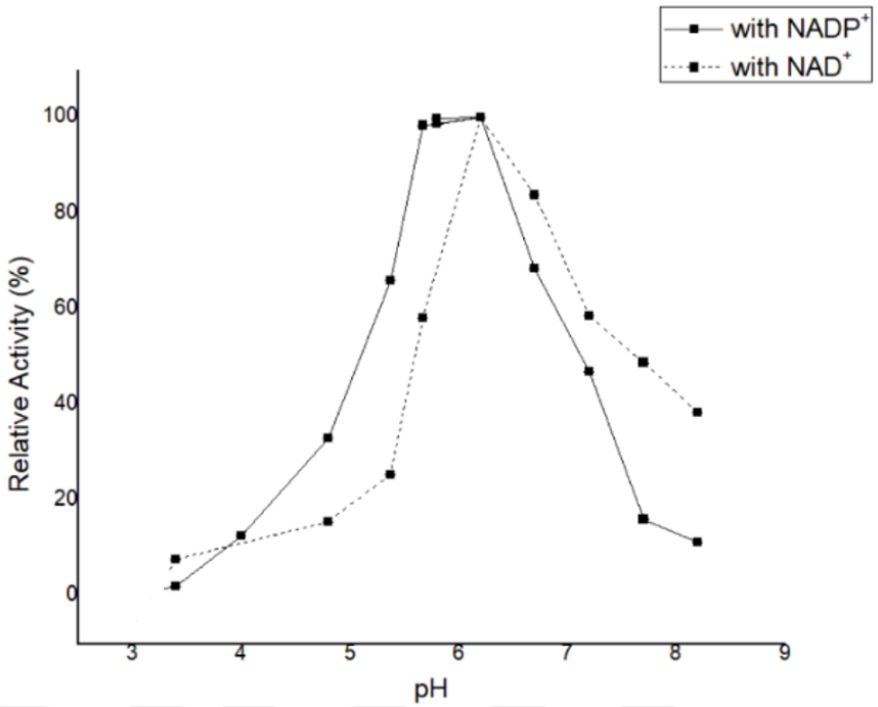



Figure 4.26 Activity-pH profile of *Bd*FDH

The pH effect on enzyme activity was investigated at pH range of 3.8–10.5 by ensuring the similarity of ionic strength of buffers. The pH-activity assay resulted with the optimum pH value is between 5.8 and 6.2 for reduction of each cofactor at 37 ˚C (ionic strength, μ= 0.49 M). The data indicated that it keeps 50% of its activity with each coenzymes in a certain pH range (pH 5.4-6.7 with $NADP^+$; pH 5.7-7.2 with $NAD^+$). At pH 3.4 and 8.0, the enzyme activity is almost equal to zero (Figure 4.26).

The optimum temperature of enzyme was detected by assaying the enzyme activity between the 15–60 ˚C. As indicated in Figure 4.27 the BdFDH has an optimum activity at 37 ºC with each coenzymes. The enzyme acts in a wide range of temperature with $NADP^+$ (20-50°C; having more than 75 % activity) than with $NAD^+$ (34-40°C). The thermostability of enzyme was also determined *via* measuring its activity at various temperatures from 37 to 60 ˚C for 0–60 min in the presence of $NADP^+$. The remaining activities of enzyme have been calculated as 94 %, 88 % and 44 % after 1 h of exposure at 37 ˚C, 45 ˚C and 60 ˚C, respectively (Figure 4.28).

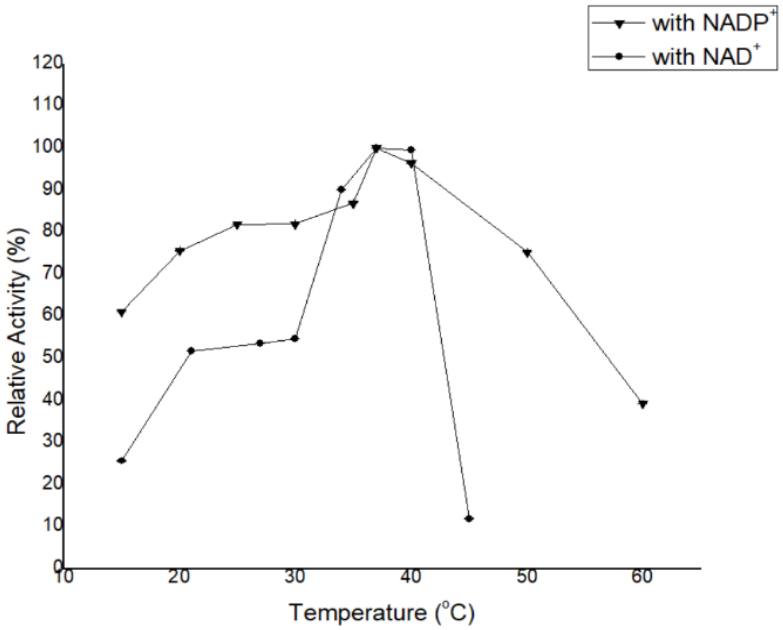



Figure 4.27 Relative activity–temperature profile of *Bd*FDH.

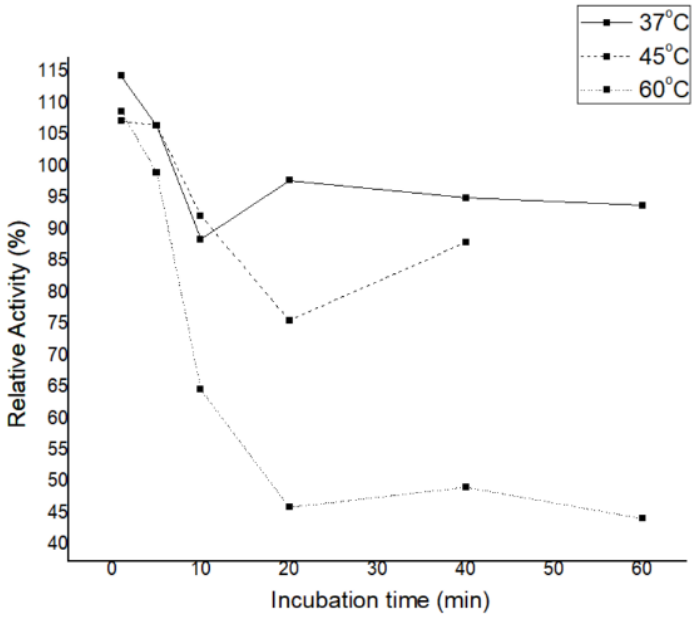



Figure 4.28 Thermostability profile of *Bd*FDH.

### 4.1.8 Effect of Metallic Ions and Organic Solvents on BdFDH

The relative enzyme activity was investigated with several cations, which were added at 1 mM and 10 mM as the final concentrations. The enzyme activity was decreased by all metallic ions at each final concentrations. However, the BdFDH was completely inactivated with $FeCl_2$, $FeCl_3$ at both concentrations and whereas the $CuSO_4$ and $MnCl_2$ inhibited the enzyme only at 10 mM (Figure 4.29). We also examined the effect of organic

solvents on enzyme stability and activity. To analyze the organic solvent effect on BdFDH, various percentages of different solvents (5, 10, 20, 30, 40 and 50%) were used. The resulted data indicated that some solvents have an enhancing effect on the enzyme activity at certain concentrations. For example, methanol, ethanol and isopropanol increased the enzyme activity up to 20% concentration. In addition, the BdFDH had the best activity (almost 170%) in 30% DMSO among the other solvents and DMSO (up to 40% (v/v) concentration) can enhance the enzyme activity (Figure 4.30). Moreover, cosolvent stability of BdFDH was investigated in the 30% DMSO due to its enhancing activity for various time intervals (from 0 to 5 h). The enzyme still has its own activity as 86% and 41%, after the incubation in 30% DMSO for 2 and 3 hours, respectively.

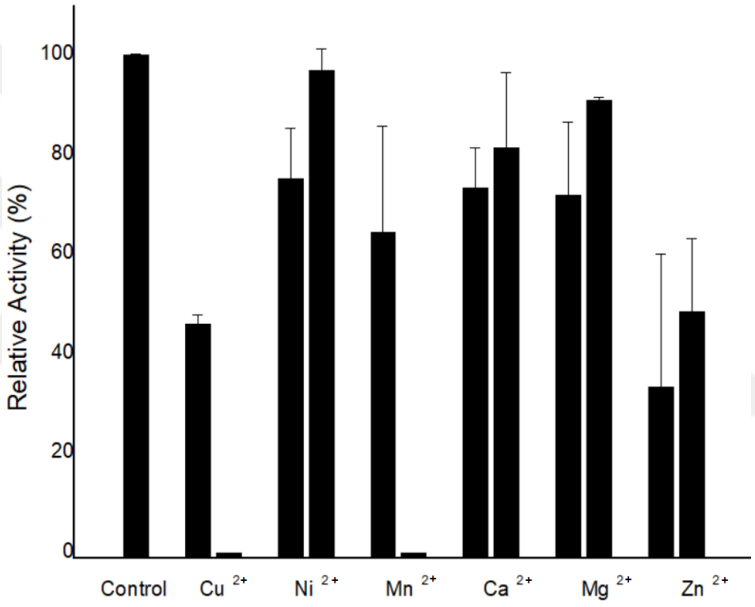



Figure 4.29 Effect of metallic ions on *Bd*FDH (First columns indicate 1mM and second ones are for 10mM at final concentration for each cations).

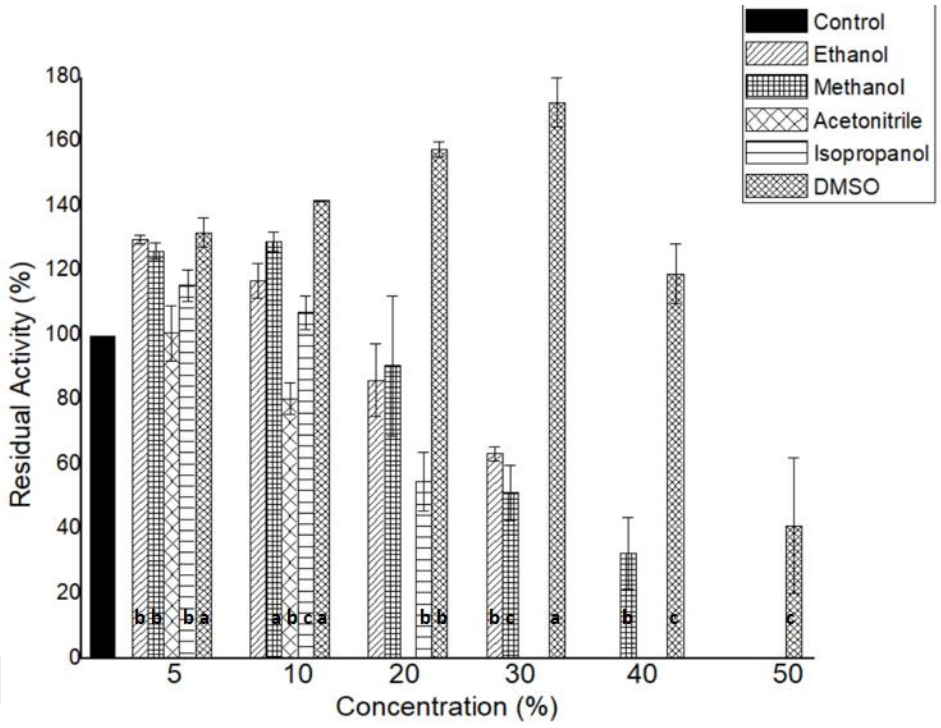



Figure 4.30 Residual activity of *Bd*FDH in some organic solvents (letters refer to difference from control and a for p≤0.001; b for p≤0.01; c for p≤0.05 )

### 4.1.9 Enzymatic Assay and Steady State Kinetics

As a result of kinetic characterization, it can be said that both cofactors can be used by BdFDH. If we compare the specificity, it prefers $NADP^+$ over $NAD^+$. The kinetic values of *Bd*FDH for substrates and the spesific activities with both cofactors were detected in 75 mM sodium phosphate buffer (pH 6.2) at 37 ˚C. In the presence of cofactors, sodium formate and ammonium formate were assayed as substrates used by FDH. The BdFDH acted on both reagents with similar activity results. The apparent $k_{cat}$, $K_M$ and $k_{cat}/K_M$ values of *Bd*FDH for both cofactors and formate were given comparatively with studied native $NADP^+$ dependent FDHs in Table 4.1 and 4.2, respectively.

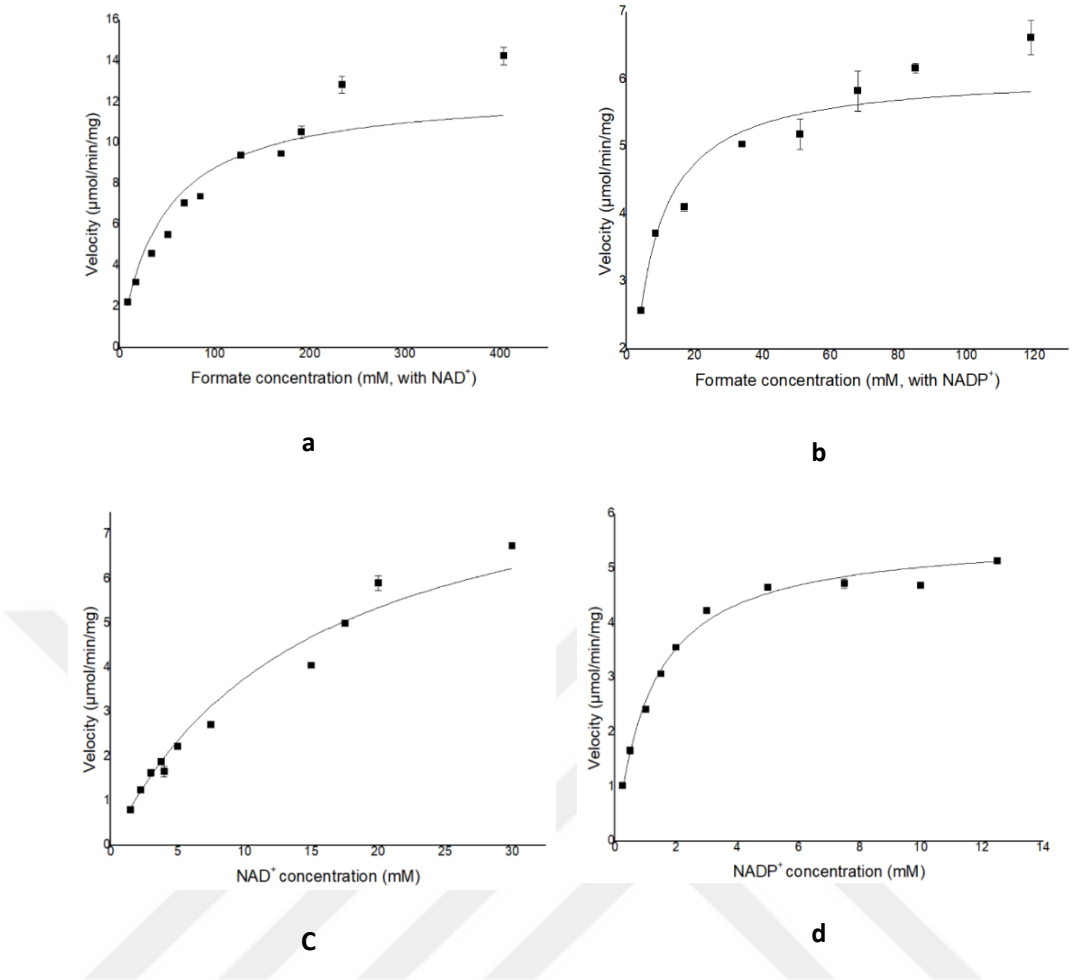



Figure 4.31 Michaelis–Menten curves (on velocity-substrate concentration) for BdFDH in presence of $NAD^+$ or $NADP^+$

As a result of kinetic parameters, the catalytic efficiency of *Bd*FDH is approximately 7.5-times higher in the presence of $NADP^+$ than in the presence of $NAD^+$. $K_M$ values for $NAD^+$, $NADP^+$ and formate (with $NADP^+$) are 14.7 mM, 1.17 mM and 5.66 mM, respectively. (Table 4.1, 4.2; Figure 4.31). The *Bd*FDH kinetic parameters are also given with its SD in Table 4.3.

Table 4.1 Kinetic constants of natural $NADP^+$ dependent FDHs for cofactors

| | **$NADP^+$** | | | **$NAD^+$** | | | |
|---|---|---|---|---|---|---|---|
| | **$K_M$ (mM)** | **$k_{cat}$ ($s^{-1}$)** | **$k_{cat}/K_M$** | **$K_M$( mM)** | **$k_{cat}$ ($s^{-1}$)** | **$k_{cat}/K_M$** | **$(k_{cat}/K_M)_{NADP+}/(k_{cat}/K_M)_{NAD+}$** |
| **BstFDH [4]** | 0.16 | 4.75 | 30 | 1.43 | 1.66 | 1.16 | 25.86 |
| **GraFDH [3]** | 0.85 | 3.96 | 4.66 | 6.5 | 5.77 | 0.88 | 5.30 |
| **Bsp184FDH [2]** | 1.1 | 3.07 | 2.79 | 15 | 0.57 | 0.04 | 73.66 |
| **Bsp383FDH [2]** | 0.7 | 2.77 | 3.96 | 7.6 | 0.82 | 0.11 | 36.76 |
| **BdFDH*** | 1.17 | 4.04 | 3.45 | 14.7 | 6.68 | 0.46 | 7.5 |

*: refers to this study

Table 4.2 Kinetics parameters of the FDHs in terms of formate (*Bd*FDH)

| | **$NADP^+$** | | | **$NAD^+$** | | |
|---|---|---|---|---|---|---|
| | **$K_M$ (mM)** | **$k_{cat}$ ($s^{-1}$)** | **$k_{cat}/K_M$ Formate** | **$K_M$ (mM)** | **$k_{cat}$ ($s^{-1}$)** | **$k_{cat}/K_M$ Formate** |
| **Bsp184FDH[2]** | 156.98 | 2.21 | 0.014 | 99.18 | 0.34 | 0.0034 |
| **Bsp383FDH[2]** | 126.79 | 6.12 | 0.048 | 50.13 | 0.77 | 0.015 |
| **BstFDH [4]** | 55.5 | - | - | - | - | - |
| **GraFDH[3]** | 200 | | | 80 | - | - |
| **BdFDH*** | 5.66 | 4.39 | 0.78 | 42.88 | 9.02 | 0.21 |

*: refers to this study

Table 4.3 Kinetics parameters of the *Bd*FDH for substrates

| | **NADP$^+$** | **NAD$^+$** | **Formate (with NAD$^+$)** | **Formate (with NADP$^+$)** |
|---|---|---|---|---|
| **$K_M$ (mM)** | 1.17±0.07 | 14.68±0.86 | 42.88±4.23 | 5.66±0.41 |
| **$k_{cat}$ ($s^{-1}$)** | 4.04±0.04 | 6.68±0.31 | 9.02±0.23 | 4.39±0.14 |
| **$k_{cat}/K_M$** | 3.45 | 0.46 | 0.21 | 0.78 |

## 4.2 Cloning, Expression and Characterization of FDH from *L. buchneri* NRRL B-30929

We screened another NADP$^+$ dependent FDH source by utilizing *Burkholderia stabilis* FDH (*Bst*FDH, ACF35003.1) as a query sequence in PHIBLAST program.

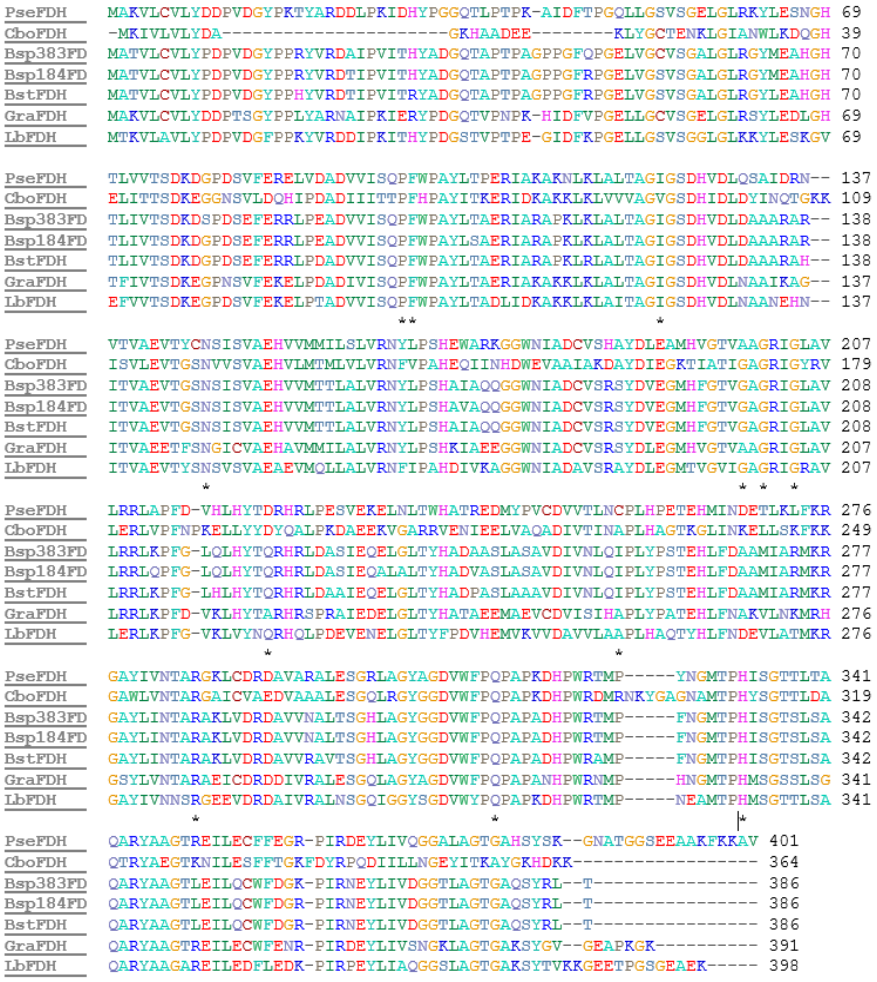



Figure 4.32 Sequence comparison of *Bd*FDH with reported NAD(P)$^+$ dependent FDHs.

An *fdh* gene from *Lactobacillus buchneri* NRRL B-30929 strain (*Lbfdh*, NC_015428; Figure 4.32) was selected among the putative FDH sequences. The given abbreviations for FDHs are; Bsp184FDH for *Burkholderia cenocepacia* PC184 FDH, BstFDH for *Burkholderia stabilis* FDH, Bsp383FDH for *Burkholderia lata* FDH, GraFDH for *Granulicella mallensis* MP5ACTX8 FDH PseFDH for Pseudomonas sp. FDH, CboFDH for *Candida boidinii* FDH in alignment. The FDH from *Lactobacillus buchneri* FDH is given as *Lb*FDH. The residues that play an important role in the catalytic cavity are shown by a star (*) symbol according to Tishkov and Popov [9]. The BioEdit software packages was used for alignment (Ibis Therapeutics, CA).

### 4.2.1 Cloning of LbFDH as C-terminal His Tagged Form

The vector pET23b(+) was used for cloning and expression, because of the His Tag region at te 3 prime of the cloning site. (Figure 4.33).

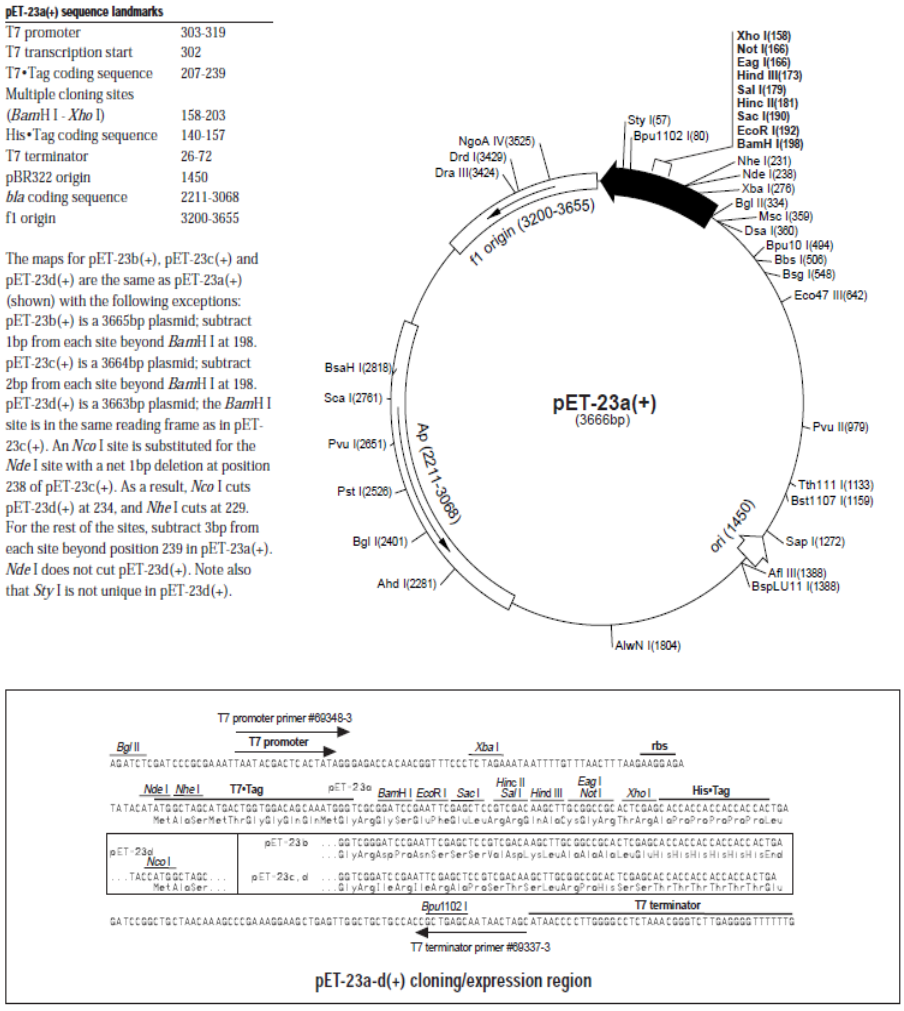



Figure 4.33 pET23b(+) vector sequence and map [99]

The sequence data of the putative *fdh* gene was used for designing mutation and cloning primers (Appendix- B Table 3). The *Lbfdh* gene was obtained as two separate fragments by PCRI and PCRII reactions using sequence-specific cloning and mutation primers (Figure 4.34). Then, the PCR products were recovered from the gel. The concentrations of these products were determined by Nanodrop spectrophotometer (PCRI: 100 ng and PCRII: 25 ng). The products were combined *via* PCR reaction and then the product was visualized on agarose gel. In addition, the *Lbfdh* was also obtained *via* PCR reaction by using only cloning primers to confirm the size of the fusion product (Figure 4.35 and Figure 4.36). As a result, to remove the *Nde*I recognition site, a silent mutagenesis was done on this gene (UniProt accession number: F4FW36) and then, the amplification process was done with cloning primers. The combined PCR product was recovered from gel and stored at -20°C.

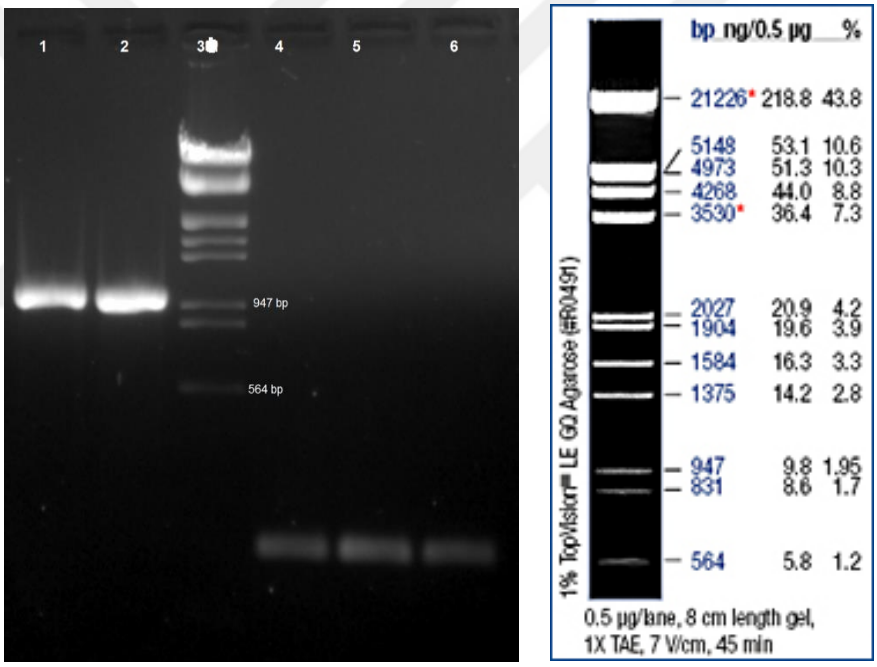



Figure 4.34 Post PCR product of *Lbfdh* on 1% agarose gel. 1,2: PCRI product (1007 bp), 3: 1 Kb DNA marker (Lambda DNA / EcoRI + HindIII), 4-5: PCRII product (206 bp)

Then, the pET23b-Lys plasmid DNA and PCR products were digested with *Nde*I and *Xho*I to get DNA with sticky ends for ligation process (Figure 4.37). The insert and vector were recovered from agarose gel and subjected to the ligation protocol. The colony PCR reaction was performed with ten colonies resulted from chemical transformation of recombinant plasmid into *E. coli* Top10. Then, 10 µl of the post PCR products were subjected to electrophoresis and the results confirmed the accuracy of ligation reaction.

The resulted DNA bands confirmed the integrity and insertion of *Lbfdh* into plasmid (Figure 4.38 and Figure 4.39). Then, the recombinant plasmids were isolated from competent cells and sequenced. The sequencing outputs confirmed that the gene including 1197 base pairs was successfully obtained with the histidine tag at C-terminus. The quantity of amino acid residues of enzyme increased to 407 by addition of hexa-histidine tag.

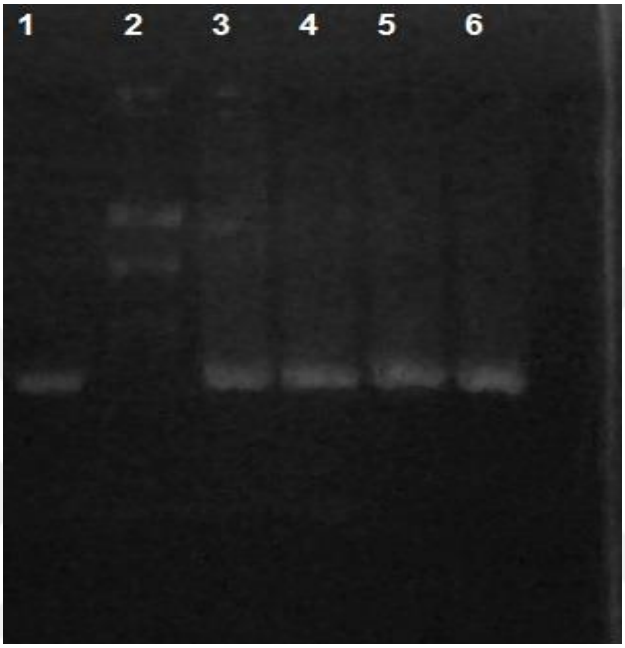



Figure 4.35 Post PCR products obtained by combining PCRI and PCRII products. 1: putative *Lbfdh* product amplified by PCR, 2: 1 Kb DNA marker (Lambda DNA / EcoRI + HindIII), 3-6: Combined PCRI and PCRII products

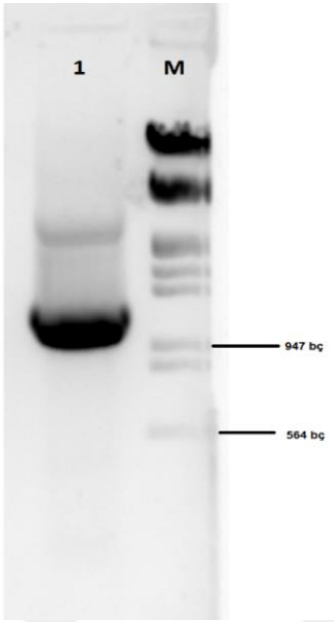



Figure 4.36 Combined PCRI and PCR II product on 1% agarose gel. 1: Post PCR product (about 1200 bp), M: DNA marker (Lambda DNA / EcoRI + HindIII)

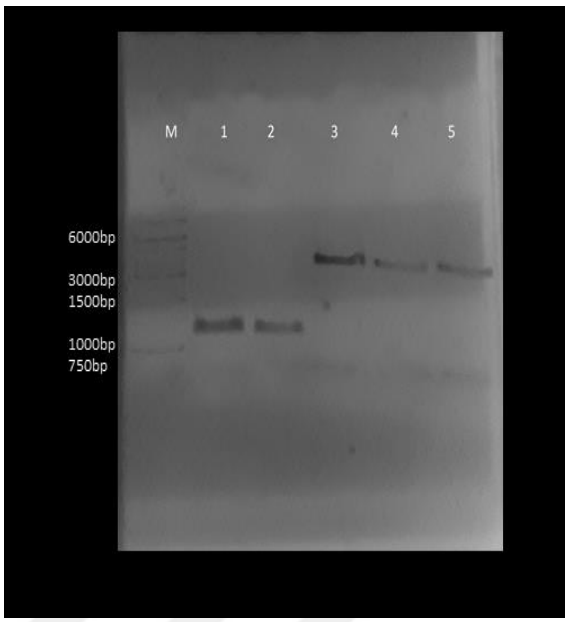



Figure 4.37 Restriction reaction products of pET23b-Lys and PCR products on agarose gel. (M) Marker; (1,2) Digested PCR product (1197bp); (3,4) Digested plasmid (3586 bp)

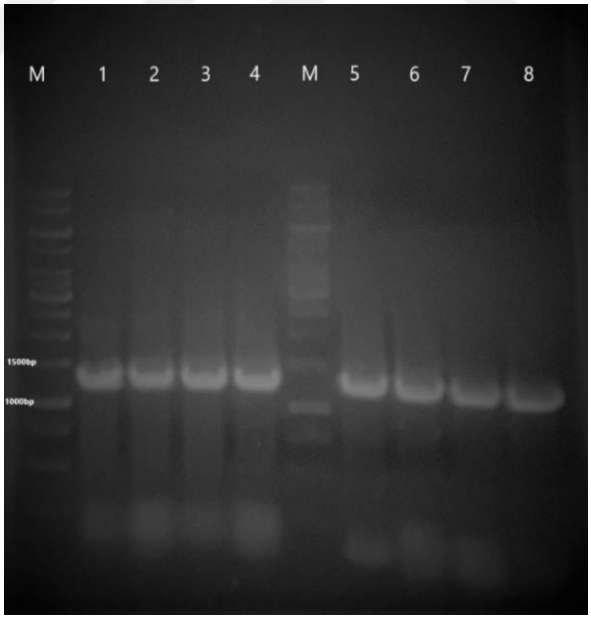



Figure 4.38 Colony PCR products on agarose gel. (M) DNA marker (1 kb); (1-8) PCR products of the eight colonies from ligation transformants, respectively

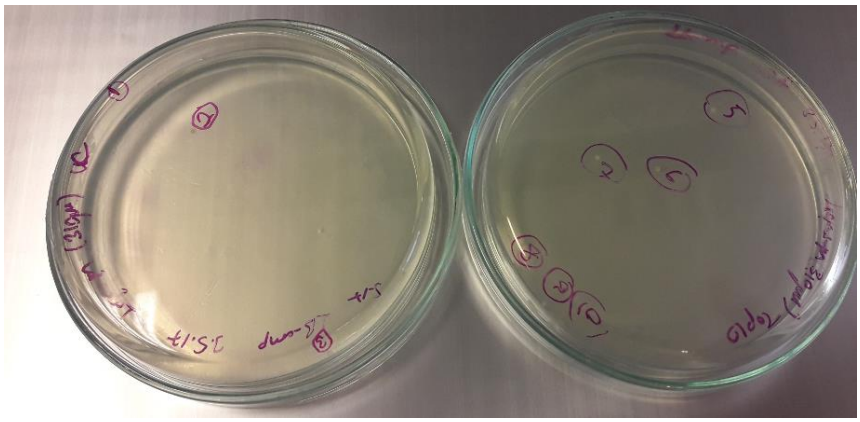


Figure 4.39 Colonies from transformation of ligation reaction

### 4.2.2 Expression and Purification of C-terminus His Tagged LbFDH

The *E. coli* BL21 (DE3)was used for protein production and the expression profile were examined on SDS-PAGE. The protein expression was induced with IPTG (0.5 mM at final concentration) at 30 °C for 8 h. The expression increased gradually during eight hours as seen on SDS-PAGE (Figure 4.40). The protein yield was approximately 25 mg/L IPTG induction at 30 ˚C for 16 h.

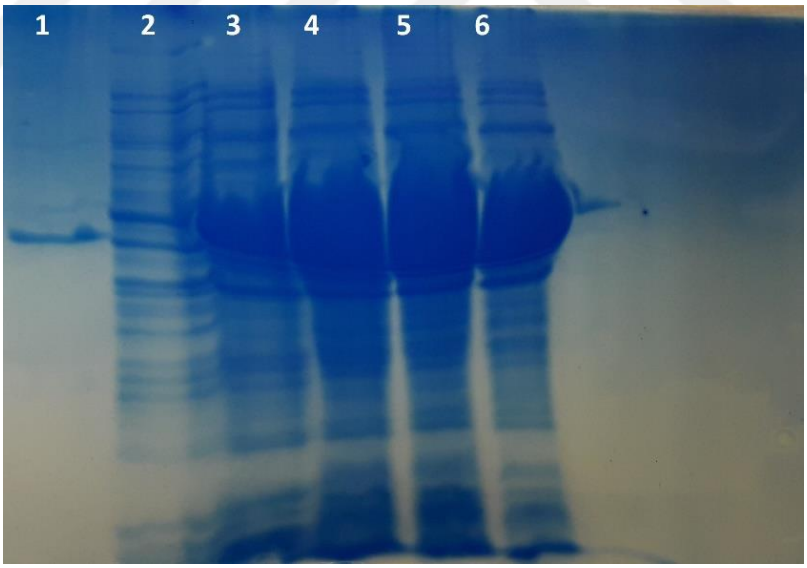



Figure 4.40 The expression profile of C-terminus His tagged *Lb*FDH at 30 °C. (1) Marker (Bsp383FDH); (2) cell pellet before IPTG induction; (3) after IPTG induction for 2 hours; (4) after IPTG induction for 4 hours; (5) after IPTG induction for 6 hours; (6) after IPTG induction for 8 hours.

The nickel affinity chromatography column was used for protein purification. According to the SDS-PAGE results, it can be said that the *Lb*FDH was expressed as a soluble protein and due to presence of a single homogeneous protein band on SDS-PAGE, the enzyme was ascertained to be pure. The SDS-PAGE results showed that the enzyme

monomer was approximately 44 kDa (Figure 4.41a). It was concluded that the overall molecular mass of enzyme was about 90 kDa according to the native-PAGE results (Figure 4.41b). The theoretically calculated mass of the LbFDH was 44,274 Da from its amino acid sequence (Figure 4.42). The MALDI-TOF method indicated that the molecular weight of the enzyme monomer is 44,801 Da (Figure 4.43). The calculated and the measured mass values are consistent with each other. The resolution power of instrument and the experimental error range might cause to this little difference between the obtained values.

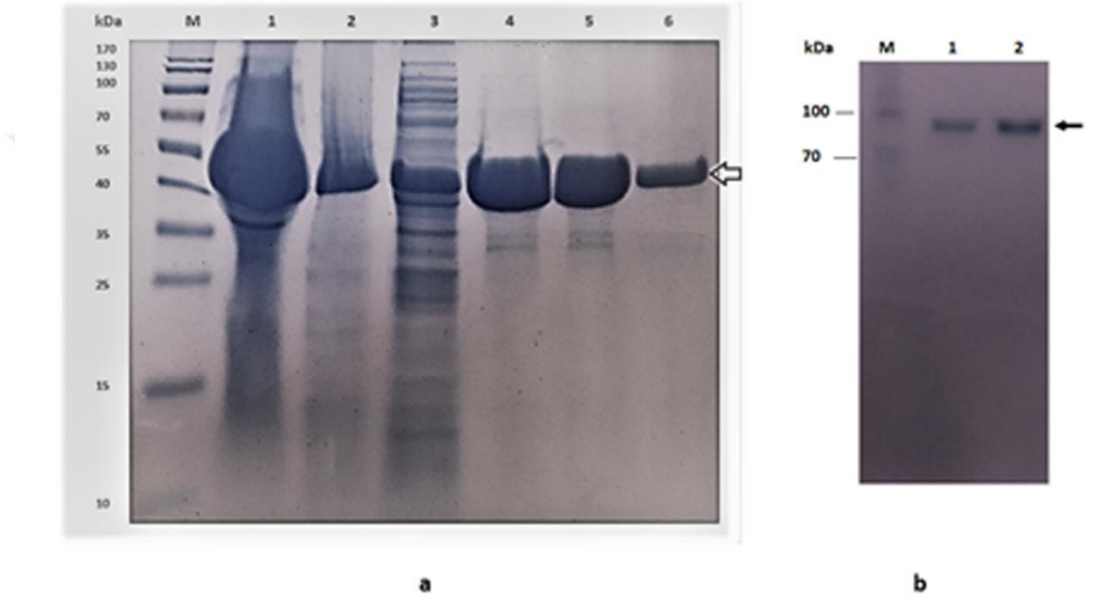



Figure 4.41 SDS-PAGE and Native-PAGE results for *Lb*FDH. **a)** The LbFDH purification fractions on SDS-PAGE. M, molecular mass marker (Thermo Scientific); 1, whole cell after autoinduction; 2, cell free extract after cell lysis; 3, washing fraction; 4-6, elution fractions with 100, 200 and 400 mM imidazole, respectively. **b)** Native-PAGE results for *Lb*FDH. Lanes: M, molecular mass marker; lanes 1st and 2nd were refer to 5 µl and 10 µl of *Lb*FDH per lane, respectively.

PROTEIN CALCULATOR v3.4

Back to the Calculator

```
MTKVLAVLYP DPVDGFPPKY VRDDIPKITH YPDGSTVPTP EGIDFKPGEL LGSVSGGLGL  60
KKYLESKGVE FVVTSDKEGP DSVFEKELPT ADVVISQPFW PAYLTADLID KAKKLKLAIT  120
AGIGSDHVDL NAANEHNITV AEVTYSNSVS VAEAEVMQLL ALVRNFIPAH DIVKAGGWNI  180
ADAVSRAYDL EGMTVGVIGA GRIGRAVLER LKPFGVKLVY NQRHQLPDEV ENELGLTYFP  240
DVHEMVKVVD AVVLAAPLHA QTYHLFNDEV LATMKRGAYI VNNSRGEEVD RDAIVRALNS  300
GQIGGYSGDV WYPQPAPKDH PWRTMPNEAM TPHMSGTTLS AQARYAAGAR EILEDFLEDK  360
PIRPEYLIAQ GGSLAGTGAK SYTVKKGEET PGSGEAEKSL EHHHHHH               407
```

**Amino Acid Count**

| Residue | Number Found |
|---|---|
| A Ala Alanine | 39 |
| R Arg Arginine | 15 |
| N Asn Asparagine | 13 |
| D Asp Aspartate | 26 |
| Q Gln Glutamine | 9 |
| E Glu Glutamate | 30 |
| G Gly Glycine | 36 |
| H His Histidine | 16 |
| I Ile Isoleucine | 19 |
| L Leu Leucine | 34 |
| K Lys Lysine | 24 |
| M Met Methionine | 8 |
| F Phe Phenylalanine | 10 |
| P Pro Proline | 27 |
| S Ser Serine | 21 |
| T Thr Threonine | 21 |
| Y Tyr Tyrosine | 16 |
| V Val Valine | 39 |
| W Trp Tryptophan | 4 |
| C Cys Cysteine | 0 |
| U SeC Selenocysteine | 0 |

**Isotopically Averaged Molecular Weight = 44273.9648**

Figure 4.42 Theoretical calculation of molecular weight of recombinant *Lb*FDH

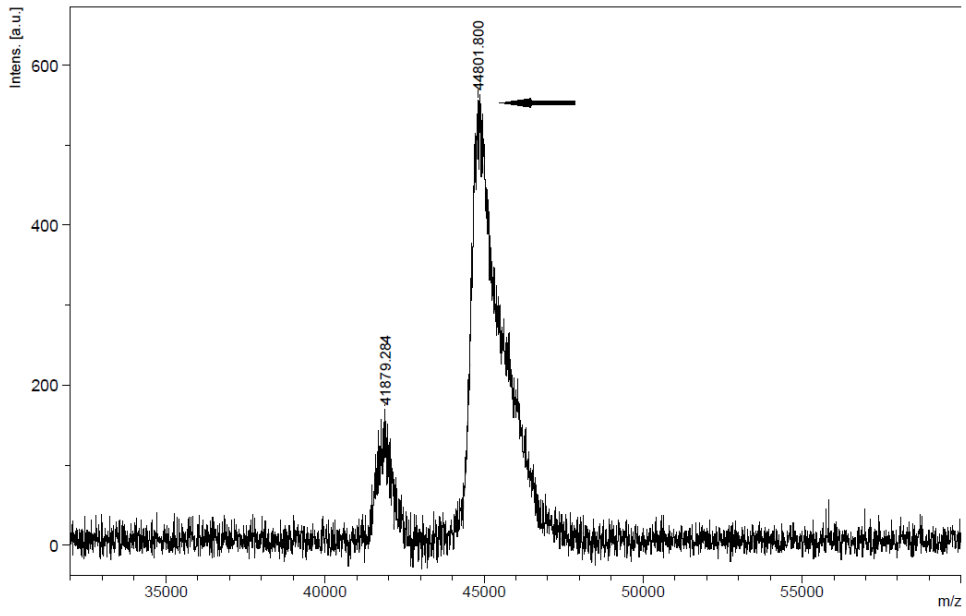
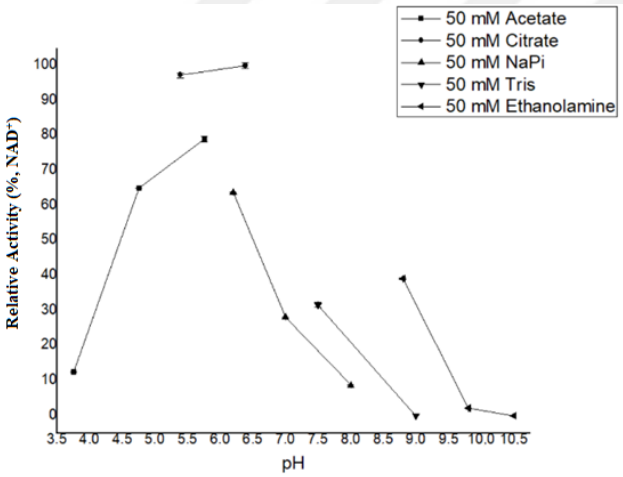



Figure 4.43 MALDI-TOF MS analysis for *Lb*FDH (highlighted by arrow).

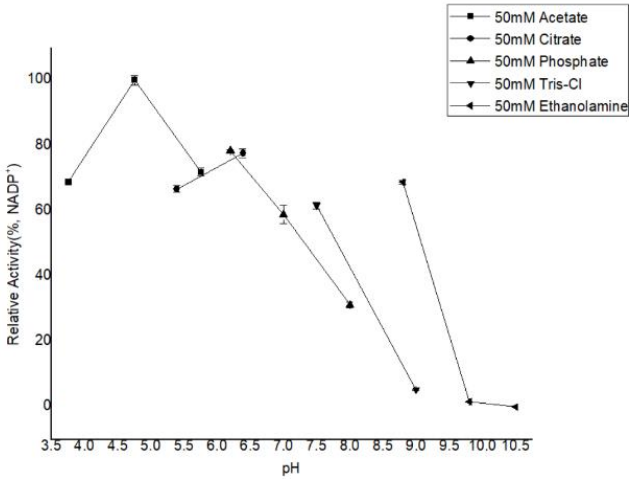
### 4.2.3 Effect of pH and Temperature on LbFDH

The pH and temperature profile of *Lb*FDH were examined *via* enzymatic activity in a certain pH range (pH 3.8–10.5) and temperature range (15–68 ºC), respectively and additionally the thermostability of enzyme was investigated. The results indicated that the LbFDH was quite active between pH 4.8-6.2 with each cofactors in terms of the formate oxidation (Figure 4.44a and Figure 4.44b).

The temperature effect on enzyme was examined by determining the variation of activity between 15-68 ˚C. The 60 ˚C (with $NADP^+$) and 50 ˚C (with $NAD^+$) were the optimum temperatures for the enzyme. The *Lb*FDH has a $T_{50}$ value between 65-68 ˚C ($T_{50}$ value: a temperature value which has the half of the activity of enzyme) (Figure 4.45). At several temperatures ranging from 50 to 60 ˚C, the thermal stability of enzyme was examined in the presence of $NADP^+$ (Figure 4.46). As a result, the half-lives of the enzyme at 50 ˚C, 55 ˚C and 60 ˚C were determined to be 9 h, more than 3 h and less than 1 h, respectively. This enzyme lost its activity at 60 ˚C and 65 ˚C, after 1 h and 1 min, respectively. In addition, DSC results indicated that the $T_m$ value for *Lb*FDH was 78 ˚C (Figure 4.47). The highest activities were obtained at pH 4.8 with $NADP^+$ (24.6 ± 0.2 U/mg at 60 ˚C) and at pH 6.4 with $NAD^+$ (0.98 ± 0.003 U/mg at 50 ºC).




**a)**




**b)**

Figure 4.44 pH- activity profile for *Lb*FDH **a)** in presence of $NAD^+$ **b)** in presence of $NADP^+$

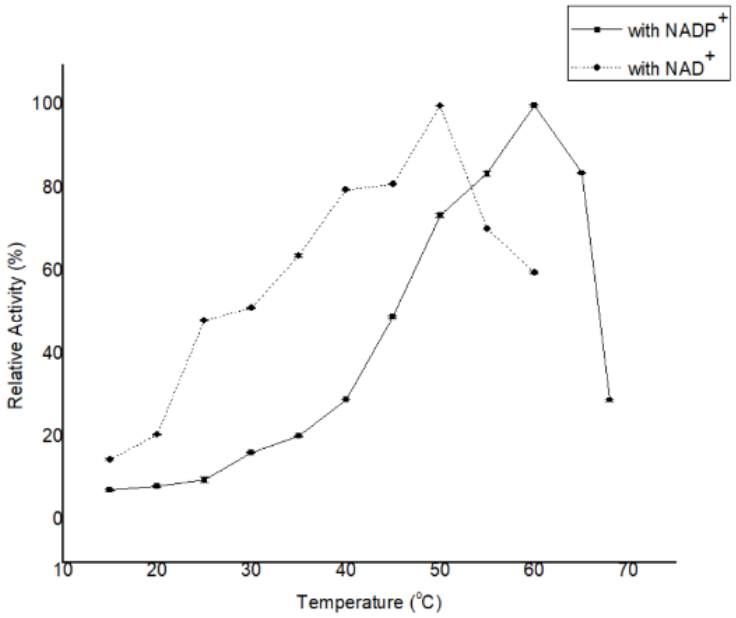



Figure 4.45 Activity-temperature profile for *Lb*FDH.

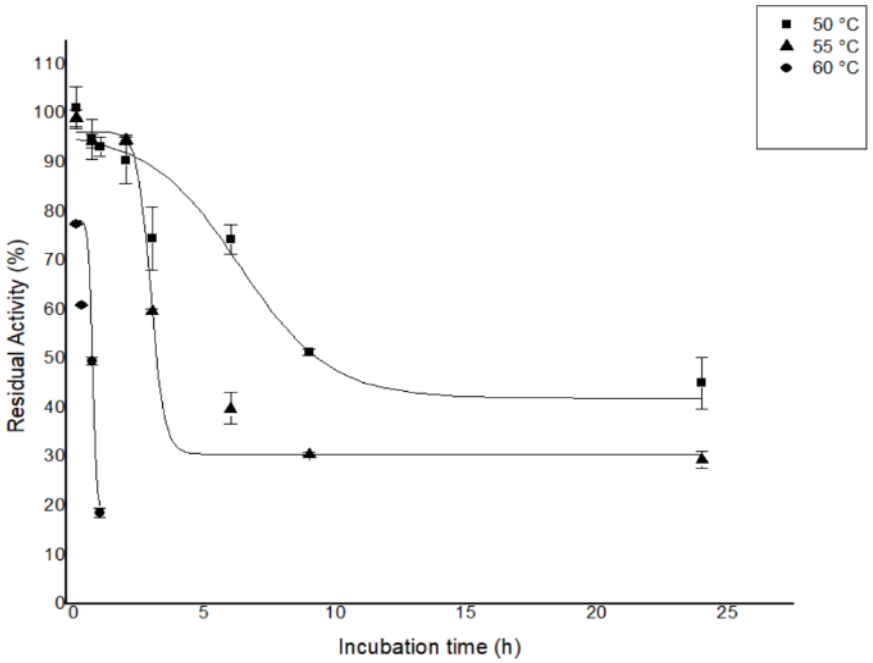



Figure 4.46 Thermostability profile for *Lb*FDH.

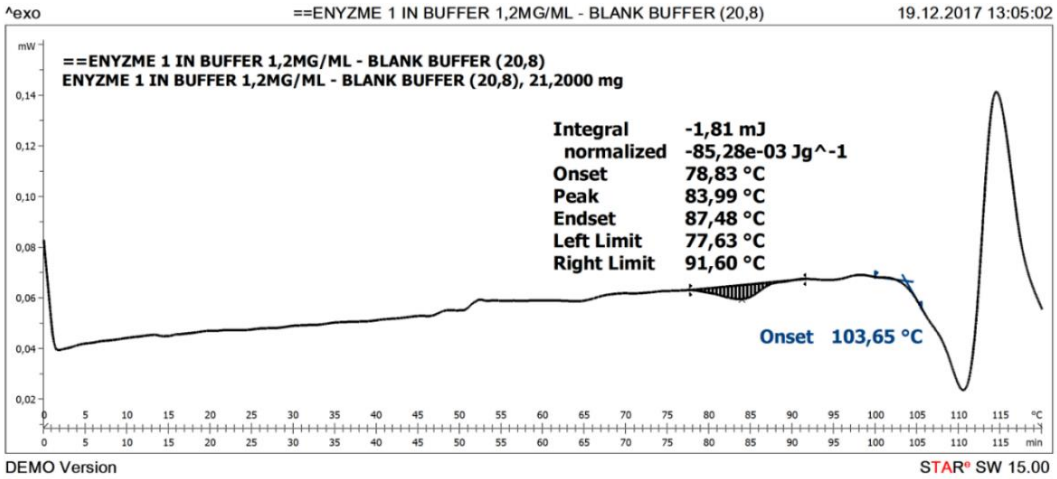



Figure 4.47 Differential scanning calorimetry (DSC) analysis for *Lb*FDH

### 4.2.4 Effects of Metal Ions and Organic Solvents on Enzyme

To investigate the effect of cations on the enzyme activity, the standard enzyme assay was performed with several metallic compounds. The results showed that this enzyme lost its overall activity by 10 mM of $FeCl_3$, $Na_2MoO_4$, $Na_2WO_4$ and 1 mM $Na_2WO_4$ at final concentration. None of following compounds, $ZnCl_2$, $NiSO_4$, $MnCl_2$, $CaCl_2$ and $MgSO_4$ at 1 mM and 10 mM concentration, affected enzyme activity in significant manner (Figure 4.48).

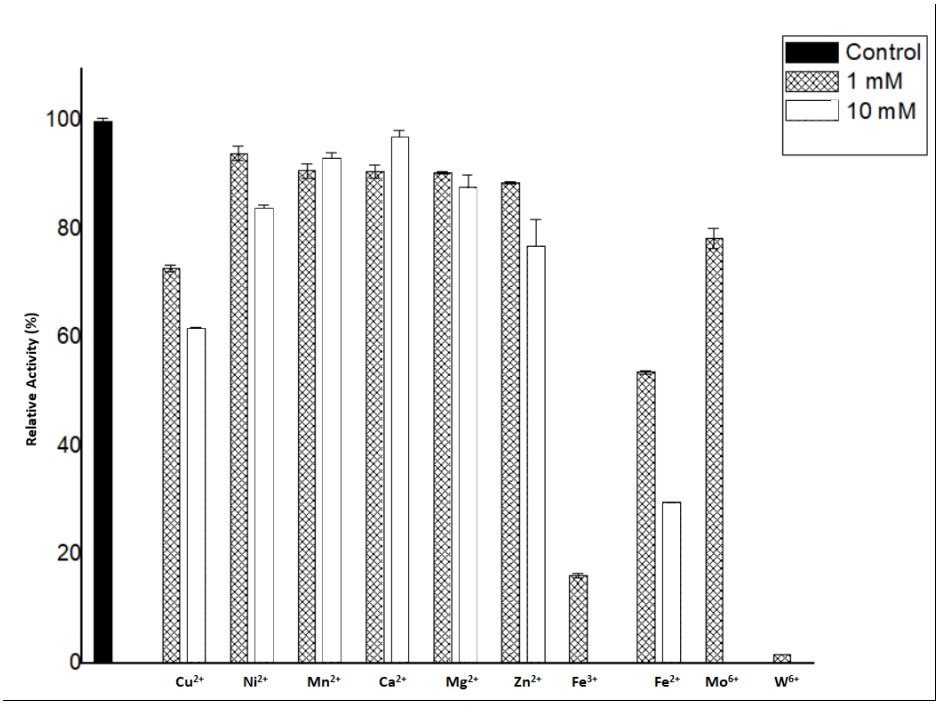



Figure 4.48 Metal ions effect on *Lb*FDH activity.

The effect of organic solvent on the enzyme activity and solvent resistance of enzyme were also investigated. The remaining activity of enzyme was determined at six concentration levels (from 5% to 50% (v/v)) of organic solvents to investigate the organic solvent effect. The LbFDH could be used with DMSO and also acetonitrile up to 20% (Table 4.4) and after incubation in 20% of acetonitrile and DMSO for 6 hours the activity of enzyme almost did not decrease (Figure 4.49). In addition, after incubation of enzyme in 20% DMSO and acetonitrile for two weeks, the protected enzyme activities were 88% and 75%, respectively.

In different storage conditions, the residual activity of *Lb*FDH was also determined by enzymatic assay without and with glycerol as a cryoprotectant (Figure 4.50). The enzyme has more stability at -80 ˚C than in the other conditions (-20 ˚C, 4 ˚C and 25 ˚C) in both cases in terms of glycerol.

Table 4.4 Residual activity profile for *Lb*FDH in various cosolvents

| **Organic Solvent** | **5%** | **10%** | **20%** | **30%** | **40%** | **50%** |
|---|---|---|---|---|---|---|
| Acetonitrile | +++ | +++ | +++ | + | - | - |
| Methanol | +++ | +++ | + | + | - | - |
| DMSO | +++ | +++ | ++ | + | + | + |
| Isopropanol | +++ | ++ | + | - | - | - |
| Ethanol | +++ | ++ | + | - | - | - |

- 66–100% (+++), 33–66% (++),1–33% (+)

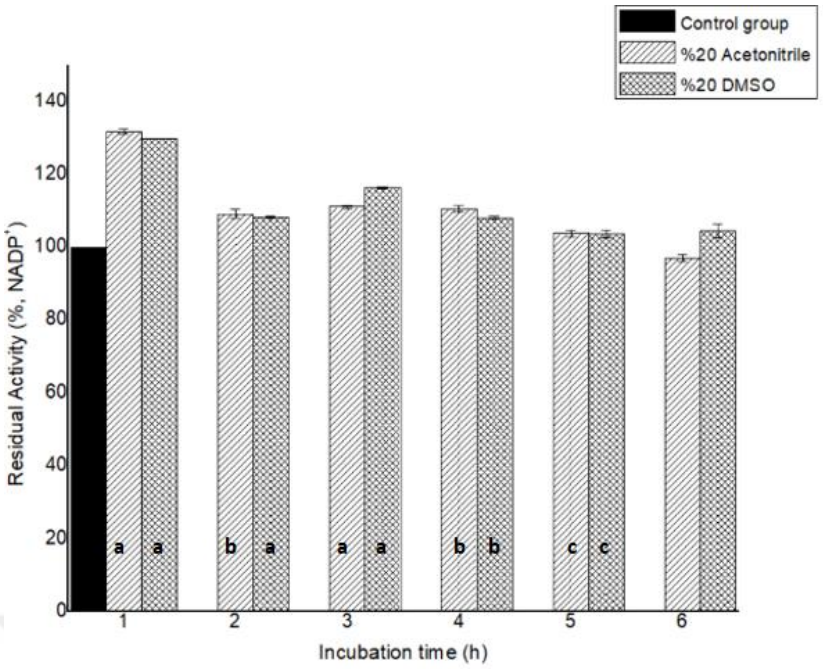



Figure 4.49 Organic solvent stability for *Lb*FDH (letters refer to difference from control and a for p≤0.001; b for p≤0.01; c for p≤0.05 ).

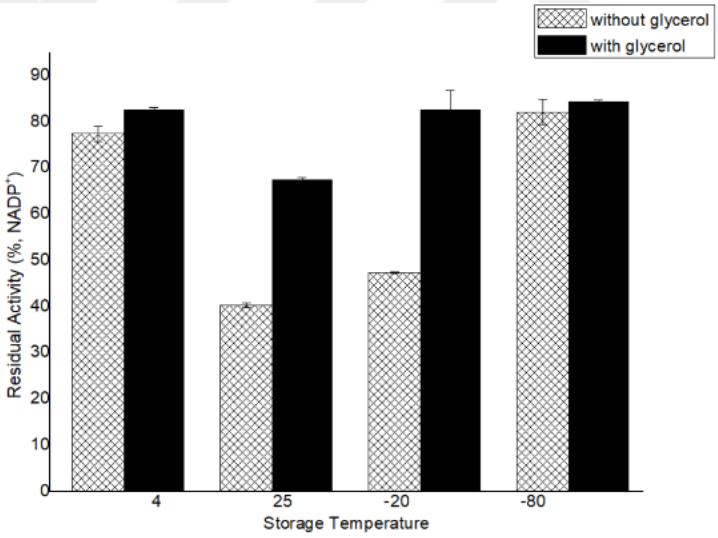



Figure 4.50 Stability profile of LbFDH in different storage conditions.

### 4.2.5 Enzymatic Assay and Steady State Kinetics

The obtained putative enzyme has a formate dehydrogenase activity. The results of experiments showed that the *Lb*FDH is able to use both cofactors. However, it has a higher specificity towards $NADP^+$. The specific activities were detected in 100 mM citrate buffer (pH 6.4) and 100 mM acetate buffer (pH 4.8) at 30 $^oC$, for $NAD^+$ and $NADP^+$, respectively. The same buffers were used for kinetic constant determination. Table 4.5 lists the $K_M$, $k_{cat}$ and $k_{cat}/K_M$ values determined for *Lb*FDH and for other $NADP^+$

dependent enzymes. The $K_M$ constants were 0.12, 1.68 and 49.8 for $NADP^+$, $NAD^+$ and formate (with $NADP^+$), respectively (Table 4.5 and 4.6; Figure 4.51).

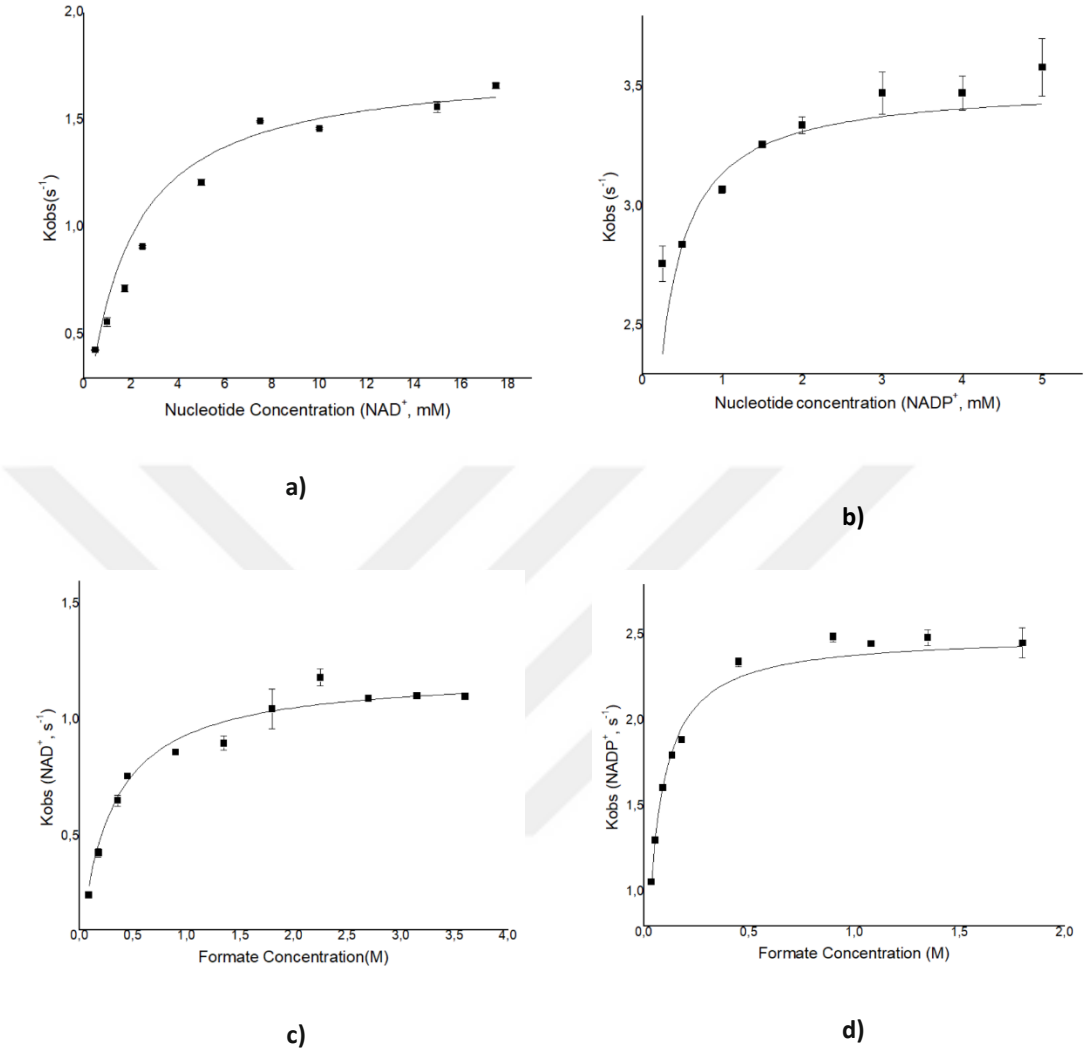



Figure 4.51 Michaelis-Menten graphs for *Lb*FDH.

Table 4.5 Kinetic constants for $NADP^+$ dependent FDHs

| | **NADP+** | | | **NAD+** | | | |
|---|---|---|---|---|---|---|---|
| | **$K_M$ (mM)** | **$k_{cat}$ ($s^{-1}$)** | **$k_{cat}/K_M$** | **$K_M$ (mM)** | **$k_{cat}$ ($s^{-1}$)** | **$k_{cat}/K_M$** | **$(k_{cat}/K_M)_{NADP+}/(k_{cat}/K_M)_{NAD+}$** |
| **LbFDH*** | 0.12 | 3.51 | 29.25 | 1.68 | 1.76 | 1.05 | 27.9 |
| **BstFDH[4]** | 0.16 | 4.75 | 30 | 1.43 | 1.66 | 1.16 | 25.86 |
| **GraFDH[3]** | 0.85 | 3.96 | 4.66 | 6.5 | 5.77 | 0.88 | 5.3 |
| **CmetFDH[2]** | 7 | 0.005 | 0.0001 | 0.2 | 1.67 | 8.35 | $8.6x10^{-5}$ |
| **Bsp184FDH [2]** | 1.1 | 3.07 | 2.79 | 15 | 0.57 | 0.04 | 73.66 |
| **Bsp383FDH [2]** | 0.7 | 2.77 | 3.96 | 7.6 | 0.82 | 0.11 | 36.76 |
| **CmetFDH D195Q[2]** | 3.8 | 1.38 | 0.36 | 1.3 | 1.67 | 1.29 | 0.28 |
| **Bsp184FDH Q223D[2]** | 111 | 0.43 | 0.004 | 0.2 | 1.82 | 9.1 | $4.22x\ 10^{-4}$ |
| **Bsp383FDH Q223D[2]** | 32 | 0.18 | 0.006 | 0.2 | 1.9 | 9.5 | $5.96x\ 10^{-4}$ |
| **CboFDH D195Q/Y196H[12]** | 1.7 | 0.44 | 0.26 | 1.8 | 0.49 | 0.27 | 0.96 |
| **CboFDH D195Q/Y196R/ Q197N[15]** | 0.029 | 0.79 | 29.1 | 0.36 | 0.62 | 1.7 | 17.1 |
| **CmFDH D195S[7]** | - | - | $8.3x\ 10^{-3}$ | 4.70 | 1.6 | 0.34 | 0.024 |
| **MycFDH 3M[16]** | 0.92 | 7.89 | 8.58 | 1.09 | 8.22 | 7.54 | 1.14 |
| **MycFDH 4M[16]** | 0.147 | 3.08 | 21 | 4.10 | 5.18 | 1.26 | 16.7 |
| **PseFDH, mutant [8]** | 0.150 | 2.5 | 16.67 | 1 | 5 | 5 | 3.3 |
| **SceFDH D196A/Y197R[8]** | 7.60 | 0.16 | 0.021 | 8.40 | 0.12 | 0.01 | 1.5 |

*: refers to this study

Table 4.6 Kinetic constants of FDHs for formate

| | NADP+ | | | NAD+ | | |
|---|---|---|---|---|---|---|
| | **$K_M$ (mM)** | **$k_{cat}$ ($s^{-1}$)** | **$k_{cat}/K_M$ Formate** | **$K_M$ (mM)** | **$k_{cat}$ ($s^{-1}$)** | **$k_{cat}/K_M$ Formate** |
| **LbFDH*** | 49.8 | 2.50 | 0.05 | 284.59 | 1.20 | 0.004 |
| **BstFDH[4]** | 55.5 | - | - | - | - | - |
| **GraFDH[3]** | 200 | | | 80 | - | - |
| **CmetFDH[2]** | - | - | - | 8.29 | 6.99 | 0.84 |
| **Bsp184FDH[2]** | 156.98 | 2.21 | 0.014 | 99.18 | 0.34 | 0.0034 |
| **Bsp383FDH[2]** | 126.79 | 6.12 | 0.048 | 50.13 | 0.77 | 0.015 |

*: refers to this study

Recombinant DNA methods are frequently used to produce proteins in order to get high levels of expression for both applied and fundamental research purposes. These proteins are generally expressed as fusion or chimeric proteins. To provide a tag is one of the application of fusion partner [100]. For large scale purification of chimeric proteins, the affinity tags are generally used because of the relatively quick, easy and efficient purification steps [101]. Engineered histidine affinity tags and Immobilized-Metal Affinity Chromatography (IMAC) have advantages for easy isolation of recombinant proteins [101]. As an affinity tag, polyhistidine-tag has an amino acid chain that contains of at least six histidines inserted at the C- or N-terminus of sequence [102], [103]. The decision about the positioning of the tag usually remains difficult and it related with the conformity and primary structure of the protein and should be detected in experimental manner [99]. If judged from the most of papers reported, the more universal and appropriate solution for the position of His tag is that to insert it on the N-terminus of the protein . The histidine tags generally do not interfere the protein function and protein folding [101]. Furthermore, the biochemical properties of the target protein may enhance *via* incorporating an affinity tag. However, it has some drawbacks such as changes in the protein conformation, alteration in biological activity, misfolding or loss of solubility or activity of the protein and lovering expression level [101], [104], [105]. Although His-tag engineering has been extensively carried out for protein purification, the effect of the tagging position on enzyme has not been investigated well [106]. Herein, we firstly aimed to get a new and efficient $NADP^+$ dependent FDH and after that to examine the C- and N-terminal histidine tag effect on the activity and solubility of enzyme. Therefore, both C- and N-terminus His tagged *Bdfdh* plasmids were constructed and the protein was

expressed. Then, the expression profiles of each proteins were analysed on SDS-PAGE and the results indicated that the expression level may not affected by the His tag position at a visible rate. Then, the C- and N- terminus His tagged *Bd*FDH protein were purified by IMAC and we realized that the N-terminus His tagged protein couldn't be released into cell free axtract, attributable to the protein was inclusion body. Hence, to get the fusion protein as a soluble form, a slower expression was carried out by decreasing temperature and expression time optimization was performed at the proper temperature. Just a few quantity (~0.5 mg) of BdFDH recovered after the expression at 16 °C by IPTG induction despite all these efforts. Because of the few quantity and activity of enzyme, we concluded that N-term His tag may be inconvenient for this region. As we learned from literature, N- terminal portion of bacterial FDHs is a prolonged loop and it contains a remarkable part of the subunit of enzyme. Therefore, this structure plays role in configuration of intersubunit contacts [9]. In addition, Tishkov and Popov [9] ascertained that the formate dehydrogenase is a greatly conservative enzyme. The analysis of conserved residues locations in the sequence of the *Pseudomonas* sp. 101 FDH has indicated that the roles of them are various such as some of these residues (e.g., the ion pair Lys2-Asp89) maintain the stability of the subunit form, others (Arg163, Asn164, Trp177, Ala180, Asp188) are involved in intersubunit interactions and only some of them are involved in catalytic process [9]. Therefore, we thought that the his tag at the N-terminal region may have an unfavourable effect on the interaction and stabilization of intersubunit contact, so that the protein may be unfolded or misfolded and may lost its three dimensional structure that is essential for functionality and solubility. Then, the C-terminal His tagged construct was used for production of the enzyme in an active and soluble form. After protein purification, SDS-PAGE analysis and all characterization steps were performed on C terminal His tagged enzyme. The results showed that the BdFDH was expressed as a soluble protein and it has a formate dehydrogenase activity (Figure 4.21 and Figure 4.22).

The $NAD^+$ dependent FDHs and also the enzymes in D-isomer specific 2-hydroxy acid dehydrogenases superfamily include a conserved nucleotide binding pattern Gly(Ala)XGlyXXGly$X_{17}$Asp for $NAD^+$ [68]. According to the protein engineering studies on FDHs indicated that the mutagenesis of the aspartate in the $NAD^+$ binding pattern to some aminoacids such as alanine, glutamine or serine is particularly favourable for $NADP^+$ binding [7], [8], [12], [15]. We selected the protein sequences that lack

aspartatic acid at this conserved point to get the $NADP^+$ dependent FDH. The *Bd*FDH includes a serine residue instead of aspartate. Due to its net charge equal to zero, the enzyme can accept both cofactors. Our enzymatic assay results are consistent with this information and the cofactor binding region of *Bd*FDH has this structure, which is appropriate for double cofactor binding, however it prefers $NADP^+$ over $NAD^+$. As understood from kinetic values in Table 4.1, the catalytic efficiency of *Bd*FDH in the presence of $NADP^+$ is almost 7.5 fold higher than the $(k_{cat}/K_M)^{NAD+}$ value of *Bd*FDH. Wu et al. [15] carried out site saturation mutagenesis for *Cbo*FDH in Asp195 and Tyr196 residues to get $NADP^+$ dependent FDHs and two mutant FDHs, D195Q/Y196R and D195S/Y196P, were obtained. Both of them had a significant $NADP^+$ specificity. The $(k_{cat}/K_M)^{NADP+}/(k_{cat}/K_M)^{NAD+}$ value of D195S/Y196P and D195Q/Y196R are 0.2 and 2.1, respectively. These residue alterations in that points were also utilized in our protein sequence mining stage to get a feasible $NADP^+$ dependent FDH. The *Bd*FDH has both variations at these regions and our experimental results were compatible with these informations on $NADP^+$ preference. The $K_M$ constants for formate (with $NADP^+$), $NADP^+$ and $NAD^+$ and, are 5.66, 1.17 and 14.7 mM, respectively (Table 4.1 and 4.2; Figure 4.31). As seen in Table 4.2, in the presence of each coenzymes, the $K_M$ for formate was relatively low among the other reported $NADP^+$ dependent FDHs [2], [3], [4]. The $k_{cat}/K_M$ value of *Bd*FDH for formate were higher than the value for the aforementioned $NADP^+$ dependent FDHs in the presence of both cofactors, separately (Table 4.2). It can be concluded that the interaction of formate with *Bd*FDH is better than the other FDHs which have a specificity towards $NADP^+$ with both cofactors.

The molecular mass of the monomer for this protein was predicted to be about 43 kDa by SDS-PAGE and almost 90 kDa according to native-PAGE results. Therefore, it can be suggested that it has a homodimer structure, that is it has two identical subunits of about 43 kDa. The native form of other known FDHs, such as the enzyme from Pseudomonas sp. 101 [107], *M. vaccae* N10 [54], *C. boidinii* [14], *Bacillus* sp. F1 [55] is also homodimer. The $NAD(P)^+$ dependent bacterial FDHs display an optimum temperature between 50-60 ˚C. Some reported FDHs from *Bacillus* sp. F1 [55], *Burkholderia stabilis* [4] and Pseudomonas sp. 101 [68] can act at 60, 55 and 50 °C, respectively. The *Bd*FDH has an optimum temperature at 37 °C which is the lowest value among bacterial $NAD(P)^+$ dependent FDHs. Therefore, it can be utilized in biocatalysis that require mild

temperatures. The optimum pH of enzyme is between 5.8 and 6.2, making *Bd*FDH a promising enzyme for reactions that need to be carried out in acidic pHs.

In addition, *Bd*FDH is highly tolerant to DMSO. As known from literature, enzymatic reactions containing organic solvents have many applications due to their abilities on substrate solubility and enzymatic selectivity. Therefore, the availability of enzymes in organic solvents can increase the utilization of enzymes in biotechnological applications rather than aqueous media [108]. DMSO, ethanol and methanol are recognized as quite efficient denaturing organic solvents for lots of proteins, because they have a negative effect on the secondary and tertiary forms of proteins due to their high polarity and solubilisation capability [109]. However, the *Bd*FDH has a strong tolerance to the abovementioned organic solvents, particularly DMSO. The *Bd*FDH activity can be enhanced by certain DMSO concentrations (up to 40% (v/v)). There is no reported information about activity enhancing ability of DMSO on $NADP^+$ dependent FDHs. Both increasing substrate solubility and enhancing the *Bd*FDH activity makes DMSO more valuable. In terms of stability, *Bd*FDH had almost protected 86% of its activity in 30% DMSO after 2 hours incubation. Therefore, it could be used for recycling processes of coenzymes in certain enzyme based reactions containing low water solubility substrates (coupled with cyclohexanone monooxygenase, cytochrome P450 etc.) [2]. Either rational design or random mutagenesis could be used to increase the enzyme activity in DMSO to benefit much more from this solvent tolerant enzyme.

In addition, we used a pathogenic bacterium, *L.buchneri* NRRL B-30929, as an enzyme source and obtained another $NADP^+$ dependent FDH and also suggested that it may be used as a cofactor regenerator in various biotransformations. The *Lb*FDH was fully characterized in terms of temperature range of activity, molecular mass, optimum pH, kinetic values, cofactor preference, organic solvent and metallic ion resistance. The *Lb*FDH has a homodimeric structure as *Bd*FDH according to the SDS-PAGE and native-PAGE results and consistent with the literature [14], [54], [55], [107].

According to thermal stability results, *Lb*FDH has a beneficial thermostability in comparison with patented $NADP^+$ dependent Bsp184FDH and Bsp383FDH [2] and it is better than earlier reported *Gra*FDH [3] since it kept about 100% of its activity at 55 °C for 2 h. Moreover, the *Lb*FDH has the highest Tm value with 78 °C among all studied FDHs. Pseudomonas sp. 101 FDH is reported with its higher Tm value with 67.6 °C so far and the melting temperatures of known FDHs are in the range of 57.9–64.5 °C [6].

Therefore, we can concluded that the thermostability of *Lb*FDH is better than mentioned FDHs.

Organic solvent tolerant capability is a crucial point for industrial usage of enzymes because of solubilisation effect of organic solvents rather than water. Since water has a weak solvent ability in organic chemistry [108]. The *Lb*FDH has a favorable tolerance to acetonitrile and DMSO for a long period (Table 4.4), therefore, it may be utilized as a promising regenerator in bioconversion of substrates which have low solubility index in water. As an example, the NADPH dependent cyclohexanone monooxygenase can be used with $NADP^+$ dependent formate dehydrogenases in the synthesis of chiral lactones, to supply cofactor economically [2]. Because of the monooxygenase substrates are mostly hydrophobic, the helper solvents such as DMSO is required for solubility of substrates [109]. Therefore, *Lb*FDH may be used as an attractive organic solvent stable regenerator in such reactions. The statistical analysis indicated that the data were significant.

The pH value around 7.0 is an optimum pH for $NAD^+$ dependent FDHs. At pH values below 6.0, these group of enzymes generally deceive their activity [68]. On the other hand, most of $NADP^+$ dependent FDHs reported so far display an optimum pH between 6.0-7.5 [2], [3], [4]. Therefore, we can indicate that *Lb*FDH is a significant enzyme among aforementioned FDHs with being active at low pHs (pH 4.8-6.2) and in the presence of $NADP^+$ it has a broader pH range for activity and narrower range with $NAD^+$. We can compare it with mutant FDHs from *C. methylica and C. boidinii* which have activity at pH 5.5-6.0. Even so, the *Lb*FDH has lower optimum pH than aforementioned mutants [12], [18]. In this aspect, *Lb*FDH may be utilized as an NADPH regenerator for reactions required acidic pH values [2].

In addition, the glycerol effect for storage of *Lb*FDH at various temperatures was examined. According to experimental results, for long term storage, protect the enzyme in glycerol at -80 ◦C is preferable. This feature may be ascribed to the capability of glycerol to protect the stability of enzyme in aqueous solution.

As we mentioned before, there is a higher specificity towards $NAD^+$ over $NADP^+$ in most of the reported $NAD(P)^+$ dependent FDHs. The outputs evidently showed that this enzyme has activity with both cofactors. Albeit, the *Lb*FDH displayed its highest specific activity in presence of $NADP^+$. The activity value with $NAD^+$ was only 11% of the specific activity of enzyme with $NADP^+$. The crucial amino acid related with specificity

of $NAD^+$ has been indicated as the Asp195 in the sequence of the FDH from *Candida boidinii* and Asp221 in the Pseudomonas sp. 101 FDH enzymes in the literature [9]. In the protein sequences of LbFDH and the query sequence (*Bst*FDH), the motif (Gly(Ala)XGlyXXGly$X_{17}$Asp) terminates with a glutamine residue [6], [66]. Thus, the negative charge is eliminated and the repulsion between the two acidic groups may be disappear and the $NADP^+$ can bind easily [3]. Another reason of preferring this bacterial source was likely because of its amino acid combination. It has not any cysteine residues. As we know, the modification of cysteine residues with impurities in the solution and with the high temperatures and also oxidation are main reasons for the inactivation of most FDHs [110]. Thus, we estimated that the absence of cysteine residues may lead to an enhancement in the stability of enzyme. As seen from the outputs, the multi aspect stability of novel enzyme confirms our estimations.

The enzyme has a greater specificity for $NADP^+$ than $NAD^+$ denoted as the $(k_{cat}/K_M)^{NADP+}/(k_{cat}/K_M)^{NAD+}$ value, which was approximately 27.86. The $NADP^+$ preference of *Lb*FDH is greater than all *Cm*FDH mutants [18]. For the same value, the *Lb*FDH is better than the other formate dehydrogenases given in Table 4.5 except for patented *Bsp*383FDH and *Bsp*184FDH. Although other reported equivalent formate dehydrogenase have close values for $NADP^+$ affinity, the *Lb*FDH has the best $K_M$ value with 0.12 mM among them. Its $k_{cat}/K_M$ constant has almost similar value with *Bst*FDH and *Cbo*FDH D195Q/Y196R/Q197N mutant in presence of $NADP^+$, however, it is better than the other FDHs, which are given in Table 4.5. The $K_M$ constant for formate is also better than the reported native $NADP^+$ dependent FDHs. The *Lb*FDH has a 24.6 U/mg specific activity in presence of $NADP^+$ at pH 4.8 and 60 °C. When the assay was performed at pH 7.0 and 30 °C, the activity value decreased to 2 U/mg. Therefore, it can be said that *Lb*FDH has about the same activity with *Bst*FDH in neutral pH [4]. In conclusion, we suggest that the *Lb*FDH can be utilized as a cofactor recycler in reactions that require high temperatures and acidic conditions.

In conclusion, all our estimations and output of genome and protein sequence mining procedure resulted with desired two $NADP^+$ dependent FDHs from *Burkholderia dolosa* PC543 and *Lactobacillus buchneri* NRRL B-30929, respectively. *Bd*FDH is tolerant to DMSO and it has dual coenzyme specificity. It can act at acidic conditions and low temperatures. Therefore, BdFDH is a promising enzyme for $NAD(P)^+$ regeneration in the chiral chemical synthesis carried out in organic solvents or at acidic pH and mild

temperatures. The solubility and activity of BdFDH can be affected by the addition of histidine residues at the N-terminal portion of enzyme. This result suggests that the mentioned region has a significant role in folding and the formation of the 3D structure of the protein. On the other hand, the second enzyme, LbFDH, has a significant tolerance for high temperatures, acidic pH values and some organic solvents. The catalytic efficiency in the presence of $NADP^+$ is also favourable and its specific activity is the highest value among reported native and mutant FDHs at 60 °C. For the production of valuable intermediates in food and pharmaceutical industries, the LbFDH can be utilized as a promising regenerator for NAD(P)H supplementation due to its multiaspect stability and cofactor preference, too. Further studies can be applied with these two enzymes such as their utilization for coupling reactions, immobilization with different materials for performing in reactor based synthesis applications and benefit from them in sensor and enzyme technologies.

# REFERENCES


[1] Rozzell, J., Hua, L., Mayhew, M. and Novick, S., (2004). Mutants of enzymes and methods for their use, US20040115691A1, Great Britain.

[2] Davis, B.G., Celik, A., Davies, G.J. and Ruane, K.M., (2009). Novel enzyme, US20130029378 A1, United States.

[3] Fogal, S., Beneventi, E., Cendron, L. and Bergantino, E., (2015). "Structural basis for double cofactor specificity in a new formate dehydrogenase from the acidobacterium *Granulicella mallensis* MP5ACTX8", Applied Microbiology and Biotechnology, 99:9541-54.

[4] Hatrongjit, R. and Packdibamrung, K., (2010). "A novel $NADP^+$ dependent formate dehydrogenase from *Burkholderia stabilis* 15516: Screening, purification and characterization", Enzyme and Microbial Technology, 46:557-561.

[5] Tishkov, V.I., Galkin, A.G., Fedorchuk, V.V., Savitsky, P.A., Rojkova, A.M., Gieren, H. and Kula, M.R., (1999). "Pilot scale production and isolation of recombinant $NAD^+$ and $NADP^+$ specific formate dehydrogenases", Biotechnology and Bioengineering, 64:187–193.

[6] Tishkov, V.I. and Popov, V.O., (2006). "Protein engineering of formate dehydrogenase", Biomolecular Engineering, 23:89 –110.

[7] Gul-Karaguler, N., Sessions, R.B., Clarke, A.R. and Holbrook, J., (2001). "A single mutation in the $NAD^+$ specific formate dehydrogenase from *Candida methylica* allows the enzyme to use NADP", Biotechnology Letters, 23:283–287.

[8] Serov, A.E., Popova, A.S., Fedorchuk, V.V. and Tishkov, V.I., (2002). "Engineering of coenzyme specificity of formate dehydrogenase from Saccharomyces cerevisiae", Biochemical Journal, 367:841–847.

[9] Tishkov, V.I. and Popov, V.O., (2004). "Catalytic mechanism and application of formate dehydrogenase", Biochemistry, 69:1252–1267.

[10] Nanba, H., Takaoka, Y. and Hasegawa, J., (2003). "Purification and characterization of an alpha-haloketone-resistant formate dehydrogenase from Thiobacillus sp. strain KNK66MA, and cloning of the gene", Bioscience, Biotechnology and Biochemistry, 67:2145–2153.

[11] Nanba, H., Takaoka, Y. and Hasegawa J., (2003). "Purification and characterization of formate dehydrogenase from Ancylobacter aquaticus strain

KNK607M and cloning of the gene", Bioscience, Biotechnology and Biochemistry, 67:720–728.

[12] Andreadeli, A., Platis, D., Tishkov, V.I., Popov, V.O. and Labrou, N.E., (2008). "Structure-guided alteration of coenzyme specificity of formate dehydrogenase by saturation mutagenesis to enable efficient utilization of $NADP^+$", The FEBS Journal, 275:3859–3869.

[13] Labrou, N.E., Rigden, D.J. and Clonis, Y.D., (2000). "Characterization of the $NAD^+$ binding site of Candida boidinii formate dehydrogenase by affinity labelling and sitedirected mutagenesis", European Journal of Biochemistry, 267:6657–6664.

[14] Schirwitz, K., Schmidt, A. and Lamzin, V.S., (2007). "High-resolution structures of formate dehydrogenase from Candida boidinii", Protein Science, 16:1146–1156.

[15] Wu, W., Zhu, D. and Hua, L., (2009). "Site-saturation mutagenesis of formate dehydrogenase from *Candida boidinii* creating effective $NADP^+$ dependent FDH enzymes", Journal of Molecular Catalysis B, 61:157–161.

[16] Hoelsch, K., Sührer, I., Heusel, M. and Weuster-Botz, D., (2013). "Engineering of formate dehydrogenase: synergistic effect of mutations affecting cofactor specificity and chemical stability", Applied Microbiology and Biotechnology, 97:2473–2481.

[17] Ihara, M., Kawano, Y., Urano, M. and Okabe, A., (2013). "Light driven $CO_2$ fixation by using cyanobacterial photosystem I and NADPH dependent formate dehydrogenase", PLOS One, 8: e71581.

[18] Özgün, G.P., Ordu, E.B., Tütüncü, H.E., Yelboğa, E., Sessions, R.B. and Karagüler, N.G., (2016). "Site Saturation Mutagenesis Applications on *Candida methylica* Formate Dehydrogenase", Scientifica, 4902450: 1-7.

[19] Chánique, A.M. and Parra, L.P., (2018). "Protein Engineering for Nicotinamide Coenzyme Specificity in Oxidoreductases: Attempts and Challenges", Frontiers in Microbiology, 9:194.

[20] Denard, C.A., Hartwig, J.F. and Zhao, H., (2013). "Multistep one-pot reactions combining biocatalysts and chemical catalysts for asymmetric synthesis", ACS Catalysis, 3:2856–2864.

[21] Wang, Y. and Zhao, H., (2016). "Tandem reactions combining biocatalysts and chemical catalysts for asymmetric synthesis", Catalysts, 6:194.

[22] Sun, H., Zhang H., Ang, E.L. and Zhao, H., (2018). "Biocatalysis for the synthesis of pharmaceuticals and pharmaceutical intermediates", Bioorganic & Medicinal Chemistry, 26:1275–1284.

[23] Nguyen, L.A., He, H. and Pham-Huy, C., (2006). "Chiral drugs: an overview", International Journal of Biomedical Science, 2(2): 85-100.

[24] Patel, R.N., (2013). "Biocatalytic Synthesis of Chiral Alcohols and Amino Acids for Development of Pharmaceuticals", Biomolecules, 3:741-777.

[25] Choi, J.M., Han, S.S. and Kim, H.S., (2015). "Industrial applications of enzyme biocatalysis: Current status and future aspects", Biotechnology Advances, 33:1443–1454.

[26] Klibanov, A.M. and Cambou, B., (1987). “Enzymatic production of optically active compounds in biphasic aqueous-organic systems”, Methods in Enzymology, 136: 117-137.

[27] Wohlgemuth, R., (2010). “Biocatalysis–key to sustainable industrial chemistry”, Current Opinion in Biotechnology, 21:713–24.

[28] Nestl, B.M., Nebel, B.A. and Hauer, B., (2011). “Recent progress in industrial biocatalysis”, Current Opinion in Chemical Biology, 15:187–193.

[29] Hall, M. and Bommarius, A.S., (2011). “Enantioenriched Compounds via Enzyme-Catalyzed Redox Reactions”, Chemical Reviews, 111:4088–4110.

[30] Kirk, O., Borchert, T.V. and Fuglsang, C.C., (2002). “Industrial enzyme applications”, Current Opinion in Biotechnology, 13(4): 345-351.

[31] Zhang, W. and Cue, B.W. (2012). Green Techniques for Organic Synthesis and Medicinal Chemistry, Second Edition, John Wiley & Sons, Ltd, New Jersey.

[32] May, S.W., (1999). “Applications of oxidoreductases”, Current Opinion in Biotechnology, 10:370–375.

[33] Xu, F., (2005). “Applications of oxidoreductases: recent progress”, Industrial Biotechnology, 1(1):38–50.

[34] Vidal, L.S., Kelly, C.L., Mordaka, P.M. and Heap, J.T., (2018). “Review of NAD(P)H-dependent oxidoreductases: Properties, engineering and application”, BBA - Proteins and Proteomics, 1866:327–347.

[35] Torres Pazmiño, D.E., Winkler, M., Glieder, A. and Fraaije, M.W., (2010). “Monooxygenases as biocatalysts: classification, mechanistic aspects and biotechnological applications”, Journal of Biotechnology, 146:9–24.

[36] Knaus, T., Paul, C.E., Levy, C.W., de Vries, S., Mutti, F.G., Hollmann, F. and Scrutton, N.S., (2016). “Better than nature: nicotinamide biomimetics that outperform natural coenzymes”, Journal of the American Chemical Society, 138:1033–1039.

[37] Determination of NADH and NADPH Using Ion Chromatography and High Resolution Accurate Mass Spectrometry, https://www.thermofisher.com/content/dam/tfs/ATG/CMD/CMD%20Documents/Application%20&%20Technical%20Notes/Chromatography/Ion%20Chrom atography/TN-149-IC-MS-NADH-N ADPH-TN70943-EN.pdf, 25 May 2018.

[38] Nealon, C.M., Musa, M.M., Patel, J.M. and Phillips, R.S., (2015). “Controlling substrate specificity and stereospecificity of alcohol dehydrogenases”, ACS Catalysis, 5:2100–2114.

[39] Altaş, N., Sevinç-Aslan, A., Karataş, E., Chronopoulou, E., Labrou, N.E. and Binay, B., (2017). “Heterologous production of extreme alkaline thermostable $NAD^+$ dependent formate dehydrogenase with wide-range pH activity from *Myceliophthora thermophila*”, Process Biochemistry, 61:110-118.

[40] Wichmann, R. and Vasic-Racki, D., (2005). “Cofactor regeneration at the lab scale”, Advances in Biochemical Engineering/Biotechnology, 92:225–226.

[41] Chenault, H.K. and Whitesides, G.M., (1987). “Regeneration of nicotinamide cofactors for use in organic synthesis”, Applied Biochemistry and Biotechnology, 14:147.

[42] Kratzer, R., Pukl, M., Egger, S. and Nidetzky, B., (2008). "Whole-cell bioreduction of aromatic α-keto esters using Candida tenuis xylose reductase and Candida boidinii formate dehydrogenase coexpressed in Escherichia coli", Microbial Cell Factories, 7:37.

[43] Zhai, X.H., Ma, Y.H., Lai, D.Y., Zhou, S. and Chen, Z.M., (2013). "Development of a whole-cell biocatalyst with NADPH regeneration system for biosulfoxidation", Journal of Industrial Microbiology & Biotechnology, 40:797-803.

[44] Bäumchen, C., Roth, A.H., Biedendieck, R., Malten, M., Follmann, M., Sahm, H., Bringer-Meyer, S. and Jahn, D., (2007). "D-mannitol production by resting state whole cell biotransformation of D-fructose by heterologous mannitol and formate dehydrogenase gene expression in Bacillus megaterium", Biotechnology Journal, 2:1408-1416.

[45] Bastos, F.M., Santos, A.G., Jones, J., Oestreicher, E.G., Pinto, G.F. and Paiva, L.M.C., (1999). "Three different coupled enzymatic systems for in situ regeneration of NADPH", Biotechnology Techniques, 13:661–664.

[46] Kubo, T., Peters, M.W., Meinhold, P. and Arnold, F.H., (2006). "Enantioselective Epoxidation of Terminal Alkenes to (*R*)- and (*S*)-Epoxides by Engineered Cytochromes P450 BM-3", Chemistry-A European Journal, 12:1216–1220.

[47] Weckbecker, A. and Hummel, W., (2004). "Improved synthesis of chiral alcohols with *Escherichia coli* cells co-expressing pyridine nucleotide transhydrogenase, $NADP^+$ dependent alcohol dehydrogenase and $NAD^+$ dependent formate dehydrogenase", Biotechnology Letters, 26:1739–1744.

[48] Johannes, T.W., Woodyer, R.D. and Zhao, H., (2005). "Directed evolution of a thermostable phosphite dehydrogenase for NAD(P)H regeneration", Applied and Environmental Microbiology, 71:5728–5734.

[49] Johannes, T.W., Woodyer, R.D. and Zhao, H., (2007). "Efficient regeneration of NADPH using an engineered phosphite dehydrogenase", Biotechnology and Bioengineering, 96:18–26.

[50] Boonstra, B., Rathbone, D.A., French, C.E., Walker, E.H. and Bruce, N.C., (2000). "Cofactor regeneration by a soluble pyridine nucleotide transhydrogenase for biological production of hydromorphone", Applied and Environmental Microbiology, 66:5161-5166.

[51] Ichinose, H., Kamiya, N. and Goto, M., (2005). "Enzymatic redox cofactor regeneration in organic media: functionalization and application of glycerol dehydrogenase and soluble transhydrogenase in reverse micelles", Biotechnology Progress, 21:1192–1197.

[52] van der Donk, W.A. and Zhao, H., (2003). "Recent developments in pyridine nucleotide regeneration", Current Opinion in Biotechnology, 14(4):421-426.

[53] Yamamoto, H., Mitsuhashi, K., Kimoto, N., Kobayashi, Y. and Esaki, N., (2005). "Robust NADH regenerator: improved α-haloketone-resistant formate dehydrogenase", Applied Microbiology and Biotechnology, 67:33–39.

[54] Galkin, A., Kulakova, L., Tishkov, V., Esaki, N. and Soda, K., (1995). "Cloning of formate dehydrogenase gene from a methanol-utilizing bacterium

*Mycobacterium vaccae* N10", Applied Microbiology and Biotechnology, 44:479–483.

[55] Ding, H.T., Liu, D.F., Li, Z.L., Du, Y.Q., Xu, X.H. and Zhao, Y.H., (2011). "Characterization of a thermally stable and organic solvent–adaptative $NAD^+$ dependent formate dehydrogenase from Bacillus sp. F1", Journal of Applied Microbiology, 111:1075–1085.

[56] Wichmann, R., Wandrey, C., Buckmann, A.F. and Kula, M.R., (1981). "Continuous enzymatic transformation in an enzyme membrane reactor with simultaneous NAD(H) regeneration", Biotechnology and Bioengineering, 23:2789–2802.

[57] Leuchtenberger, W., Huthmacher, K. and Drauz, K., (2005). "Biotechnological production of amino acids and derivatives: current status and prospects", Applied Microbiology and Biotechnology, 69(1):1-8.

[58] Jayabalan, R., Sathishkumar, M., Jeong, E.S., Mun, S.P. and Yun, S.E., (2012). "Immobilization of flavin adenine dinucleotide (FAD) onto carbon cloth and its application as working electrode in an electroenzymatic bioreactor", Bioresource Technology, 123:686–689.

[59] Goldberg, S.L., Nanduri, V.B., Chu, L., Johnston, R.M. and Patel, R.N., (2006). "Enantioselective microbial reduction of 6-oxo-8-[4-[4-(2-pyrimidinyl)-1-piperazinyl] butyl]-8-azaspiro [4.5] decane-7,9-dione: Cloning and expression of reductases", Enzyme and Microbial Technology, 39(7):1441-1450.

[60] Hanson, R.L., Goldberg, S.L., Brzozowski, D.B., Tully, T.P., Cazzulino, D., Parker, W.L., Lyngberg, O.K., Vu, T.C., Wong, M.K. and Patel, R.N., (2007). "Preparation of an Amino Acid Intermediate for the Dipeptidyl Peptidase IV Inhibitor, Saxagliptin, using a Modified Phenylalanine Dehydrogenase", Advanced Synthesis & Catalysis, 349: 1369–1378.

[61] Shabalin, I.G., Polyakov, K.M., Tishkov, V.I. and Popov, V.O., (2009). "Atomic Resolution Crystal Structure of $NAD^+$ dependent Formate Dehydrogenase from Bacterium Moraxella sp. C-1", Acta naturae, 3: 89-93.

[62] Yu, X., Niks, D., Mulchandani, A. and Hile, R., (2017). "Efficient reduction of $CO_2$ by the molybdenum-containing formate dehydrogenase from *Cupriavidus necator (Ralstonia eutropha)*", Journal of Biological Chemistry, 292:16872–16879.

[63] Jormakka, M., Byrne, B. and Iwata, S., (2003). "Formate dehydrogenase – a versatile enzyme in changing environments", Current Opinion in Structural Biology, 13:418–423.

[64] da Silva, S.M., Voordouw, J., Leita, C., Martins, M., Voordouw, G. and Pereira, I.A.C., (2013). "Function of formate dehydrogenases in *Desulfovibrio vulgaris* Hildenborough energy Metabolism", Microbiology, 159:1760–1769.

[65] Alissandratos, A., Kim, H.K., Matthews, H., Hennessy, J.E., Philbrook, A. and Easton, C. J., (2013). "*Clostridium carboxidivorans* Strain P7T Recombinant Formate Dehydrogenase Catalyzes Reduction of CO2 to Formate", Applied and Environmental Microbiology, 79(2):741–744.

[66] Alekseeva, A., Savin, S. and Tishkov, V., (2011). "$NAD^+$ dependent formate dehydrogenase from plants", Acta Naturae, 4:38–54

[67] Shabalin, I.G., Serov, A.E., Skirgello, O.E., Timofeev, V.I., Samygina, V.R., Popov, V.O., Tishkov, V.I. and Kuranova, I.P., (2010). "Recombinant Formate Dehydrogenase from Arabidopsis thaliana: Preparation, Crystal Growth in Microgravity, and Preliminary X-Ray Diffraction Study", Crystallography Reports, 55(5):806–810.

[68] Popov, V.O. and Lamzin, V.S., (1994). "$NAD^+$ dependent formate dehydrogenase", Biochemical Journal, 301:625–643.

[69] Shabalin, I.G., Filippova, E.V., Polyakov, K.M., Sadykhov, E.G., Safonova, T.N., Tikhonova, T.V., Tishkova, V.I. and Popova, V.O., (2009). "Structures of the apo and holo forms of formate dehydrogenase from the bacterium Moraxella sp. C-1: towards understanding the mechanism of the closure of the interdomain cleft", Acta Crystallographica, D65:1315–1325.

[70] Ragsdale, S.W., (2008). "Enzymology of the Wood-Ljungdahl pathway of acetogenesis", Annals of the New York Academy of Sciences, 1125:129–136.

[71] Wood, G.E., Haydock, A.K. and Leigh, J. A. (2003). "Function and regulation of the formate dehydrogenase genes of the methanogenic archaeon Methanococcus maripaludis". Journal of Bacteriology, 185: 2548–2554.

[72] des Francs-Small, C.C., Ambard-Bretteville, F., Small, I.D. and Remy, R., (1993). "ldentification of a Maior Soluble Protein in Mitochondria from Nonphotosynthetic Tissues as $NAD^+$ dependent Formate Dehydrogenase", Plant Physiology, 102:1171-1177.

[73] Igamberdiev, A.U., Bykova, N.V. and Kleczkowski, N.A., (1999). "Origins and metabolism of formate in higher plants", Plant Physiology and Biochemistry, 37:503-513.

[74] Lou, H.Q., Gong, Y.L., Fan, W., Xu, J.M., Liu, Y., Cao, M.J., Wang, M.H., Yang, J.L. and Zheng, S.J., (2016). "Rice bean VuFDH functions as formate dehydrogenase that confers tolerance to aluminum and low pH", Plant Physiology, 171:294–305.

[75] Kruse, J.A., (1992). "Methanol poisoning", Intensive Care Medicine, 18(7):391-397.

[76] World Health Organization. Methanol poisoning outbreaks, http://www.who.int/environmental_health_emergencies/poisoning/methanol_information.pdf, 26 May 2018.

[77] Hovda, K.E., Urdal, P. and Jacobsen, D., (2005). "Increased serum formate in the diagnosis of methanol poisoning", Journal of Analytical Toxicology, 29(6):586-588.

[78] Barceloux, D.G., Bond, G.R., Krenzelok, E.P., Cooper, H. and Vale, J.A., (2002). "American Academy of Clinical Toxicology practice guidelines on the treatment of methanol poisoning", Journal of Clinical Toxicology, 40(4): 415-446.

[79] Bozza-Marrubini, M., Brucato, A., Locatelli, C. and Ruggeroni, M.L., Methanol, http://www.inchem.org/documents/pims/chemical/pim335.htm, 26 May 2018.

[80] Hovda, K.E., Gadeholt, G., Evtodienko, V. and Jacobsen, D., (2015). "A novel bedside diagnostic test for methanol poisoning using dry chemistry for formate", Scandinavian Journal of Clinical and Laboratory Investigation, 75(7): 610-614.

[81] Brzica, H., Breljak, D., Burckhardt, B.C., Burckhardt, G. and Sabolic, I., (2013). "Oxalate: from the environment to kidney stones", Arhiv za higijenu rada i toksikologiju, 64(4):609-630.

[82] Rose, G.A.,(Eds.), (1988). Oxalate Metabolism in Relation to Urinary Stone. The Bloomsbury Series in Clinical Science, Springer-Verlag, Berlin.

[83] Miller, C.A., (1993). "Diagnosis of trichomonas vaginitis by detecting formate in vaginal fluid", EP0556685A2.

[84] Alvarez-Guerra, M., Quintanilla, S. and Irabien, A., (2012). "Conversion of carbon dioxide into formate using a continuous electrochemical reduction process in a lead cathode", Chemical Engineering Journal, 207–208: 278–284.

[85] Innocent, B., Liaigre, D., Pasquier, D., Ropital, F., Léger, J.-M. and Kokoh, K.B., (2009). "Electroreduction of carbon dioxide to formate on lead electrode in aqueous medium", Journal of Applied Electrochemistry, 39:227–232.

[86] Rees, N.V. and Compton, R.G., (2011). "Sustainable energy: a review of formic acid electrochemical fuel cells", Journal of Solid State Electrochemistry, 15:2095–2100.

[87] Reda, T., Plugge, C.M., Abram, N.J. and Hirst, J., (2008). "Reversible interconversion of carbon dioxide and formate by an electroactive enzyme", PNAS, 105:10654–10658.

[88] Kim, S., Kim, M.K., Lee, S.H., Yoon, S.H. and Jung, K.D., (2014). "Conversion of $CO_2$ to formate in an electroenzymatic cell using Candida boidinii formate dehydrogenase", Journal of Molecular Catalysis B: Enzymatic, 102: 9–15.

[89] Zhang, Z., Schäffer, A.A., Miller, W., Madden, T.L., Lipman, D.J., Koonin, E.V and Altschul, S.F., (1998). "Protein sequence similarity searches using patterns as seeds", Nucleic Acids Research, 26(17):3986-90.

[90] Papadopoulos, J.S. and Agarwala, R., (2007). "COBALT: constraint-based alignment tool for multiple protein sequences", Bioinformatics, 23:1073-1079.

[91] Workentine, M.L., Surette, M.G. and Bernier, S.P., (2014). "Draft Genome Sequence of Burkholderia dolosa PC543 Isolated from Cystic Fibrosis Airways", Genome Announcements, 2(1): e00043-14.

[92] Studier, F.W., (2005). "Protein production by auto-induction in high density shaking cultures", Protein Expression and Purification, 41:207–234.

[93] Bradford, M.M., (1976). "A rapid and sensitive method for the quantitation of microgram quantities of protein utilizing the principle of protein-dye binding", Analytical Biochemistry, 7:248-254.

[94] Galante, Y. and Hatefi, Y., (1978). "Resolution of complex *I* and isolation of NADH dehydrogenase and an iron-sulfur protein", Methods in Enzymology, 53:15-21.

[95] Liu, S., Leathers, T.D., Copeland, A., Chertkov, O., Goodwin, L. and Mills, D.A., (2011). "Complete genome sequence of *Lactobacillus buchneri* NRRL B-30929, a novel strain from a commercial ethanol plant", Journal of Bacteriology, 193(15):4019-4020.

[96] Hussain, H. and Chong, N.F., (2016). "Combined Overlap Extension PCR Method *for* Improved Site Directed Mutagenesis", Biomed Research International, 2016: 8041532.

[97] Novagen, pET14b vector, https://www.helmholtz-muenchen.de/fileadmin/PEPF /pET_vectors/pET-14b_map.pdf, 26 May 2018.

[98] Novagen, pET22b vector, https://www.helmholtz-muenchen.de/fileadmin/PEPF/ pET__vectors/pET-22b_map.pdf, 26 May 2018.

[99] Novagen, pET23b vector, https://www.chemistry.mcmaster.ca/berti/safety/Manuals/pET23a.pdf, 26 May 2018.

[100] Horchani, H., Sabrina, L., Régine, L., Sayari, A., Gargouri, Y. and Verger, R., (2010). "Heterologous expression and N-terminal His-tagging processes affect the catalytic properties of staphylococcal lipases: a monolayer study", Journal of Colloid and Interface Science, 350(2):586-94.

[101] Gaberc-Porecar, V. and Menart, V., (2001). "Perspectives of immobilized-metal affinity chromatography", Journal of Biochemical and Biophysical Methods, 49:335-360.

[102] de Costa, F., Barber, C.J., Pujara, P.T., Reed, D.W. and Covello, P.S., (2016). "Purification of a recombinant polyhistidine-tagged glucosyltransferase using immobilized metal-affinity chromatography (IMAC)", Methods in Molecular Biology, 1405:91-97.

[103] Kim, E.Y., Choi, H.J., Chung, T.W., Jang, S.B., Kim, K. and Ha, K.T., (2015). "Expression and efficient one-step chromatographic purification of a soluble antagonist for human leukemia inhibitory factor receptor in E. coli*",* Journal of Microbiology and Biotechnology, 25:1307-1314.

[104] Chant, A., Kraemer-Pecore, C.M., Watkin, R. and Kneale, G.G., (2005). "Attachment of a histidine tag to the minimal zinc finger protein of the Aspergillus nidulans gene regulatory protein AreA causes a conformational change at the DNA binding site", Protein Expression and Purification, 39(2):152-159.

[105] Horchani, H., Ouertani, S., Gargouri, Y. and Sayari, A., (2009). "The N-terminal His-tag and the recombination process affect the biochemical properties of Staphylococcus aureus lipase produced in Escherichia coli", Journal of Molecular Catalysis B: Enzymatic, 61:194-201.

[106] Hyun, J., Abigail, M., Choo, J.W., Ryu, J. and Kim, H.K., (2016). "Effects of N-/ C-Terminal Extra Tags on the Optimal Reaction Conditions, Activity, and Quaternary Structure of Bacillus thuringiensis Glucose-1-Dehydrogenase", Journal of Microbiology and Biotechnology, 26(10):1708-1716.

[107] Lamzin, V.S., Dauter, Z., Popov, V.O., Harutyunyan, E.H. and Wilson, K.S., (1994). "High resolution structures of holo and apo formate dehydrogenase", Journal of Molecular Biology, 236: 759–785.

[108] Klibanov, A.M., (2001). "Improving enzymes by using them in organic solvents", Nature, 409:241–246.

[109] Wu, X., Yang, C. and Ge, J., (2017). "Green synthesis of enzyme/metal-organic framework composites with high stability in protein denaturing solvents", Bioresources and Bioprocessing, 4(24):1-8.

[110] Bommarius, A.S. and Karau, A., (2005). “Deactivation of formate dehydrogenase (FDH) in solution and at gas-liquid interfaces”, Biotechnology Progress, 21:1663–1672.

# APPENDIX-A

## MEDIUMS/SOLUTIONS

**Luria Bertani (LB) Medium**

10 g tryptone or casein pepton tryptic digest, 5 g yeast extract, 5 g NaCl were dissolved in deionized water and filled up to 1 L. The pH was adjusted to 7.0 and sterilized for 15 minutes under 1.5 atm at 121 °C. The medium was kept at room temperature.

**LB Agar Medium**

10 g tryptone, 5 g yeast extract, 5 g NaCl and 15 g agar were dissolved in deionised water up to 1 L and the pH is adjusted to 7.0. Media is sterilized by autoclaving for 15 min at 121 °C. The medium was poured to the plates. The plates were kept at +4°C.

**SOC Medium**

2 g bactotryptone, 0.5 g bactoyeast extract and 50 mg NaCl were dissolved in distilled water. 250 µL of 1M KCl was added to the solution and the pH was adjusted to 7.0 with NaOH. Volume was adjusted to 100 mL with distilled water and the solution was autoclaved. 2 M MgCl2 and 1 M glucose were added just before the usage.

**50X TAE (Tris/Acetate/EDTA) Buffer**

57.1 ml of glacial acetic acid, 242 g of Tris base, 100 ml of 0.5 M EDTA (pH 8.0) in 1000 ml water.

**APS (10%) Solution**

Add 1g Ammonium persulphate per 10 ml water. Mix thoroughly - APS will dissolve readily. Solution may be kept at 4'C up to 6 months.

**SDS (10%) Stock Solution**

Dissolve 10 g of SDS in 80 mL of $H_2O$, and then add $H_2O$ to 100 mL. This stock solution is stable for 6 month at room temperature.

**30% Acrylamide Solution**

Acrylamide (30 g ) ve N,N'-methylbisacrylamide (0.8 g) Dissolve in 60ml of water, adjust the volume to 100 ml with water. Filtration through 0.45 micron pore size filter. Store at +4°C.

## APPENDIX-B

## PRIMERS FOR CLONING AND MUTAGENESIS

Table 1. N-terminus his tagged cloning primers for *B.dolosa* PC543

| **Direction** | **Sequence** |
|---|---|
| Forward (*Nde*I) | 5’-CGGTGTC**CATATG**GCGAAAGTGCTTTGCG-3’ |
| Reverse (*BamH*I) | 5’- CGCT**GGATCC**CTACGTCAGGCTGTACG-3 ’ |

Table 2. C-terminus his tagged cloning primers for *B.dolosa* PC543

| **Direction** | **Sequence** |
|---|---|
| Forward (*Nde*I) | 5’-CGGTGTC**CATATG**GCGAAAGTGCTTTGCG-3’ |
| Reverse (*Not*I) | 5’-ATAAAT**GCGGCCGC**CGACGTCAGGCTGTACGACGC-3’ |

Table 3. C-terminus his tagged cloning primers and mutation primers for *L.buchneri NRRL B-30929*

| **Primer type** | **Direction** | **Sequence** |
|---|---|---|
| Cloning Primers | Forward (*Nde*I) | 5’CGGTGTC**CATATG**ACCAAAGTGTTAGCAGTTC-3’ |
| | Reverse (*Xho*I) | 5’ATAAAT**CTCGAG**CGACTTCTCAGCTTCCCCACTTC-3’ |
| Mutagenesis Primers | Forward | 5’- CCCCACACATGTCCGGAACAAC-3’ |
| | Reverse | 5’- CCGGACATGTGTGGGGTCATAGC-3’ |

## CURRICULUM VITAE

**PERSONAL INFORMATION**


**Name Surname** : Saadet ALPDAĞTAŞ

**Place of Birth** :VAN

**Foreign Languages** :English

**E-mail** :saadetalpdagtas@gmail.com


**EDUCATION**

| Degree | Department | University | Date of Graduation |
|---|---|---|---|
| Master | Biology | Yuzuncu Yil University | 2012 |
| Undergraduate | Biology Education | Marmara University | 2005 |

**WORK EXPERIENCE**

| Year | Corporation/Institute | Enrollment |
|---|---|---|
| 2009-Present | Yuzuncu Yil Univ. | Research Assistant |
| 2005-2009 | Public Schools | Biology Teacher |

## PUBLISHMENTS

### Papers

1. Alpdağtaş, S., Celik, A., Ertan, F. and Binay, B., (2018). "DMSO tolerant, NAD(P)H recycler enzyme from a pathogenic bacterium, *Burkholderia dolosa* PC543: effect of N-/C-terminal His Tag extension on protein solubility and activity", Engineering in Life Sciences, 0:1-11.

2. Alpdağtaş, S., Yucel, S., Kapkac, H.A., Liu, S. and Binay, B., (2018). "Discovery of an acidic, thermostable and highly $NADP^+$ dependent formate dehydrogenase from *Lactobacillus buchneri* NRRL B-30929", Biotechnology Letters, 40(7): 1135-1147.

3. Hazini, A., Cemek, M., Işıldak, I., Alpdağtaş, S., Önül, A., Şenel, Ü., Kocaman, T., Dur, A., Iraz, M. and Uyarel, H., (2015). "Investigation of ischemia modified albumin, oxidant and antioxidant markers in acute myocardial infarction", Advances in Interventional Cardiology. Postepy Kardiol Interwencyjnej, 11(4): 298–303.

4. Keleş, İ, Bozkurt, M.F., Cemek, M., Karalar, M., Hazini, A., Alpdağtaş, S., Keleş, H., Yıldız, T., Ceylan, C. and Büyükokuroğlu, M.E., (2014). "Prevention of cyclophosphamide-induced hemorrhagic cystitis by resveratrol: A comparative experimental study with mesna", International Urology and Nephrology, 46(12): 2301-10.

5. Cemek, M., Büyükokuroğlu, M.E., Sertkaya, F., Alpdağtaş, S., Hazini, A., Önül, A. and Göneş, S., (2014). "Effects of food color additives on antioxidant functions and bioelement contents of liver, kidney and brain tissues in rats", Journal of Food and Nutrition Research, 2(10): 686-694.

### Conference Papers

1. Esen, H., Alpdağtaş, S., Çakar, M.M. and Binay, B., (2018). "Polyhistidine Tag Effect on Solubility and Activity of *Chaetomium thermophilum* Formate Dehydrogenase (*Ct*FDH)", 1st EBAT Congress, 27-30 October 2018, Antalya.

2. Çakar, M.M., Duraksoy, B.B., Alpdağtaş, S., Turner, N.J., Woodley, J. and Binay, B., (2018). "Engineering and large-scale producing of formate dehydrogenase for CO2 reduction", 6th Novel Enzymes, 9-12 September 2018, Darmstadt, Germany

3 Alpdağtaş, S., Yucel, S., Kapkac, H.A.., Liu, S. and Binay, B., (2018). "A novel NADPH regenerator for industrial biocatalysis", 4th MECP18, 19-22 March 2018, Trondheim, Norway.

4 Rasolonjatovo, M.A., Cemek, M., Şenel, Ü., Kocaman, T., Göneş, S., Alpdağtaş, S., Ortaç, D., Konuk, H.B. and Karaman E., (2015). "Investigation of the

Effectiveness of Natural and Chemical Solvents on the Removal of Pesticide Residues in Tomatoes", VII. National Veterinary Biochemistry and Clinical Biochemistry Congress, 28-30 May 2015, Samsun.

5 Cemek, M., Ortaç, D., Karaca, T., Büyükokuroğlu, M.E., Özdemir, Z.Ö., Kocaman, T., Alpdağtaş, S., Karaman, E. and Konuk, H.B., (2015). "Investigation of Anti-Ulcer Effect of Okra (Abelmoschus Esculentus L.) on Acute Stomach Mucosal Damage", VII. National Veterinary Biochemistry and Clinical Biochemistry Congress, 28-30 May 2015, Samsun.

6 Cemek, M., Büyükokuroğlu, M.E., Sertkaya, F., Alpdağtaş, S., Hazini, A., Önül, A. and Göneş, S., (2014). "Effects of Food Color Additives on Antioxidant Functions and Bioelement Contents of Liver, Kidney and Brain Tissues in Rats". Bioengineering Conference Proceeding, International BIO ENG14, 27-28 November 2014, Istanbul.

7 Hazini, A., Cemek, M., Işıldak, İ., Alpdağtaş, S., Önül, A., Dur, A., Iraz, M. and Uyarel, H., (2014). "Investigation of ischemia modified albumin, oxidant and antioxidant markers in acute myocardial infarction", International BIO ENG14, Bioengineering Coference Proceeding, 27-28 November 2014, Istanbul.

8 Hazini, A., Cemek, M., Sarı, I., Onul, A., Onat, D. And Alpdagtas, S., (2014). "Honey and propolis based wound dressing: A promising biomaterial for skin wound healing", International Symposium on Sustainable Development ISSD 2014, Biotechnology for Sustainable Development, 15-18 May 2014, Sarajevo, Bosnia and Herzegovina.

9 Cemek, M., Hazini, A., Onul, A., Isıldak, I., Onat, D., Sarı, I., Alpdagtas S. and Gones S., (2014). "Cardiac markers and ischemia modified albumin on acute myocardial infarction". International Symposium on Sustainable Development ISSD 2014. Biotechnology for Sustainable Development, 15-18 May 2014, Sarajevo, Bosnia and Herzegovina.

10 Keleş, İ., Bozkurt, M.F., Cemek, M., Karalar, M., Hazini, A., Alpdağtaş, S., Keleş, H., Yıldız, T., Ceylan, C. and Büyükokuroğlu, M.E., (2014). "Prevention of Cyclophosphamide Induced Hemorrhagic Cystitis by Resveratrol: A comparative study with mesna", XXIII. National Urology Congress, Ekim 2014, Antalya.

11 Alpdagtas, S., Senler, N.G. and Yıldız, İ., (2014). "Morphological and Taxonomic Investigations on Pleuronema coronatum (Protista, Ciliophora, Pleuronematida)", 22. National Biology Congress, June 2014, Eskisehir.

12 Ocak, S., Atik, N. and Alpdagtas, S., (2011) "Heavy Metals from Solid Waste and Its Bioremediation", International Conference of Ecosystems (ICE) , International Conference of Ecosystems (ICE), June 2011, Tirana, ALBANIA.

13 Alpdagtas, S., Ucar, F., Birgul, C. and Coban, S., (2003). “Autoantibodies and autoimmune diseases”, X. th National Student Congress, Marmara University, Istanbul.

**Projects**

1. Morphological and Taxonomical studies on Pleuronema (Protista, Ciliophora) species, Yuzuncu Yıl University, Scientific Projects Department/ MSc projects, Researcher, 2009-2012.

2. Investigation of Novel $NADP^+$ Dependent Format Dehydrogenase Enzymes, Yıldız Technical University, Scientific Projects Department / PhD Projects, Researcher, 2018-2019.

**AWARDS**

1. Turkish Higher Education Council Institution fellowship for MSc students (YOK Fellowship), 2011 ( Smith College / Massachusetts / USA, for 3 months)

2. National FARABI fellowship for MSc students, 2009-2010 (Karadeniz Technical University / Trabzon / TURKEY, for fall term)